1994

Ecological Aspects Of Iron Acquisition In Synechococcus Sp (cyanophyceae)

Steven Wray Wilhelm

ECOLOGICAL ASPECTS OF IRON ACQUISITION IN *SYNECHOCOCCUS* SP. (CYANOPHYCEAE)

by

Steven W. Wilhelm

Department of Plant Sciences

Submitted in partial fulfilment
of the requirements for the degree of
Doctor of Philosophy

Faculty of Graduate Studies
The University of Western Ontario
London, Ontario
April, 1994

ISBN 0-315-93242-2

Canada

As primary producers, marine cyanobacteria regulate the biological and biogeochemical cycles of aquatic ecosystems and influence ocean-atmosphere gas exchange. The purposes of this project were to determine if a *Synechococcus* sp. was capable of utilizing a high-affinity iron transport system during periods of iron-limited growth and if physiological changes due to iron limitation could be identified. Resolution of these factors was achieved by maintaining the cyanobacterium *Synechococcus* sp. PCC 7002 in continuous culture chemostats over a range of iron availabilities.

Changes in physiology were detected over a range of iron concentrations. Reductions in the levels of photosynthetic pigments were accompanied by a deterioration of thylakoid integrity and changes in cellular carboxysome and polyphosphate bodies. Polypeptide profiles of thylakoid, cytoplasmic, and outer membrane fractions demonstrated the enhanced production of specific proteins during iron-limited growth. The photosynthetic efficacy (measured as oxygen evolution and carbon fixation) is significantly reduced during iron-limitation, with carbon incorporation being reduced from luxury levels to the minimum requirements for cellular carbon turnover.

Steady state cell densities within chemostats, combined with growth data obtained from batch cultures, demonstrate a non-linear response between iron concentration and cyanobacterial proliferation. Results suggest that this is brought about by changes in the cellular iron quotient, coupled with the activation of an energy dependant high-affinity iron transport system. The

activation of this system involves the release of four novel iron-regulated, iron-binding cell products (siderophores) by *Synechococcus* sp. PCC 7002.

To determine the prevalence of siderophore production, ten species of cyanobacteria were examined for the ability to produce siderophores under iron-limiting conditions. In all cases these cyanobacteria were found to produce siderophores, and, in many species, the production of multiple siderophores was detected. Analysis of the chemical moieties associated with these compounds demonstrated that hydroxamate-type, catechol-type, and atypical-type iron chelators are produced by these cyanobacteria.

The presence of siderophores enhances the ability of cyanobacteria, grown under iron-limiting conditions, to assimilate iron from the environment via membrane-associated receptor proteins. Ferrisiderophore receptors are not expressed by cyanobacteria grown under iron-replete conditions.

An amalgamation of these results infers that some cyanobacteria utilize high-affinity iron transport systems, involving the serial transport of iron via soluble and membrane-associated ferrisiderophore complexes, in a process which requires the presence of membrane-specific receptors and ATP. This work demonstrates that the definition of affinity in iron transport must consider the biologically available and unavailable pools of iron in the environment. This work suggests that high-affinity iron transport in cyanobacteria involves the conversion of biologically unavailable iron to an available form.

Acknowledgements

As with any endeavour, this thesis would not have been possible without the effort and support of numerous people. My particular appreciation is given to my supervisor, Dr. C.G. Trick, whom was willing to provide me with this opportunity when many others were not. The fact that this thesis exists is a testament to his patience, guidance and trust. I am, and will remain, deeply indebted to Charlie for the opportunities and experiences he has presented me.

I also own a great deal of gratitude to Dr. M.A. Lachance, who functioned as my "spiritual" supervisor throughout my graduate experience at Western. André deserves a great deal of credit for my development as an academic.

The content of this thesis has been also greatly influenced my advisory committee, Dr. R.B. van Huystee and Dr. N.P.A. Huner, both of whom have provided me with a great many answers to problems I might still be struggling with. Others also deserve credit for there influence on this work: Dr. J.B. Stothers, Dr. D. McKnight, and D. Moyles all provided insight and assistance with problems that I may not have overcome alone.

My experience during my tenure here has also been greatly influenced by my many peers, only a few of whom I have space to mention. I would be remiss if I did not acknowledge (Dr?) D.P. Maxwell, whom made my studies of the photosynthetic parameters more bearable. I would also like to acknowledge C.M. Brown, Dr. V. Hurry, and (Drs?) G. Gray and J.E. Kaden. Without there academic input and sense of humour, this would have been a much less pleasant experience.

Finally I am indebted to my family and personal friends for all their support in allowing me this little adventure; hopefully you will not be disappointed by its outcome. A final note of thanks to Barb Sudeyko, whose charm and sense of humour has helped maintain a small amount of sanity in my life.

Table of Contents

List of Tables

List of Figures

Nomenclature

$ABS_{x\ nm}$ ...	Absorbance @ x nm
amol.....	Attomoles
ATP.....	Adenosine triphosphate
CAS.....	Chrome azural S
Chl*a*.....	Chlorophyll *a*
CCCP.....	Carbonylcyanide *m*-chlorophenylhydrazone
D.....	Chemostat diultion rate
d^{-1}.....	Per day
Da.....	Daltons
DCMU.....	3-(3' 4'-dichloromethyl)-1,1-dimethyl urea
2,3-DHBA	2,3-dihydroxybenzoic acid
DNP.....	2,4-dinitrophenyl
EDDA.....	Ethylene diamine di(o-hydroxyphenyl acetic acid)
EDTA.....	Ethylene diamine tetra-acetic acid
eV.....	Electron volts
h^{-1}.....	Per hour
HDTMA...	Hexadecyltrimethyl-ammoniumbromide
HEPES....	N-2-hydroxethyl-piperazine-N'-2-ethanesulfonic acid
HPLC...	High performance liquid chromatography
K_{sol}.....	Solubility constant
m^{-2}.....	Per meter squared
min^{-1}.....	Per minute
μ.....	Growth rate (d^{-1})
NADP...	β-Nicotinamide adenine dinucleotide phosphate
PC.....	Phycocyanin
PCC.....	Pasteur Culture Collection
pFe.....	- Log [Fe^{3+}]
Φ_{app}.....	Apparent quantum yield
PMSF...	Phenyl-methylsulfonyl fluoride
Q_{Fe}.....	Cellular iron quotient
s^{-1}.....	Per second
SOD.....	Superoxide dismutase
TES.....	N-tris(hydroxymethyl) aminomethane
TLC.....	Thin layer chromatography
TRIS.....	Tris(hydroxymethyl) aminomethane
UTEX....	University of Texas at Austin Collection of Algae
X_t.....	Cell density at time = t

1. Introduction

The flux of photosynthetically derived carbon into the ocean is potentially regulated by several factors that function to restrict the growth rate and cell density of the primary producers in aquatic systems The regulation of primary productivity is important in our understanding of the global carbon cycle and in the potential of regional scale fisheries.

The role of nutritional factors in limiting primary productivity in marine systems has received considerable attention, but the precise roles remain unclear. Limitation in most freshwater systems is now accepted, in general, to be due to the low availability of phosphorus (Schindler 1981), although other nutrients such as nitrogen, silicon (Schindler 1981) and iron (Wetzel 1966, Murphy et al. 1983; Storch and Dunham 1986) have also been implicated. Early work in marine systems suggested that N and P may limit these systems On a geological scale (long term), Redfield et al. (1963) suggested that P availability must have ultimately limited phytoplankton abundance while arguments on short term scales have suggested that the availability of N in open-ocean communities was the growth limiting factor (Eppley et al. 1973; DiTullio et al. 1993). More recent considerations now suggest that phytoplankton growth and species composition in these regions may in fact be co-determined by the availability of macro- (N, P, or Si) and micro- (iron, trace metals, vitarnin B_{12}) nutrients (Morel and Hudson 1984).

The concept of co-limiting factors is not a new one. Nathanson (1908),

in response to Brandt's suggestion that aquatic systems should be limited by whatever nutrient was in the lowest concentration according to Leibig's Law of the Minimum, stated that the complex interactions of light, temperature, salinity, and gas exchange were too numerous, and that a single limiting factor would be replaced by a complex of factors (Brandt and Raben 1922).

Gran (1931) was one of the first to suggest that "the growth of the plankton diatoms is determined by factors other than the concentration of phosphates and nitrates and besides temperature and light". Hart (1941), concluded from his work in the Weddell Sea and other Antarctic regions that iron may be one of the limiting growth factors. Since then a number of other researchers, predating the past two decades, investigated the potential of iron to act as a limiting nutrient (Harvey 1933, 1937, 1947; Menzel and Ryther 1961). All of these studies were discounted, however, due to the levels of contaminating iron.

The paradoxical existence of high nutrient : low chlorophyll regions in the oceans has supported the notion that the level of biologically available iron in some marine systems may indeed regulate the new production within these systems. Evidence from Martin and co-workers (Martin et al. 1989, 1990; Martin and Fitzwater 1988) preceded a flurry of reports suggesting that certain areas of the oceans, including the sub-arctic Pacific gyre, the equatorial pacific, and the vast southern ocean may be limited by the amount of available iron (Figure 1). These regions have been shown to acquire most of the iron utilized

Figure 1a). False colour satellite image of seven year mean pigment levels in the oceans. Chlorophyll levels in aquatic areas were derived from data accumulated using the Coastal Zone Colour Scanner satellite. Pink regions demonstrate areas of low chlorophyll concentration (< 0.10 mg m^{-3}). Oceanic regions in the equatorial Pacific, sub-arctic Pacific gyre, and the vast Southern Ocean are among those regions in which primary productivity has been suggested to be limited by the availability of iron. **b).** Colour representation bar correlated to chlorophyll concentration (mg m^{-3}) for 1a). From Mitchell et al., 1991.

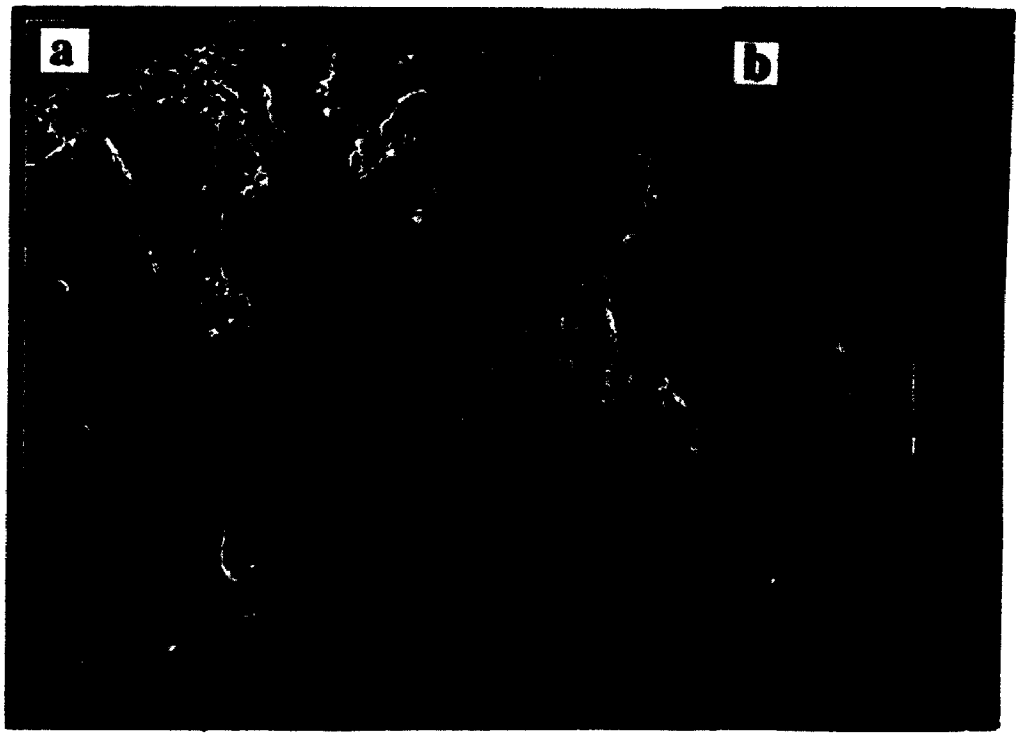
a
b

in new production by aeolian input (Moore et al. 1984, Duce and Tindale 1991). Unlike coastal and mid-Atlantic regions, these areas are not subjected to large anthropogenically determined iron fluxes. Further to this, Martin's group demonstrated that the upwelling rate of iron, when examined as a ratio of biological nutrient necessity, was significantly lower than that of the macronutrients (nitrogen and phosphorous) in these oceanic regions (Martin et al. 1988). From this information, Martin and co-workers suggested that, in these regions, primary productivity is limited by the availability of iron. This became of national interest when it was suggested that the infusion of a large amount (about 300,000 tonnes) of iron, in a soluble form, would alleviate the repression of primary productivity by iron limitation causing an algal bloom capable of driving two billion tons of carbon dioxide into the oceans. This was proposed as the "geritol solution" to the problem of global warming (Chisholm and Morel 1991). The increased flux of carbon dioxide into the ocean would help to offset the affect of the anthropogenically introduced carbon dioxide. This buildup of CO_2 is believed to be responsible for the period of global warming currently being experienced (the "green-house" effect).

In order to resolve some of the specific effects of iron on primary productivity, I have focused on the effect of iron-limited growth on the physiology of a coccoid cyanobacterium, and the associated high-affinity iron acquisition response brought about by iron-limited growth.

1.1 Importance of Cyanobacteria in Aquatic Systems

The cyanobacteria constitute one of the largest groups of the Gram-negative prokaryotes. Their maintenance of two photosystems and ability to undertake oxygenic photosynthesis (as in higher plants) combined with their rapid growth and ability to be cultured has made them an integral tool in many research labs. Traditional assignments of these organisms to the algae resulted in an early classification by phycologists within the provisions of the botanical code (Stafleu et al. 1972). Discrimination at these morphological, ecological and physiological levels resulted in an early description of some 150 genera containing well over 1000 species (Rippka et al. 1979). The reclassification of cyanobacteria by Rippka et al. (1979) lead to the development of five sections of cyanobacteria. These sections are created by dividing the cyanobacteria into filamentous and unicellular groups, and then subgrouping these based on reproductive characteristics. The coccoid cyanobacteria of the genus *Synechococcus* as well as those of the genera *Gloeothece*, *Gloeobacter*, *Gloeocapsa*, *Synechocystis* and *Chamaesiphon* comprise Section I (Table 1).

The importance of cyanobacteria in pelagic ocean has only recently been appreciated, in part due to the small size of the coccoid species and the early difficulties in enumerating them. Early reports suggested that the marine, planktonic cyanobacterial species, unlike their freshwater counterparts, were limited to a few nostocalean species such as *Trichodesmium* (Fogg 1973).

Table 1. Cyanobacterial assignments to sub-groups. Grouping of cyanobacteria and the assignment into sections.

Unicellular; cells single or forming colonial aggregates held together by additional outer cell wall layers	**Section I.** Reproduction by binary fission or budding **Section II.** Reproduction by multiple fission giving rise to small daughter cells (baeocytes), or by both multiple fission and binary fission		
Filamentous; a trichome (chain of cells) which grows by intercalary cell division	**Reproduction by random trichrome breakage, by formation of hormagonia and (Sections IV and V only) sometimes by germination of akinetes**	**Trichome always composed of only of vegetative cells** **In the absence of combined nitrogen, trichome contains heterocysts; some also produce akinetes**	**Section III.** Division in only one plane **Section IV.** Division in only one plane **Section V.** Division in more than one plane

Table 1b. Section I: Unicellular cyanobacteria dividing by binary fission.

		Division in one plane	Division in two or three planes
Reproduction by binary fission	Thylakoids absent	Sheath present *Gloeobacter*	
	Thylakoids present	Sheath present *Gloeothece*	Sheath present *Gloeocapsa*
		Sheath absent *Synechococcus*	Sheath absent *Synechocystis*
Reproduction by budding	Thylakoids present	*Chamaesiphon*	

from Rippka et al. 1979.

Utilization of epifluorescent techniques and the advent of flow cytometry (DiTullio et al. 1993) have been used to analyze the previously disregarded 0.2-2.0 µm planktonic fraction (isolated by selective filtration) and permitted the realization of the importance of the picoplanktonic fraction (Waterbury et al. 1979; Johnson and Sieburth 1979). Of primary interest are the coccoid cyanobacteria (especially those of the genus *Synechococcus*), that are ubiquitously distributed throughout temperate and tropical regions in numbers within an order of magnitude on either side of 10^4 cells mL^{-1} (Fogg 1987). Cyanobacterial numbers decrease significantly as one goes toward the poles (Murphy and Haugen 1985), although evidence does exist for limited cyanobacterial proliferation as far as 68°North (Northern Foxe Basin, Smith et al. 1985) and a coccoid, phycocyanin rich, psychrophilic cyanobacterium (tentatively proposed as *Synechococcus*) from the True Love Lowlands on Devon Island (75° 33" North) has been isolated (Wilhelm, Renaud and Trick, unpublished).

Estimates of the importance of cyanobacteria, with respect to carbon flux, have suggested that 60% of the photosynthesis in pelagic systems may be carried out by organisms < 1.0 µm in size (Platt et al. 1983). A great deal of discrepancy does still exist, however, with researchers often finding a great flux in the range of photosynthetic potential: Li et al. (1983) found that 25 to 90% of the biomass and 20 to 80% of the photosynthesis in the eastern tropical Pacific Ocean was attributable to cells passing through a 1 µm filter.

The other major role of cyanobacteria in pelagic systems may be accredited to their potential role as nitrogen fixers (see Fogg 1987; Capone and Carpenter 1982). *Trichodesmium* is the principal organism responsible for the fixation of nitrogen in marine ecosystems. It has been estimated that 4.8 megatonnes of nitrogen are fixed each year in pelagic environments, two-thirds of which occurs in the Indian Ocean contrasting only 0.34 Mt fixed in the Pacific Ocean (Carpenter 1983). It appears, however, that cyanobacterial fixation of nitrogen still represents only a small fraction of the total nitrogen required by phytoplankton (Fogg 1987).

1.2 Iron Availability

Iron is the fourth most abundant element on the planet (after oxygen, aluminum and silicon) (Boyer et al. 1987). Although iron represents almost 33% of the total mass of the planet, the dynamics of iron in biologically viable environments dictates that this element becomes unavailable to organisms. Aqueous ferric iron quickly precipitates as ferric hydroxide with a very low solubility constant for the ferric form ($K_{sol} = 10^{-38}$; Biedermann and Schindler 1957). Using this value, the availability of Fe^{3+} can be determined for natural conditions:

$$Fe^{3+} + 3OH^- \longrightarrow Fe(OH)_3$$

$$K_{sol} = [Fe^{3+}][OH^-]^3$$

$$K_{sol} = 10^{-38}$$

$$[Fe^{3+}] = 10^{-38} / [OH^-]^3$$

$$[Fe^{3+}] = 10^{-38} / [10^{-7}]^3 = 10^{-17} \text{ M at pH 7.0}$$

Thus ferric iron, at it's maximum solubility under biological conditions, is available at a pFe value (defined as -log[Fe^{3+}]) of 17.0. The other free form of iron, Fe^{2+}, is found in only small concentrations in marine waters and has been suggested to be oxidized to the Fe^{3+} form within 2 to 200 seconds (Andersen and Morel 1982), suggesting it may be of little importance in the total iron pool. Other reports, however, contradict this by suggesting that the rate of photochemical and/or biological reduction of Fe^{3+}, with respect to the rates of Fe^{2+} oxidation, may be sufficient so as to maintain a steady state concentration of Fe^{2+}, and that this Fe^{2+} may be biologically significant (O'Sullivan et al. 1991).

Due to its insolubility in oxic environments, concentrations of iron in pelagic marine environments are quite low (0.02 - 0.05 nM, Hutchins et al. 1993), while river water typically contains from 0.18 to 25 µM (Bowen 1966). Laboratory studies suggest iron uptake rates from colloidal and particulate sources is quite low (Wells et al. 1983; Rich and Morel 1990), and it is felt that the "biologically available" iron must exist in the dissolved Fe^{3+} state. Hudson (1989) demonstrated for the two species of phytoplankton that the availability of Fe^{3+} was indeed the factor regulating iron uptake, while selective chelation of Fe^{2+} had little effect on iron acquisition.

Variations in pH can also dramatically affect the availability of iron. With a pH shift from pH 7.0 to 7.4, the free ferric ion in concentration decreases from pFe 17.0 to 18.2. A further increase to pH 8.1 (the pH of most marine systems) reduces the iron level a further 2 orders of magnitude (to pFe 20.3). This

availability is further complicated by the presence of other compounds in natural systems. Attempts to model this have resulted in a variety of computer programs focused on determining the chemical speciation of components in aquatic systems. Such programs have become of paramount importance as the scientific community accepts the fact that the biologically available iron may vary due to a number of factors independent of total iron concentration, and thus reporting iron in pFe values has become the norm.

1.3 Biological Requirements for Iron

Iron has been suggested to be required for most forms of life, with the potential exception of the *Lactobacillus* spp. (Neilands and Leong 1986). The importance of iron is brought about by a versatility that allows it to function as both an electron acceptor and electron donor; it's stability in both ionic states allows it to function as an effective biological catalyst. Phytoplankton, in particular, have a number of demonstrated requirements for this trace nutrient. Iron is an essential component in cellular photosystems, the cytochrome b_6/f complex, and in a number of soluble electron carriers such as cytochrome c and ferredoxin. While photosynthetic pigments (chlorophyll, phycobilin pigments) contain no iron in themselves, the pathways for their synthesis include a number of iron-dependant steps (Guikema and Sherman 1984; Pakarasi et al. 1985).

Elemental iron is also a crucial component of nitrogen assimilation

mechanisms in phytoplankton. Iron-sulphur and heme-containing compounds serve as integral cofactors in elemental N assimilation by organisms during NO_3^- or NO_2^- reduction, and the reductive transfer of amide-nitrogen (Hall et al. 1982). Nitrogen fixation also requires the integrated iron/molybdenum nitrogenase enzyme to split the strong diazo bonds of N_2; the nitrogenase enzyme itself requires 28 to 36 atoms of iron (Averall and Orme-Johnson 1978). The importance of iron can thus be inferred on an ecological scale, in considering the demands for Fe in N acquisition.

Iron is also required for some forms of the metalloenzyme superoxide dismutase (SOD). These catalysts bring about the elimination of superoxide anions (O_2^-) and thus protect the cells from their destructive effect. While eukaryotic algae contain manganese and copper/zinc SOD, iron-type SOD are found in cyanobacteria including in *Anacystis nidulans*, *Plectonema boryanum* and *Spirulina platensis* (Laudenbach et al. 1989 and references therein). While a number of other iron-containing metalloenzymes have been identified, these enzymes account for only 10 to 18% of the total cellular iron quota of cyanobacteria and thus a great portion of cellular iron remains unaccounted for (Boyer et al. 1987).

The actual quantity of iron required to maintain cellular growth has become an issue of great interest due to questions regarding the status of iron in some marine regions. Determination of cellular iron quotas for cells are often hampered by contamination from trace levels of iron present in chemicals

utilized for growth, as well as contamination from iron in laboratory equipment.

Estimated iron quotas (Q_{Fe}) for various eukaryotic algae have suggested that cellular requirements range from 0.04 to 0.23 pg (Boyer et al. 1987). Estimates of Q_{Fe} in cyanobacteria have been less successful, as they are complicated by a variety of factors. A non-linear relationship between iron concentration and cell growth (Kerry et al. 1988; Brown and Trick 1992; Rueter and Unsworth 1991) suggests that alterations in iron availability do not directly relate to changes in growth potential. The ability of cyanobacteria to vary cellular iron requirements (ie. utilizing flavodoxins instead of ferredoxins) as well as to produce siderophores affects the apparent Q_{Fe} of the cells.

Other physiological factors such as nitrogen source (ie. NO_3^-, N_2 or NH_4^+) directly affect the physiological requirements for iron as the activation of nitrogen assimilating enzymes places an increased iron demand on the cell. Calculations by Morel et al. (1991) suggest that utilization of NO_3^- instead of NH_4^+ will increase cellular iron requirements in *Thalassiosira weissflogii* by 13 amol $cell^{-1}$, an amount greater than 15% of the total cellular iron. Further calculations suggest that N_2 fixation requires a further 1.6 times as much iron as NO_3^- reduction (Raven 1988).

Measured quotas for some oceanic phytoplankton have, however, been significantly lower than the calculated minimum requirements for Fe catalysts, emphasizing the difficulty in determining iron requirements (Morel et al. 1991; Raven 1988).

1.4 Iron-Limited Cyanobacterial Physiology

Perhaps the most obvious manifestation of iron-limitation in cyanobacteria is the associated chlorosis (Boyer et al. 1987). The specific changes associated with pigment content (and absorption maxima) were first noted by Öquist (1971, 1974a,b). These variations were later confirmed in *Anacystis nidulans* as well as identified in *Agmenellum quadruplicatum* by a variety of researchers who expounded the results (Peschek 1979; Hardie et al. 1983a; Sherman and Sherman 1983; Guikema and Sherman 1984). Due to the involvement of iron in the catalyses of pigment synthesis, the decrease in chlorophyll·cell^{-1} as well as phycocyanin·cell^{-1} seen in *A. nidulans* and *A. quadruplicatum* (Peschek 1979; Hardie et al. 1983) was expected. Boussiba and Richmond (1980) have suggested that the degradation of cellular phycocyanin may be only a secondary effect of iron-limitation; nitrogen deficiency caused by a reduction in the level of iron-containing enzymes required for nitrogen assimilation may cause the cells to degrade phycocyanin pools and utilize them as a source of N.

Guikema and Sherman (1984) further showed an alteration in pigmentation changes as an increase in the phycocyanin to chlorophyll ratio, suggesting that some pathways may be more strongly affected than others. The decrease in cellular chlorophyll levels due to iron-limitation has been confirmed in the natural environment, as Murphy and Lean (1975) showed a decrease to one-third the control level of chlorophyll in field studies.

Iron-limited growth has also been shown to bring about specific changes in components of the electron transport chain. By culturing *Aphanocapsa* 6714 at 10% of the control level of iron, Sandmann and Malkin (1983) were able to bring about a switch from iron containing ferredoxin to the non-iron containing flavodoxin in this phytoplankton's electron transport chain. A further reduction, to 1% of the control iron level, brought about a reduction in all the iron-containing photosynthetic redox proteins.

Iron deficiency also leads to a number of morphological changes in cyanobacteria. A size decrease in *Anacystis nidulans* R2 to between ½ and ⅓ of the iron-satiated cell length has been documented (Sherman and Sherman 1983). Gorham et al. (1964) similarly showed a variation in size as well as a pronounced filament coiling in iron-deficient cultures of *Anabaena flos-aquae*.

Electron microscopy has allowed for the identification of a number of iron-deficiency induced changes (Hardie et al. 1983b; Sherman and Sherman 1983). A pronounced rearrangement of the thylakoids, culminating with their degradation as well as the degradation of the cytoplasmic membrane has been seen in *A. quadruplicatum* and *A. nidulans*. A depletion of ribosomes and peripheral lipid bodies as well as an increase in glycogen storage bodies has also been seen. *A. nidulans* has also been reported to decrease its number of cellular carboxysomes (Sherman and Sherman 1983) although no coordinate alteration was seen in *A. quadruplicatum* (Hardie et al. 1983). Similar analysis in the filamentous cyanobacterium *Calothrix parietina* showed no obvious

changes in carboxysome formation during iron-limitation although there was an unrelated formation of colourless, multicellular hairs and the development of false branching (Douglas et al. 1986). An increase in heterocyst frequency was also seen in *C. parientina*, but this contradicts other reports that iron deficiency decreases heterocyst formation in the nitrogen-fixing cyanobacterium *Anabaena catenula* (Rooney and Trick 1993).

Another set of changes often associated with low nutrient availablitiy is the production of stress specific proteins in specific membrane or cell fractions. Factors such as salinity (Apte and Bhagwat 1989), oxidative stress (Mittler and Tel-Or 1991), heat shock (Borbely et al. 1985), as well as magnesium, calcium and phosphate (Scanlan et al. 1989) limitation have been shown to bring about the induction of specific proteins in cyanobacteria. Iron-limitation has also been implicated as a potential inducer of protein production. Guikema and Sherman (1984) noted the presence of an iron-limitation inducible 34 kDa protein in *A. nidulans*, similar in size to a siderophore receptor found in *Escherichia coli*. Such proteins have been implicated as potential ferrisiderophore transport proteins (see High-Affinity Transport Systems).

1.5 Microbial Iron Acquisition

The ability of microorganisms to synthesize iron sequestering compounds (siderophores), and actively transport them into cells has been well studied in eubacterial and fungal systems. Siderophores (greek: σιδερος {=siderous} iron,

φορευς {=phorus} bearer) are low molecular weight (400-1200 Da), iron-binding compounds (siderophore + Fe^{3+} = ferrisiderophore complex) which facilitate the transport of ferric ions into cells during periods of iron-deficiency. All aerobic and anaerobic bacteria and fungi (with the exceptions of *Lactobacillus* spp., *Legionella* spp., and *Sacchromyces* spp.) appear to produce siderophores (Neilands and Leong 1986), including microorganisms found in marine environments (Trick 1989).

The detection of aspergillic acid production by *Aspergillus flavus* in 1947 is perhaps the first report of siderophore production (Neilands and Nakamura 1991). The isolation of ferrichrome in 1952, however, is often thought of as the original identification of a siderophore. Propagation of the smut fungus *Ustilago sphaerogena* under iron-deficient conditions gave high yields of ferrichrome (Emery and Neilands 1961). Other siderophores discovered concurrent with ferrichrome include coprogen, mycobactin, the ferroxamines and albomycin (grisein), all of which were identified around the same time (Neilands and Nakamura 1991).

Escherichia coli is capable of activating at least 5 high-affinity iron acquisition systems, each with specific siderophore and transport components associated with them (Braun et al. 1987). Other bacterial systems, such as those found in many *Pseudomonas* spp., *Bacillus* spp., and *Salmonella* spp. have all been shown to possess high affinity iron acquisition systems. The production of ferric specific, iron-regulated, low molecular iron-chelating

compounds is now a well accepted mechanism of microbial iron acquisition (Winkelmann 1991).

The growth response of cyanobacteria under iron-limiting conditions suggests that a recovery in growth rate occurs at low levels of iron availability. When iron availability drops to a sufficiently low level (e.g., below pFe 20), activation of high-affinity acquisition systems, in combination with a probable reduction in cellular iron requirements, brings about a recovery in growth. This recovery rate has been demonstrated for a number of siderophore-producing cyanobacteria in batch culture conditions including *Synechococcus* sp. PCC 7942, *Anabaena variablis*, and *Oscillatoria tenuis* (Kerry 1988; Brown and Trick 1992) (Figure 2). Iron acquisition in iron-replete environments has been suggested to be driven primarily by diffusion of Fe^{3+} along a diffusion gradient into the cells via porin channels in the outer membrane, with decrease in growth rate concomitantly associated with a proportional decrease in iron concentration. In systems where no high-affinity is found (ie. *Plectonema boryanum*), this growth rate decreases to zero as iron levels drop (Kerry, 1988). The presence of a high-affinity system changes the predicted growth rate in iron-limited cultures, with an actual increase in growth rate being observed (Figure 2). The ability of cyanobacteria to produce siderophores has been known for some time. Murphy et al. (1976), Estep et al. (1975) and Simpson and Neilands (1976) were among the first to demonstrate that cyanobacteria were capable of siderophore production during iron limitation (Table 2). These

Figure 2. Affect of iron on the growth rate profiles of cyanobacteria. The growth of cyanobacteria in batch culture over a range of iron concentrations (X-axes presented as pFe values) demonstrates that cultures capable of producing siderophores show recoveries in growth at levels where siderophores are produced. *Anacystis nidulans*, *Anabaena variablis* and *Oscillatoria tenuis* have been shown to produce extracellular iron chelators while no such compounds have been detected in iron-deficient *Plectonema boryanum* cultures (from Kerry 1988; Brown 1991). Values are in doublings d^{-1} (± S.E.)

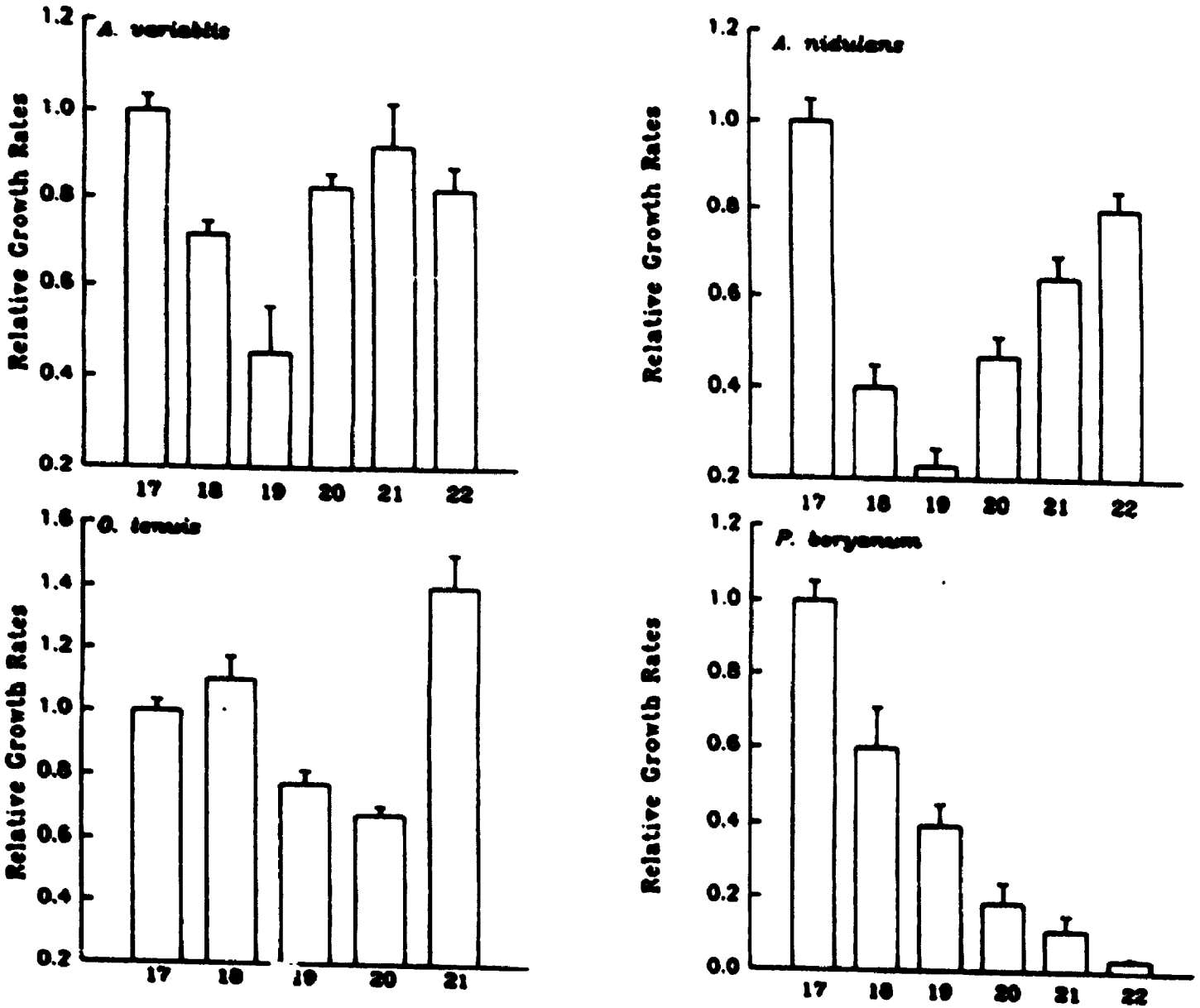
A. variabilis
A. nidulans
O. tenuis
P. beryanum
Relative Growth Rates
17
18
19
20
21
22

Table 2. Previously reported siderophore production by cyanobacteria.

ESTEP et al. 1975.
-Examination of cyanobacteria from near shore waters
-Produced a hydroxamate-type siderophore

MURPHY et al. 1976.
-Examined relationship between iron and nitrogen-fixing cyanobacterium
-Found a hydroxamate-type siderophore

SIMPSON AND NEILANDS 1976.
-Isolated dihydroxamate-type siderophore

ARMSTRONG AND VAN BAALEN 1979.
-Survey of marine cyanobacteria
-Most produced hydroxamate-type siderophores
-one (*Synechococcus*) produced a chloroform-soluble hydroxamate

LAMMERS and SANDERS-LOEHR 1982.
-siderophore-mediated iron uptake

GOLDMAN et al. 1983.
-Production of Schizokinen in *Anabaena*

CLARKE et al. 1987.
-Siderophore production and its affects on toxic copper

KERRY et al. 1988.
-Hydroxamates from *Synechococcus* and *Anabaena*

MAHASNEH 1991.
-Siderophore production in *Rivulariaceae*

HUTCHINS et al. 1991.
-Hydroxamate from *Synechococcus*

BROWN and TRICK 1992.
-Hydroxamates from *Oscillatoria tenuis*

TRICK AND KERRY 1992
-siderophores from *Synechococcus* and *Anabaena*

studies have demonstrated that a wide variety of cyanobacterial species are capable of producing hydroxamate-type siderophores. These siderophores utilize hydroxamic acid moieties to coordinate iron molecules (Figure 3). While detection of these iron chelators has been quite common, detection of iron-chelating catecholate-type siderophores has only been reported in one instance (Brown and Trick 1992). As of yet, no reports of atypical-type (recently termed "complexone-type") siderophore production by cyanobacteria are in the literature. These compounds utilize carboxyl-, alkyl- and keto- moieties to coordinate iron chelation. This group also contains the class of siderophores termed phytosiderophores, which are a novel class of higher plant siderophores based on diaminobutyrate and the amino acid azetidine. Members of this group are commonly secreted from plants roots and include avenic acid from oats, 3-hydroxymugenic acid form rye, and mugenic acid as well as distichonic acid A from barley (Bienfait 1987).

1.6 Detection of Siderophores

Isolation of iron chelators from aquatic environments has been approached with a variety of techniques. The utilization of a variety of ion exchange HPLC technology (Speirs and Boyer 1991), as well as the popular use of a variety of XAD resins (XAD-2, XAD-4, XAD-7, XAD-8), has brought some success in the isolation of iron chelators (Yamamoto et al. 1992 [XAD-7]; Brown 1992 [XAD-2]).

Figure 3. The molecular structure of typical siderophores and the associated functional groups. **A)** Representation of the different functional moieties associated with specific siderophores. In each case, coordination of iron requires electrostatic alignment of the Fe with six oxygen. **R-**: non-specific carbohydrate chains or structures. **B)** Enterobactin (catechol-type siderophore). **C)** Rhodotorulic acid (hydroxamate-type siderophore). **D)** Rhizobactin (atypical-type siderophore). **E)** Schizokinen, the only characterized cyanobacterial siderophore (from *Anabaena* sp.), is a hydroxamate-type iron chelator (Matzanke 1991).

A.

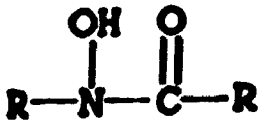

Hydroxamate Moiety

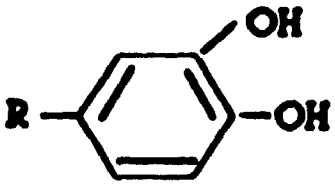

Catechol Moiety

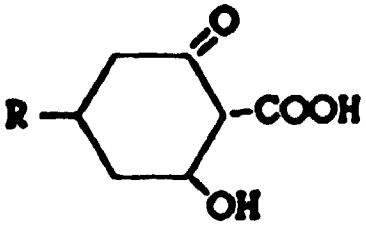

Atypical Moieties

B.

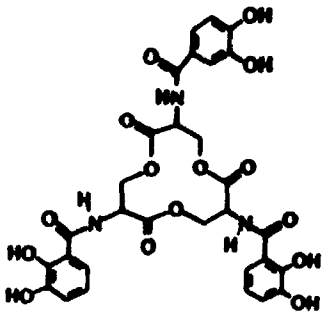

C.

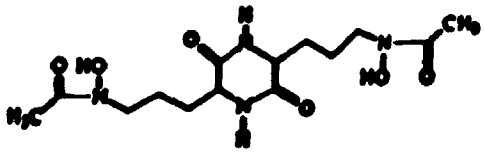

D.

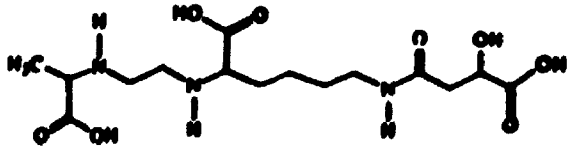

E.

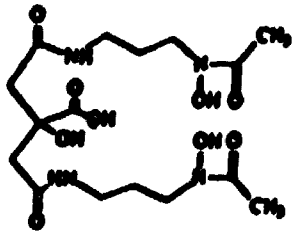

A variety of chemical methods for siderophore detection exist. Colourimetric analyses allow not only for the determination of siderophore production, but also allow for a semi-quantitative resolution of the rate of synthesis. The chrome azural S (CAS) assay of Schwynn and Neilands (1987) has been developed as a general test in order to identify any iron-sequestering compounds produced by cells grown on either plates or in liquid medium. More conventional chemical tests are available however to identify the specific types of siderophores. The test of Arnow (1937) utilizes the nitrite-molybdate reaction in order to detect catechol-type siderophores while the modified Czaky test (Gillam et al. 1981) uses acid cleavage to assay the hydroxamates (Figure 3) that are associated with some siderophores.

A variety of useful but limited biological tests of siderophore production also exist. In these tests, microbial mutants which require, but do not produce, siderophores are provided with a putative siderophore. Growth response of the bioassay organism is then guaged against the application of a specific, isolated siderophore. *Escherichia coli* RW193 (Neilands 1981), *Salmonella typhimurium* enb-1 (Luckey et al. 1972) and *Salmonella typhimurium* enb-7 (Pollack et al. 1970) are common bioassay organisms to detect an external supply of catecholate siderophores. Similarly, *Arthrobacter flavens* JG-9 is an obligate auxotroph for hydroxamate-type siderophores (Neilands 1984). These bioassays are limited. Not all siderophores are detected with these methods.

A final technique for determining the presence of siderophore production

is the EDDA bioassay (Kerry 1988). Ethylene diamine di-(o-hydroxyphenyl acetic acid) [EDDA] chelates iron with an affinity constant approaching 10^{30} (Kroll et al. 1957). This is substantially higher than other commonly used commercially available chelating agents such as EDTA (ethylene diamine tetra-acetic acid $K_A \approx 10^{16}$), which also has affinities for other divalent cations, such as Ca^{2+}. This assay utilizes EDDA in a competition with the organism's natural iron acquisition systems, giving an interspecies comparison of iron-sequestering ability based on the concentration of EDDA at which growth no longer occurs .

1.7 High-Affinity Transport Systems

The presence of high-affinity iron transport systems in microorganisms is generally based on the identification of the specific components involved in siderophore-mediated iron transport. Transport of siderophores into cells has been attributed to membrane associated, ferrisiderophore specific proteins. These proteins are required in any membrane fraction or compartment which the intact ferrisiderophore complex is transported into or through. Neilands (1977) summarized the transport of aerobactin into Enterobacteria (Figure 4) in a model that is still the basis for iron transport schemes in microorganisms.

Examinations of the induced or enhanced expression of membrane specific proteins in cyanobacteria during periods of iron-limited growth has focused primarily on the alterations that occur in the photosynthetic machinery. Guikema and Sherman (1983, 1984) have determined the effects of iron

Figure 4. The two iron-acquisition systems of microorganisms (Neilands 1977). When the concentration of extracellular, free ferric iron is high, organisms obtain sufficient iron to supply their cellular requirements by simple diffusion of iron through the porin channels in the outer membranes. When cells encounter a situation of iron-deficiency, a high-affinity system for iron assimilation is activated and its components expressed. These systems are comprised of specific carriers for iron ("siderophores"), and their cognate membrane receptors.

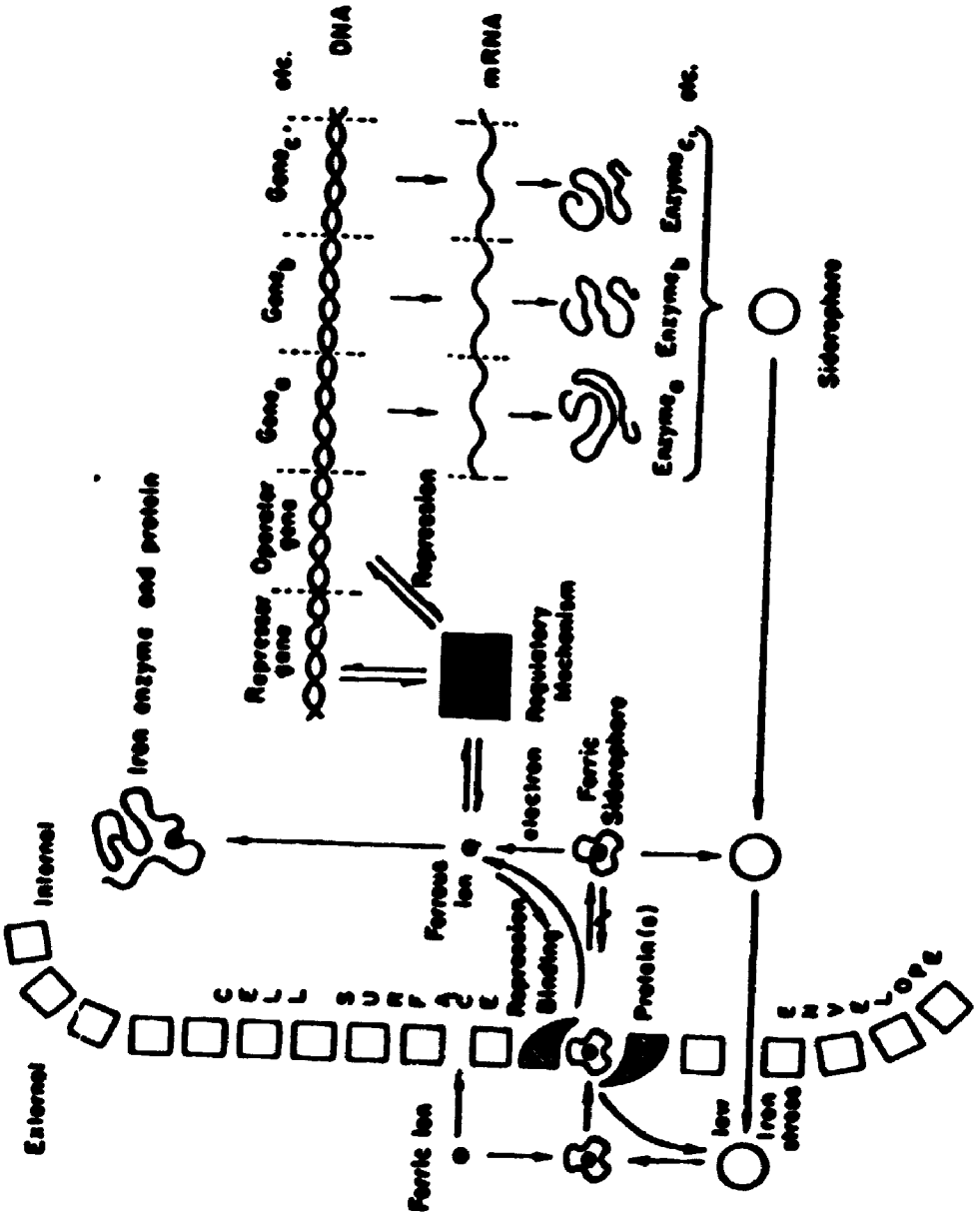
External
Internal
Iron enzyme and protein
Ferric ion
Ferrous ion
Reduction
Blocking
Protein(s)
Low iron stress
Ferric Siderophore
Repressor gene
Operator gene
Gene a
Gene b
Gene c
etc.
DNA
Repression
Repressor
mRNA
Enzyme a
Enzyme b
Enzyme c
etc.
Siderophore

starvation (not limitation) on the thylakoid membranes of *Anacystis nidulans* R2 and *Synechococcus cedorum* (UTEX 1191), two freshwater coccoid cyanobacteria. Work by Scanlan et al. (1989) demonstrated the effect of iron-limited batch culture growth on the outer membrane profile of *Synechococcus* PCC sp. 7942 (aka. *Anacystis nidulans* R2). Their findings suggested that this cyanobacterium is capable of producing a variety of outer membrane proteins in response to iron-deficient growth. They concluded (owing to the detection of hydroxamate-type siderophore production in this cyanobacterium by Kerry et al. 1988) that *Synechococcus* sp. PCC 7942 may harbour a high-affinity iron acquisition system similar to that found in eubacteria.

Changes in polypeptide composition the photosynthetic apparatus have also been examined by an analysis of the spectral peaks of the associated pigments. Iron-deficiency induces an *in vivo* shift of the main red chlorophyll^a absorbance peak (from 679 nm to 673 nm) in *Anacystis nidulans* (Öquist 1971), as well as a similar *in vitro* shift in isolated lamellae (Öquist 1974a,b). Shifts of such nature are attributed to changes in the protein-pigment association as a result of nutrient deprivation.

Although the production of extracellular siderophores by cyanobacteria has been utilized as evidence for high-affinity iron transport, it remains to be determined if cyanobacterial siderophores function to increase the affinity of cyanobacteria for iron. Demonstration of this would not only confirm that these extracellular chelators are functioning as true siderophores, but also provide

strong evidence to support the contention that cyanobacterial iron-siderophore transport systems are truly high-affinity in nature.

It is thus important to distinguish between high-"affinity" and high "velocity" nutrient uptake systems. The affinity of a system is a reflection of that systems attractiveness for the nutrient in question. High-affinity nutrient transport systems are thus those systems within organisms which, when induced, will increase the organisms ability to utilize the pool of the nutrient within the environment. In the case of iron, speciation in the environment renders the majority of iron biologically unavailable to organisms utilizing conventional diffusion-mediated iron acquisition systems (Sections 1.2, 1.3). For an organism to utilize the biologically unavailable pool of iron in the system, it must change its ability to attract iron so as to increase its ability to scavenge it. High-affinity iron acquisition systems may therefore be defined as any inducible systems which allow organisms to tap into the pool of biologically unavailable iron.

These systems further function to increase the organisms ability to scavenge the available Fe^{3+} which is already available in the environment. This results in a shift in the $Fe(OH)_3$ -----→ Fe^{3+} + $3OH^-$ equilibria to the right which renders more Fe^{3+} available. This utilization of the previously biologically unavailable iron is of importance to the ecosystem as a whole as it increases the amount iron in the biological iron cycle allowing for the iron to be ultimately available to the other organisms in the system.

1.8 Alternative Iron Transport Mechanisms

Although some plants have been shown to release or utilize iron chelating compounds, a variety of alternate mechanisms are utilized by plants in order to acquire iron from their environment. The release of organic acids or protons (via an inducible ATPase dependant proton pump), as well as the preferential uptake of cations has been proposed as mechanisms by which organisms may decrease the pH in the specific environment around itself. Such a drop in pH makes more iron biologically available to the organism (Bienfait 1987). Changes in the pH of aquatic environments driven by iron-limited algae have yet to be determined. This arises from the difficulty of monitoring such a factor in a closed batch culture environment, where the utilization of nutrients, decreases in the concentration of CO_2, and fluctations in cell density would perturb the measurements. Only work in a continuous culture system would allow for an appropriate determination.

Another mechanism involves an accumulation of citrate driving NADP to a highly reduced state. This system (termed "Turbo Reductase") then functions using a surface associated reductase which utilizes the buildup of NADPH as an electron pool. In such a system, citrate is known to accumulate in the roots, where it is thought to function in proton extrusion. It may also however be converted to isocitrate by mitochondrial aconitase and the isocitrate act as an electron donor to $NADP^+$ via isocitrate dehydrogenase (Critchon 1991). This system is however severely constrained by its dependence on a variety of

external factors, and often leaves critics questioning its feasibility to the host. Due to its systemic complexity, it may be almost completely ruled out as a possible cyanobacterial mechanism for iron acquisition.

The utilization of a reductase-type system has been suggested for nutrient scavenging in an *Anabaena* sp. (Boyer and Morse 1992). The system involves the activity of a surface associated B_6 reductase which liberates organically associated iron and allows for its assimilation into cells.

1.9 Nutrient-Limited Culturing of Algae

The growth of algae and cyanobacteria under nutrient-limited conditions has been attempted in a number of ways. Nutrient-limitation suggests a situation where organisms are limited in their growth potential by the flux of a single nutrient. Growth experiments have been utilized to determine the effect of other nutrient manipulations on cyanobacteria. Complete removal of a nutrient from a non-limited culture to look at its effect on the cells (starvation) provides data about a culture with a different previous nutrient history (see Hardie et al. 1983a,b). Such a situation occurs when exponentially growing cells are transferred from a nutrient-replete culture to a nutrient-deficient culture. In order to abolish the effects of starvation, researchers often take batch cultures through several subcultures in medium of the specific test nutrient level prior experimentation. This protocol still results in a nutrient flux; upon the initial inoculation of the culture, the level of nutrient is non-limiting and the

cell density low. Over time, the cell density will increase and the level of available nutrients in the culture decrease. The culture is thus not exposed to a static level of limiting nutrient, but instead to a transient level. This situation is further complicated by the lysis of nonviable cells and the subsequent remobilization of nutrients that occurs.

In order to avoid the perturbations that are commonly associated with batch culture techniques, the utilization of continuous culture "chemostat" systems has gained popularity for the study of nutrient-limited growth. Chemostat systems supply a continual amount of fresh, nutrient defined medium to an enclosed culture system, while at the same time providing for the maintenance of a constant volume within the chemostat reactor through the removal of spent medium and cells. Upon addition, the medium is mixed rapidly and thoroughly with the culture by vigourous stirring and bubbling with air or an air/CO_2 mixtures, providing homogeneous distribution of the limiting nutrient to the cyanobacteria.

The dilution rate of the chemostat D (d^{-1}), is defined as $D = f/v$, where f represents the flow rate of fresh medium into the chemostat reactor and v the volume of that reactor. The change in cell numbers within the reactor, dx/dt, is a function of the growth rate μ (d^{-1}), and the dilution rate such that $dx/dt = (\mu - D)X_t$, where X_t is the cell density within the reactor at a given time t. If the dilution rate of the reactor is less than the maximum growth rate of the cells (μ_{max}), then the reactor will eventually reach an equilibrium point where

dx/dt=0, and remain in steady state (ie. no change in cell number). At this point, all cells in the chemostat are growing at a rate equal to the dilution rate:

$$dx/dt = (\mu\text{-}D)\, X_t$$

$$\text{if } dx/dt = 0, \text{ then } (\mu\text{-}D)\, X_t = 0$$

$$\text{therefore as long as } X_t > 1,$$

$$\mu\text{-}D = 0 \text{ and thus } \mu = D$$

Thus, at any dilution rate at which the chemostat is capable of reaching equilibrium, one knows the precise growth rate of the culture. It is important to note, however, that when $D > \mu_{max}$, the culture is unable to maintain itself within the chemostat reactor and washout occurs (for reviews on chemostat kinetics and dynamics see Droop 1962, 1968; Rhee et al. 1981)

Growth of algae in chemostats has been utilized by a number of researchers in order to look at the effects of specific limitations on algal growth. The requirements of a number of algae for vitamin B_{12} including *Monochrysis lutheri* (Droop 1968), *Isochrysis galbana* and *Thalassiosira pseudonana* (Swift and Taylor 1974) have been examined in this manner. Monod (1950) was able to show that Michaelis-Menten kinetics applied as equally well to nutrient uptake as to enzyme activity. Such calculations have now been completed for the binding, uptake and utilization of nitrate and phosphate by algae in chemostat and cyclostatic systems (NB: cyclostats are chemostats where a light cycle is employed) (reviewed by Rhee et al. 1981). Recent work has also utilized chemostats to examine the effect of inorganic carbon levels on photosynthesis (Bloye et al. 1992; Miller et al. 1984).

2. METHODS AND MATERIALS

2.1 Strains and Growth Conditions

Synechococcus sp. PCC 7002 (*Agmenellum quadruplicatum* PR6) was obtained from D. Bryant (Pennsylvania State University) and cells were grown in modified A$^+$ medium (D. Bryant, pers. comm.) at 37°C and under a photon flux of 85 µmol m^{-2} s^{-1}. With the exception of the stock solutions of iron, vitamin B_{12} and trace metals, all waters and nutrient stocks were first treated with Chelex-100 (Price et al. 1989) to remove residual iron. Water was obtained for the Chelex treatment from a Milli-Q water treatment system (Millipore). All glassware utilized for iron-limited growth experiments was acid washed (≈1.0 N HCl) and rinsed with Chelex-treated water prior to use.

Modified A$^+$ medium was prepared in two main components (*i.* salts, *ii.* nutrients, Table 3), autoclaved, and combined to provide the indicated levels. Filter sterilized vitamin B_{12} and trace metals (*iii.* "trace" components) were then added. Filter sterilized, $FeCl_3$ (5.83 mM in 0.1 N HCl) was added to generate a concentration range of 4.2×10^{-5} M to 5.1×10^{-9} M total iron, with each increment differing by approximately one order of magnitude.

Other cyanobacterial strains, which were examined for the ability to produce siderophores under iron-limiting conditions, were batch grown in either the modified A$^+$ medium (for marine strains) or in a modified BG11 medium (for

Table 3. Concentration of components in A^+ medium. All nutrients and salts were made into concentrated stock solutions prior to the preparation of the three component stocks for A^+ synthesis. Values represent final concentrations in growth medium.

i. Salts	*ii.* Nutrients	*iii.* Trace
3.10×10^{-1} M.....NaCl	3.70×10^{-4} M.....KH_2PO_4	
8.00×10^{-2} M..... KCl	8.05×10^{-5} M.....Na_2EDTA	A) 500 mg/L Vitamin B_{12}
2.00×10^{-2} M.....$MgSO_4$	1.18×10^{-2} M.....$NaNO_3$	B) 1 mL Trace metal stock
2.45×10^{-2} M.....$CaCl_2$	8.76×10^{-3}M.....TRIS (pH 7.8)	

Trace Metal Stock

Metal Source	g L^{-1} in Stock
H_3BO_3	34.26
$MnCl_2 \cdot 3H_2O$	4.320
$ZnCl_2$	0.315
MoO_3 (35%)	0.030
$CuSO_4$	0.003
$CoCl_2 \cdot 6H_2O$	0.012

freshwater strains: Rippka et al. 1979 as modified by Brown 1991) as described in Table 4. Similar techniques were utilized in the culturing and analysis of these cyanobacteria.

The availability of free ferric ions in all media was calculated using the computer program Mineql+ ver. 2.1 (Environmental Research Software, Edgewater, MD.). Speciation of elemental components was determined via a series of algorithmic calculations, and solubility estimates made according to the lowest free energy state(s) of the system. The concentration of Fe^{3+} was converted to pFe values.

Water jacketed, thermostated, column chemostats, with working volumes of 400 mL, were maintained at a dilution rate of 0.6 d^{-1} using a multistatic pump (Buchler Instruments) to control the dilution of the culture chamber with fresh medium. Homogeneous distribution of the cells was achieved by continuous injection of sterile, filtered air. Sampling of chemostat cultures was achieved through a sampling port built into the chemostat system (Figure 5). Approximately 5 mL of sample were taken and utilized for the various daily procedures (cell density, pigment levels, pH). For all experiments, results for chemostat data were for $n \geq 3$ trials (unless stated).

Work in batch culture was carried out using 250 mL Erlenmeyer flasks containing 50 mL of medium. Cells were subcultured during exponential growth into the appropriate medium prior to experimentation in order to ensure that the cellular iron status truly reflected the desired environmental iron concentration

Table 4. Cyanobacterial species and specific medium for their culture and the isolation of siderophores. A list of cyanobacterial strains and appropriate collection codes. All strains (unless stated) were in the laboratory at the onset of the project. PCC: Pasteur Culture Collection. UTEX: The Culture Collection of Algae at the University of Texas at Austin. WH: Woods Hole Oceanographic Institute Culture Collection.

Strain	Source	Medium
Synechococcus sp. PCC 7002	D. Bryant	Modified A$^+$
Synechococcus sp. PCC 6301		Modified BG11
Synechococcus sp. PCC *6803*		Modified BG11
Synechococcus sp. PCC *6908*		Modified BG11
Synechocystis sp. PCC 7942		Modified A$^+$
Synechococcus sp. WH 8101	J. Waterbury	Modified A$^+$
Synechococcus sp. WH 7805	J. Waterbury	Modified A$^+$
Synechococcus sp. BBC2A	C. Suttle	Modified A$^+$
Oscillatoria tenuis Ag. UTEX 428		Modified BG11
Anabaena catenula UTEX 375		Modified BG11

Figure 5. Schematic design of chemostat system. Continuous culture chemostats, with working volumes of 400 mL, were established in water-jacketed glass vessels. Medium flux (0.6 vol d^{-1}) from the reservoir was maintained by the action of a peristaltic pump. Chemostat reactor temperatures were maintained at 37°C by a thermostated water pump circulating water through the outer glass jackets. Cells were maintained under a constant a constant light level (85 $\mu E\ m^{-2}\ s^{-1}$).

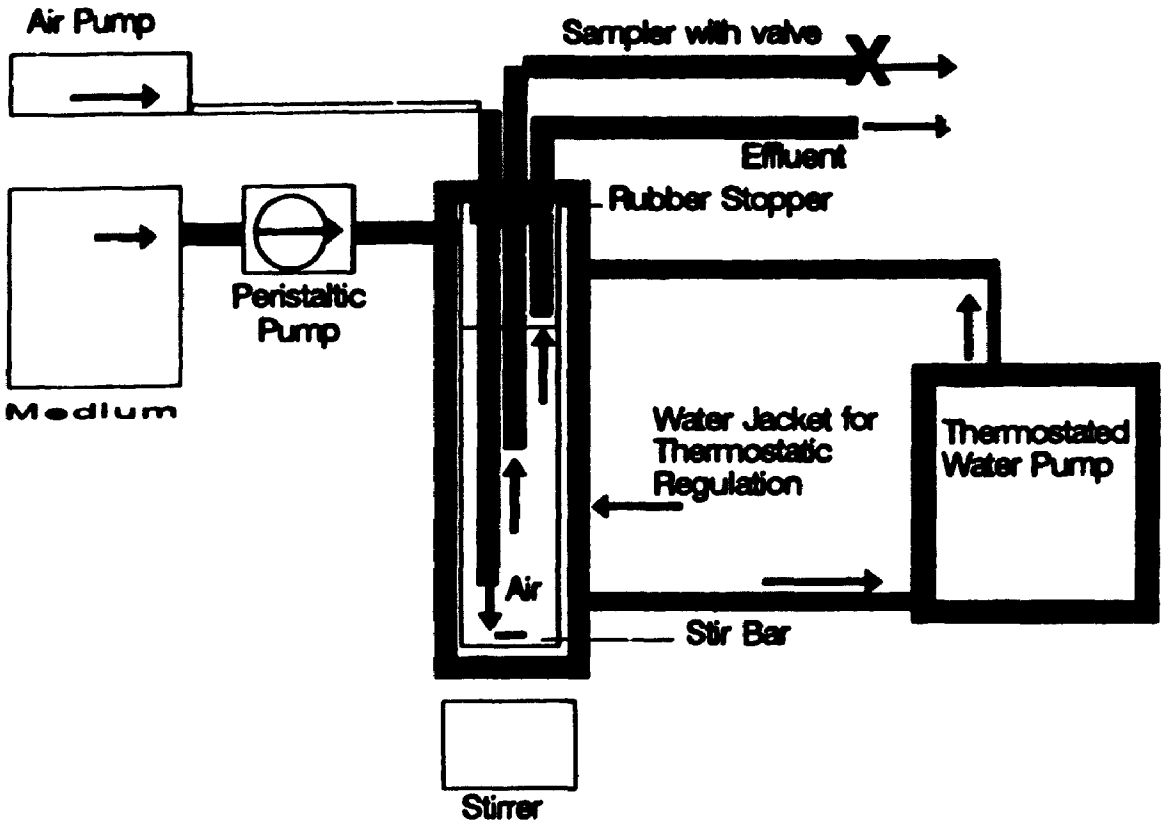
Air Pump
Sampler with valve
Effluent
Rubber Stopper
Peristaltic Pump
Medium
Water Jacket for Thermostatic Regulation
Thermostated Water Pump
Air
Stir Bar
Stirrer

and was not an artifact from a previous growth condition. Flasks were maintained on a orbital shaker at 38°C, under a photon flux of 85 μmol m^{-2} s^{-1} In order to isolate a sufficient quantity of siderophore for characterization, 8 L batch cultures of cyanobacteria were established in 9 L glass carboys. Cultures were bubbled with filtered air and circulation maintained by continuous stirring.

2.2 Analysis of Chemostat Yields and Growth Rates

I. Chemostats. In order to expediently sample cultures, a standard relationship between cell density and absorbance at 750 nm (using a LKB 4040 Novaspec II) was established. Linear regression of the data established a relationship (an absorbance unit of 0.1 equivalent to 7.83×10^6 cells mL^{-1}) which was then utilized for the precise estimation of cell density with the spectrophotometer (Figure 6).

Daily estimates of chemostat cell concentrations were obtained from absorbance readings at 750 nm and converted to cell densities (cells mL^{-1}). Chemostat cultures were maintained for at least 2.5 cycles (4 days) after steady state growth had been established in order to guarantee equilibrium.

II. Growth Rate. Cells were preconditioned for at least two cycles of 72 hours at the test iron level prior to their subculture (5%) into flasks for growth studies. This was to ensure that cells were physiologically equilibrated to the specific iron level prior to analysis of growth. Cell densities were estimated

Figure 6. Relationship between cell density and absorbance for *Synechococcus* sp. PCC 7002. Linear regression of the relationship between cell density (cells mL^{-1} as determined by haemocytometer counts) and absorbance at 750 nm demonstrates the relationship utilized to calculate cell densities spectrophotometrically.

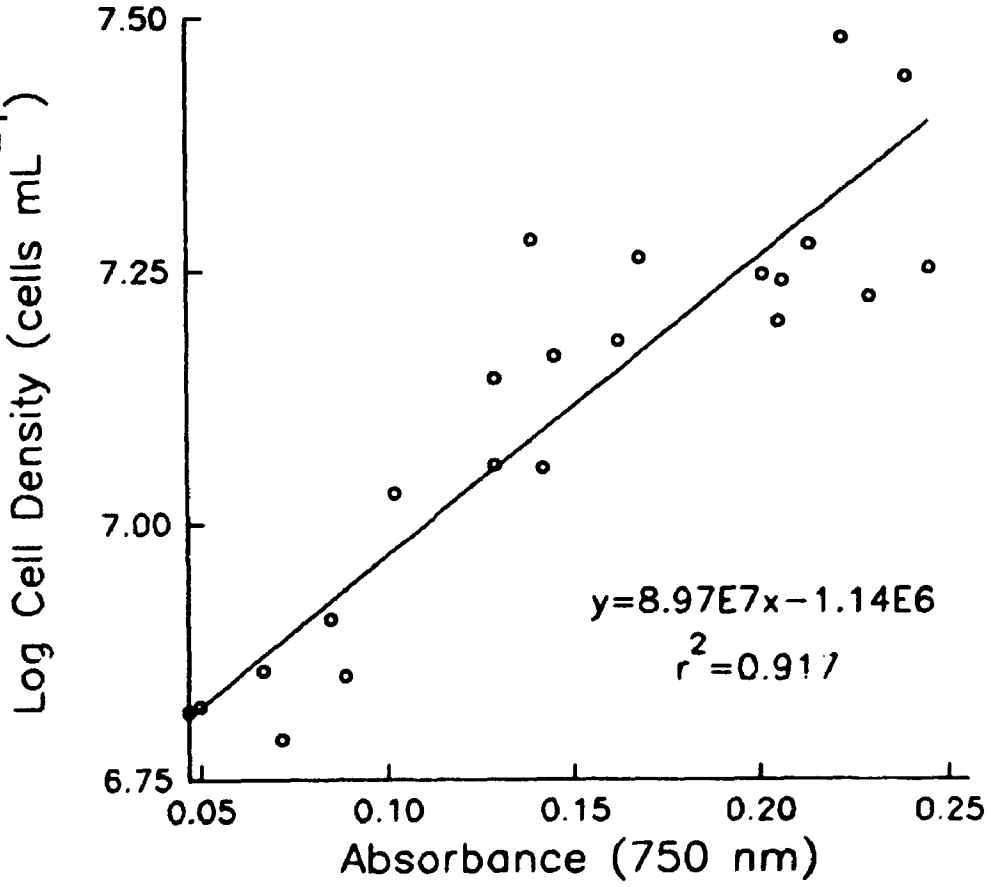
7.50
7.25
7.00
6.75
Log Cell Density (cells mL^{-1})
0.05
0.10
0.15
0.20
0.25
Absorbance (750 nm)
y=8.97E7x−1.14E6
r^2=0.917

spectrophotometrically every 6 hours at 750 nm with an LKB Biospec II spectrophotometer. Cell growth was monitored for at least 120 hours to ensure that the culture had reached stationary phase. Log normalized cell numbers were then examined with regression analysis of the exponential phase of growth and this utilized to determine specific doubling times of cells.

2.3 Whole Cell Measurement of Photosynthetic Pigments

Chlorophyll a (chla) and phycocyanin (PC) concentrations in steady state cells were estimated daily by whole cell spectra and normalized to cell biomass using the equation of Myers et al. (1980). Absorbance spectra were measured on a Shimadzu UV 160 spectrophotometer and the absorbance maxima used in pigment calculations. Shifts in the chla absorbance maxima were examined for variations between cultures under different iron regimes.

2.4 Alterations in pH

Chemostats were analyzed for shifts in hydrogen ion concentration using a Corning 215 pH meter with a Corning General Purpose Combinaiton probe. Samples removed from chemostats for pigment analysis were monitored prior to spectrophotometric analysis.

2.5 Photosynthetic Capacity and Efficiency

i. Carbon Fixation. The incorporation of carbon dioxide into cells grown under iron-replete (pFe 17) and iron-deficient (pFe 21) conditions was monitored by providing the cells with a known quantity of $NaH^{14}CO_3$. Chemo. tat grown cells were harvested by centrifugation (8,000 xg) and resuspended in fresh A* medium containing the appropriate iron level and 100 µM carbonate. Cells were dark-adapted for a period of 30 minutes prior to the introduction of 1 µCi (37 kBq = 0.119 µmol) radiotracer. After 15 minutes of dark monitoring, cells were illuminated (I = 85 µE m^{-2} s^{-1}) and photosynthetic carbon uptake monitored. A parallel set of samples was maintained in the dark in order to correct for any dark fixation of carbon into the cell.

The sampling procedure for cells involved the removal of a 1 mL aliquot of cells and filtration through 0.4 µM polycarbonate filters. Cells were rinsed with standard A* media containing 100 µM $NaHCO_3$, placed in scintillation vials and then treated with 100 µL hydrogen peroxide to degrade chlorophyll. This is an important step in the process as autofluorescence of the chlorophyll can interfere with the scintillation process when low energy emitters (such as ^{14}C) are used. Ten mL of scintillation fluid ("Ecoscint", Diamed) were then added to the samples and these were analyzed by scintillation counting after 12 hours. Results were standardized to cellular carbon turnover rates based on estimations of cell volume and mean cell carbon (vol = 1 μm^3, mean cell carbon = 125 kg C m^{-3} and 125 *f*g C $cell^{-1}$) and these values confirmed to be

approximately equivalent to the carbon per cell values of 150-290 for natural populations (Waterbury et al. 1987).

II. Oxygen Evolution. Oxygen evolution and consumption were measured in iron-replete and iron-deficient cultures of *Synechococcus* sp. PCC 7002 using a thermostated, aqueous phase Clarke-type oxygen electrode (Hansatech Ltd. King's Lynn, UK) according to the technique of Maxwell et al. (1993). Aliquots of 2 mL, with a chlorophyll density of 1-2 μg L^{-1} were brought to 4 mM with $NaHCO_3$ prior to examination. Each replicate involved the examination of a single sample through 12 different irradiances ranging form 0 to 2000 μmol photons m^{-2} s^{-1}. Actinic light from a 150 W halogen bulb was supplied via a fibre optic cable (Fibre-lite, Dolan-Jenner Ind. Rochester, NH, USA). PPFD (photosynthetic photon flux density) was measured in the middle of the cuvettes using a LICOR 185 quantum sensor. All data is reported as μmol O_2 ($cell^{-1}$) h^{-1} as well as μmol O_2 (mg chl*a*)$^{-1}$ h^{-1} (the standard method for reporting oxygen evolution rates). Apparent quantum yield (Φ_{app}) was calculated from a linear regression of the μmol O_2 (mg $chla^{-1}$) h^{-1} data for values of positive net oxygen evolution and PPFD < 250 μmol photons m^{-2} s^{-1}.

2.6 Electron Microscopy

Chemostat cultured cells were harvested by centrifugation (4,000 xg) and fixed according to the method of Burdett and Murray (1974). Thin sections were stained with lead citrate and uranyl actete (Reynolds 1963). Micrographs

were taken with a Philips EM200 electron microscope operated at an accelerating voltage of 60 kV. Exponentially growing cells from batch culture under iron-replete conditions (pFe 17) were similarly treated and utilized to compare physiological alterations that may result as a function of the specific culturing technique.

2.7 Presence of Siderophores

In order to determine extracellular siderophore concentrations in steady state chemostat cultures, cyanobacterial cells were removed by centrifugation and subsequent passage of the spent culture medium through glass microfibre filters (Whatman GF/C). Cell-free medium was concentrated (14-fold) by lyophilization in order to increase detectability. This concentrated medium was analyzed for the presence of iron chelators utilizing a number of chemical tests.

I. CAS Assay. The ternary complex, chrome azurol S-iron(III)-hexadecyltrimethylammonium bromide (CAS), was utilized as an indicator of extracellular iron-binding ligands based on a modification of the method of Schwyn and Neilands (1987). This method involves the formation of an intensely coloured iron-dye complex which, upon removal of the iron, leads to a change in colour.

$$FeDye^{3-n} + L^{k-} \rightarrow FeL^{k-} + Dye^{n-}$$

Thus the addition of a strong iron binding ligand (L: ie., a siderophore) is capable of creating a colour shift proportional to the amount of iron bound. This

procedure is standardized against the reaction of a known iron chelator (rhodotorulic acid), to generate a semiquantitative result.

The CAS assay involved the generation of a buffered test solution that was prepared and then challenged with the potential iron chelators. Six mL of 10 mM HDTMA (hexadecyltrimethylammonium bromide or CTAB) was added to an acid washed polypropylene container containing 25 mL chelex-treated H_2O. $FeCl_3$ (1.5 mL of 1 mM $FeCl_3$ in 10 mM HCl) was added prior to the addition of 7.5 mL of a 2 mM aqueous CAS solution. Ten mL of MES stock solution (0.43 g mL^{-1}, pH 5.6) was then added along with 1 mL of 10.2% 5-sulphosalicyclic acid. The 5-sulphosalicyclic acid acts as an iron "shuttle". The presence of the iron shuttle speeds up the rate of dye to ligand transfer in situations where the ligand's affinity for iron is only slightly above that of the dye. This solution was then brought to a final volume of 100 mL and utilized as the CAS test solution.

Samples, solubilized in water, were mixed 50 : 50 (v/v) with the CAS test solution and allowed to incubate for 30 min at room temperature. Samples were assayed spectrophotometrically (630 nm) and compared to a blank using H_2O to replace the potential chelator. Results are reported as a function of the following calculation:

$$ABS_{630nm}\ Blank / ABS_{630nm}\ Sample$$

Results equivalent to 1.0 suggest no iron chelating ability in the sample while those > 1.0 suggest the solution is chelating iron from the dye complex.

ii. Czaky Test for Hydroxamate-type Siderophores. The presence of hydroxamate-type siderophores was examined using the hydroxylamine production test of Czaky (1948), as modified by Gillam et al. (1981). Acid hydrolysis in 3 M sulphuric acid (4 hours at 121° C, 15 psi) cleaves bound hydroxylamine functional groups from the siderophores. The cleaved product is then oxidized with iodine to nitric acid, and reacted with sulphanilamide to produce a diazonium salt. These diazonium salts can be coupled to N-(1-naphthyl) ethylenediamine to produce an azo dye with an absorption maximum of 543 nm. Trials are blanked against a non-acidified sample in order to account for nitrite, which may interfere with the reaction. A range of hydroxylamine standards are utilized to provide a standard curve, and results are reported in hydroxylamine equivalents.

iii. Chemical Tests for Catechol-Type Siderophores. Catechol-type siderophores were quantified using two separate analyses. The Arnow test (Arnow, 1937) is specific for the detection of aromatic vic-diols in which either the 3- or 4-position is unsubstituted and not sterically blocked. The catechol moiety is nitrited in alkali to produce a complex with an intense colour. This complex is further stabilized and the colour enhanced by the addition of molybdate. The final solution is assayed at 500 nm.

The catechol determination test of Rioux et al., 1983 is not selective for specific catechols, and is based on the reduction of Fe^{3+} to Fe^{2+} by the catechols under acidic conditions. Two molecules of Fe^{3+} are reduced per

catechol, while the catechol is oxidized irreversibly to the corresponding o-benzoquinone. The addition of ammonium fluoride masks any residual Fe^{3+} after the reduction, and the Fe^{2+} generated by the reaction is then assayed in a hexamethyltetramine-buffered 1,10-phenanthroline system.

All catechol concentrations are correlated to standard curves prepared using 2,3- DHBA; results are, therefore, reported as DHBA equivalents.

2.8 Isolation of Siderophores

Extracellular siderophores were examined in the spent culture medium of low iron (pFe 21) grown cyanobacteria. The cultures were rendered cell-free by centrifugation at 8,000 xg for 20 min. Remaining cells were then removed by vacuum filtration of the culture medium through glass microfibre filters (Whatman GF/C).

The filtrate was then acidified to pH 3.0 with 12 N HCl; this allowed for the protonation of any iron chelators in the medium, so as to dissociate any ferrisiderophore complexes that may exist. The acidified medium was then passed through a column (15 cm x 3.5 cm) of Amberlite XAD-16 (Supelco), a polymeric, non-ionic absorbent of hydrophobic, cross-linked, polystyrene copolymer. This matrix adsorbs the exuded organic compounds in the spent, cell-free medium. The organic laden column was then eluted with methanol (to remove hydrophillic compounds), followed by a methanol : chloroform mix (1:1) to liberate any remaining organic compounds. Specific siderophores were

released under both elution procedures, with complete liberation possible only with methanol : chloroform (1 : 1) elution.

Methanol and chloroform were removed by rotary evaporation at 63°C. The remaining solvent and water were then expelled in a Savant SpeedVac concentrator under vacuum. Collected material was fractionated based on molecular mass and absorbance properties on a Sephadex LH-20 (Pharmacia) column (37.5 cm x 1 cm) in one of a variety of solvent systems: methanol : chloroform (90 : 10), propanol : butanol-1 : water (1 : 1 : 1), and methanol : chloroform (50 : 50) were utilized, along with other, less successful solvent mixtures. Fractions were analyzed with the CAS assay, as well as by spectrophotometric analysis at 280 nm (for potential phenolic and proteinaceous compounds) and at 405 nm (putative hydroxamate-type siderophore absorbance maxima).

In order to determine if hydrophobic, iron-chelating compounds were associated with the surface of cells, pFe 21 grown cells were harvested and then washed with a small amount of chloroform (5 mL chloroform with 20 mL wet packed cells). The chloroform component was resolved by centrifugation and examined to determine in any iron-binding compounds were present.

2.9 Thin Layer Chromatography

Whatman PE SIL G plates, with a variety of solvents, were utilized to separate the iron-binding ligands by thin layer chromatography. Organic

fractions were applied to plates utilizing capillary tubes. Samples were resolved in one of several solvent systems: propanol : butanol : water (1 : 1 : 1); butanol : acetic acid : water (25 : 15 : 60); isopropanol : water (70 : 30); methanol : water (70 : 30); chloroform : methanol (50 : 50). Iron-sequestering compounds were visualized on the plates by employing a 1.0% (w/v) $FeCl_3$ (in ethanol) spray (Brown 1991), and R_f values determined for each. In order to determine the purity of samples, plates were analyzed for organics by exposure to iodine vapour as well as examination under ultraviolet light to detect any fluorescence.

Fractions determined to contain iron sequestering compounds were analyzed by thin layer chromatography and chemical techniques. Those fractions which were to be utilized for mass spectrometric analysis were refractionated in the LH-20 column. Purity of the compounds was determined by two dimensional TLC analysis.

2.10 Chemical Ionization Mass Spectrometry

Precise mass measurements for siderophores was obtained by mass spectrometry in the Department of Chemistry, The University of Western Ontario. Purified siderophore samples (approx. 10 µg) were dissolved in methanol prior to analysis in a Finnigan MAT 9236 Mass Spectrometry Analyzer. Primary chemical ionization was accomplished with isobutane, followed by a secondary ionization of 20 *e*V, utilized for a determination of the fragmentation spectrum.

2.11 Preparation of Membrane Fractions

i. Outer Membranes. Outer membrane proteins were prepared based on the technique of Brown (1991). Cells were collected by centrifugation at 5500 xg, washed in HEPES buffer (10 mM HEPES, 5 mM NaCl, pH 7.8), and resuspended in several mL of the same buffer. Lysozyme (3 mg mL^{-1}) was added and the suspensions were incubated at 30° C for 2 h. After the addition of DNase and RNase to 5 µg mL^{-1}, and phenyl-methylsulfonyl fluoride (PMSF; included in all subsequent solutions) to 1 mM, breakage of the cells was achieved using a cell disrupter (Mini-Bead Beater, Biospec Products) with 0.1 µm glass beads. All enzymes for this were obtained from Sigma. Suspensions were pulse centrifuged (approximately 10-15 seconds) in an Eppendorf 5414 centrifuge to remove unbroken cells. Membranes were then collected by centrifugation for 30 min (4°C) in the Eppendorf centrifuge. Pellets were resuspended in 1 mL of HEPES buffer. N-Lauroyl sarcosine ("sarkosyl") was added to a final concentration of 0.5% to solubilize thylakoid and cytoplasmic membranes (Filip et al. 1973) and samples incubated at room temperature for 20 min prior to centrifugation (30 min) to pellet outer membranes. Pellets were resuspended in HEPES buffer and incubated for 20 minutes at room temperature to remove the excess sarkosyl and any remaining soluble membranes. Outer membranes were collected by a final 45 min spin in the Eppendorf centrifuge. Pellets were resuspended in 0.1% SDS and proteins quantified by a modification of the Lowry method (Hartee, 1972) The absence

of contaminating pigments from other fractions (correlated to absorbance values) is utilized as an indicator of membrane purity and was determined from UV-visible light (200-750 nm) spectra (Brown 1991). For outer membranes, chla absorbance (measured at 678 nm) was utilized to determine the presence of other membranes (Figure 7).

ii. Internal Membranes. Cytoplasmic and thylakoid membrane fractions were isolated by discontinuous density centrifugation (in sucrose) by a modification of Omata and Murata (1984). Cells were treated with lysozyme (3 mg mL^{-1} for 2 hours) and then mechanically disrupted as above. The membrane suspension was brought to 0.6 M with sucrose and the intact cells removed by a 10-15 second pulse centrifugation in the Eppendorf centrifuge. After the addition of 0.74 volumes of 90% sucrose to the supernatant (final concentration of 50% sucrose), 17 mL of the solution was placed at the bottom of a ultracentrifuge tube and successively overlayed with 8 mL of 39% sucrose, 3 mL of 30% sucrose and 7 mL of 10% sucrose. All sucrose solutions contained 10 mM TES (pH 7.8), 10 mM NaCl, 5 mM EDTA, and 1 mM PMSF. Gradients were resolved by centrifugation in a Beckman L5-50 ultracentrifuge for 16 hours at 130,000 xg and 4°C. Cytoplasmic membranes (resolved into the 30% sucrose layer) and thylakoid membranes (resolved at the 39%-50% sucrose interface) were withdrawn and diluted 5 fold with 10 mM TES (pH 7.8), 10 mM NaCl, 5 mM EDTA, and 1 mM PMSF. Membranes were collected by centrifugation at 20,000 xg. Membrane fractions were resuspended in the

Figure 7. UV-visible light spectra of sarkosyl isolated membrane fractions. Spectra of outer membrane fraction of *Synechococcus* sp. PCC 7002 isolated with N-Lauryl Sarcosine. The purity of the membrane fraction is reflected in the lack of chl*a* from potentially contaminating thylakoid membranes. **A.** Spectrum of sarkosyl insoluble fraction from 200 nm to 750 nm with peaks at 301 and 446 nm. **B.** Expansion of sarkosyl insoluble spectrum for 400 nm to 750 nm demonstrating the presence of carotenoids (446 nm) and the lack of chl*a* (678 nm) in this fraction. The identification of carotenoids at 446 nm is based on spectra from Omata and Murata, 1983. **C.** Spectrum of sarkosyl soluble membrane fractions. Peak at 674 nm (chl*a*) demonstrates the presence of thylakoid material in this fraction.

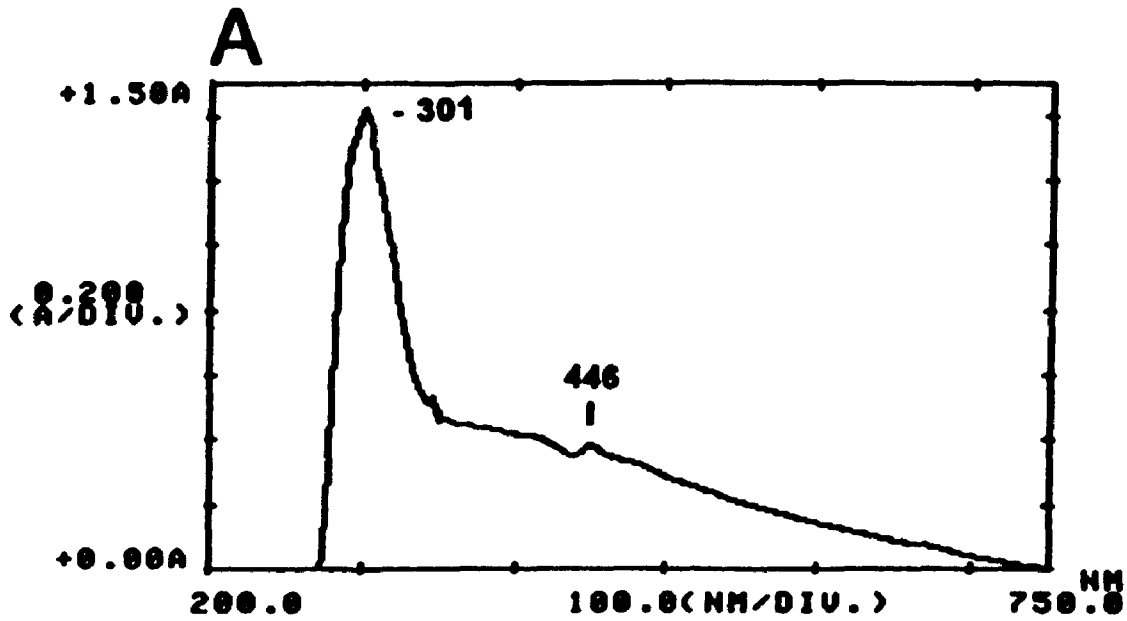
A
+1.50A
0.200
(A/DIV.)
+0.00A
301
446
200.0
100.0(NM/DIV.)
750.0
NM

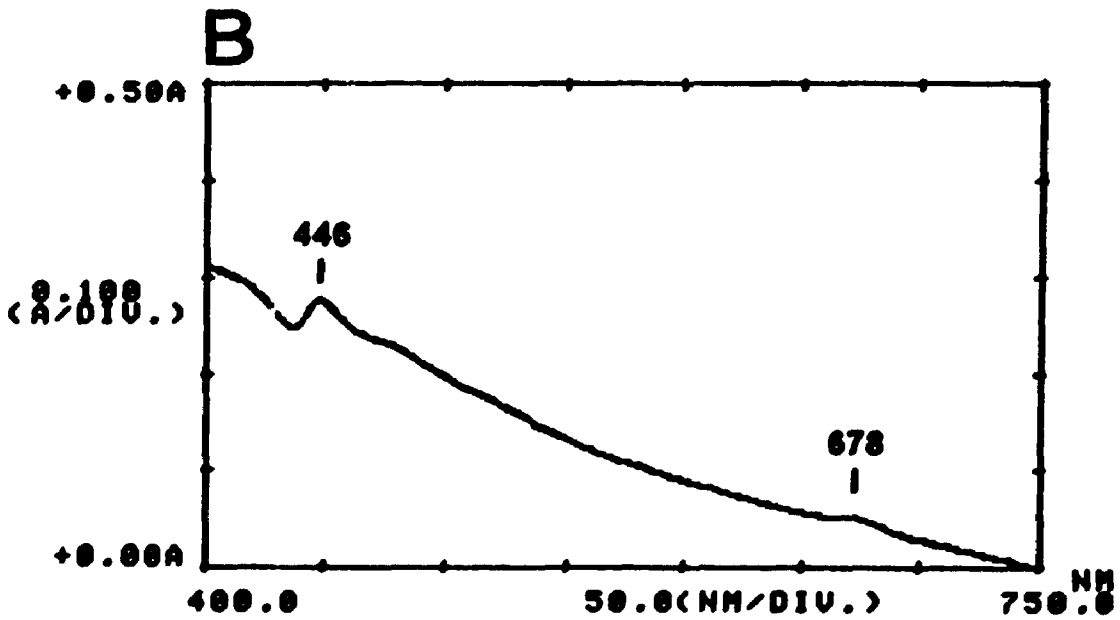
B
+0.50A
0.100
(A/DIV.)
+0.00A
446
678
400.0
50.0(NM/DIV.)
750.0
NM

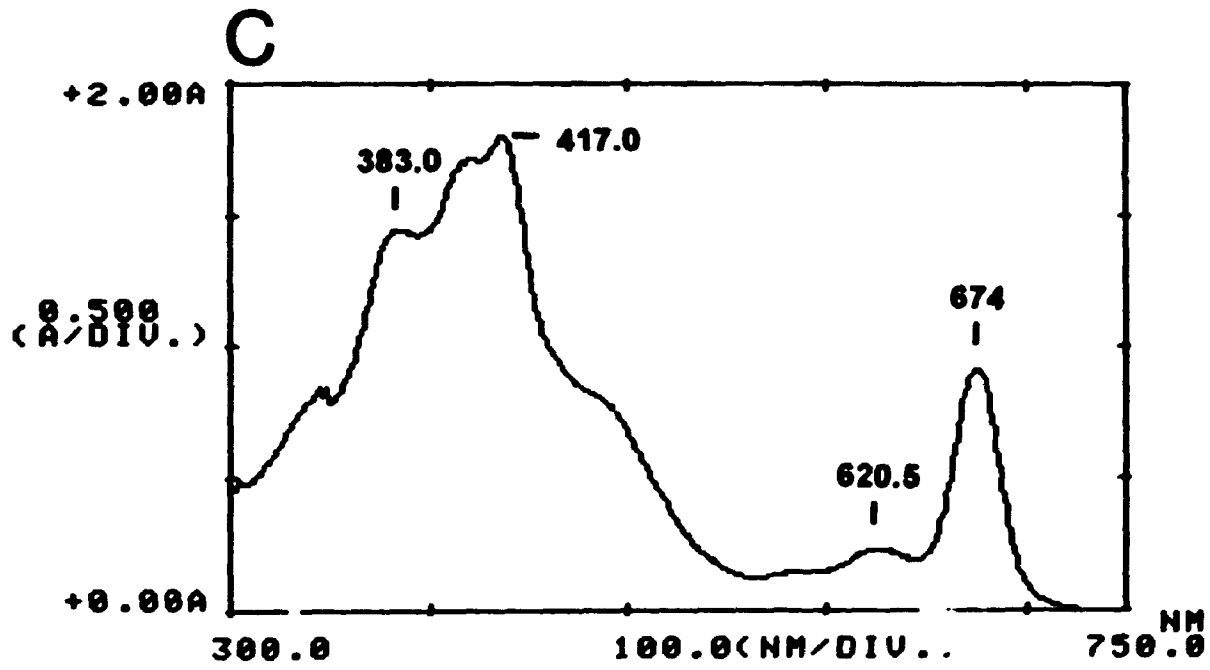
C
+2.00A
383.0
417.0
0.500
(A/DIV.)
674
620.5
+0.00A
300.0
100.0(NM/DIV..
750.0
NM

same buffer, analyzed for protein content, and stored at -20°C. The purity of all membrane fractions was assured by a visible light spectral analysis (200-750 nm)

iii. Proteins in the Periplasmic Space. To examine the proteins of the periplasmic space, the osmotic shock procedure of Neu and Heppel (1965, as modified by Brown, 1991) was employed. Chemostat grown cells were harvested by centrifugation (8000 xg) and cells quickly resuspended in 20 mL of 20% (w/v) sucrose in 0.03 M Tris (pH 7.8). Na_2EDTA was added to a final concentration of 1 mM and cells incubated for 10 min. Cells were collected by centrifugation and immediately resuspended in 20 mL of cold (4°C), chelexed H_2O. Cells were removed by centrifugation and the supernatant concentrated by lyophilization. The absence of phycocyanin in the periplasmic protein fraction (the supernatant) was utilized as an indicator that the cells did not lyse. Protein in this fraction was then quantified using the modified Lowry technique (Hartee, 1972).

2.12 SDS-Polyacrylamide Gel Electrophoresis (SDS-PAGE)

SDS-PAGE was performed using the buffer system of Laemmli (1970). Quantified protein (75 µg $lane^{-1}$) was electrophoretically resolved at 4°C in 7.5-15% polyacrylamide gradient gels (16 cm by 16 cm) and visualized first with Coomassie blue stain and then by silver staining (Merril et al. 1979).

2.13 Iron-Protein Associations

Isolated protein fractions from specific cellular components were examined to determine if any difference in iron sequestering ability was brought about by conditioning to growth-limiting levels of iron. Cells from pFe 17 and pFe 21 chemostats were harvested and the outer membrane and periplasmic components isolated as described. Material equivalent to 100 µg of protein was lyophilized to dryness and resuspended in a 8.76×10^{-3} M Tris (pH 7.8) and 8.5×10^{-5} M EDTA buffer. $^{55}FeCl_3$ (10.41 µg yielding approx. 10^7 cpm) was brought up to 900 µL in Tris-EDTA buffer. Aliquots (100 µL) of radiolabel were then dispensed to each of three protein samples. Into the first set, 25 µL of crude *Synechococcus* sp. PCC 7002 siderophore, containing all four siderophores at a total concentration equivalent to 150 µg rhodotorulic acid based on the CAS assay, was added. Crude siderophore and ß-mercaptoethanol (5 µL, 4% v/v final) was added to the second set of samples in order to disrupt the secondary structure of the proteins, and the third (control) sample was left as just $^{55}FeCl_3$/protein. All samples were then brought to 1.0 mL final volume and incubated for 30 minutes at 37°C. Samples were filtered through 0.22 µm nitrocellulose filters and rinsed with 2 mL of nutrient-free and iron-free A* medium. Filters were placed into scintillation vials and assayed after the addition of the 10 mL scintillation fluor (Ecoscint, Diamed). In order to account for the alterations in protein content that occur, results are expressed as a percent of the control iron association level.

2.14 Iron Uptake

In order to test the effects of siderophores on iron uptake in cyanobacteria, cells grown in chemostats under iron-replete (pFe 17) and iron-deficient (pFe 21) conditions were monitored for iron uptake and iron/surface associations.

Crude extracts of extracellular organics from *Synechococcus* sp. PCC 7002 were isolated using XAD-16 and quantified with the CAS assay. Fractions with an CAS determined iron-chelating equivalent of 300 µg Rhodotorulic acid were taken and used for iron uptake analysis. Cells were harvested from chemostats and resuspended in 40 mL fresh, iron-free medium, and incubated for 1 hour at 85 µE m^{-2} s^{-1} and 37° C. Cyanobacteria were then maintained for 30 minutes in the dark and the siderophore fraction added (in control samples no siderophore was added). After another 30 minutes, $^{55}FeCl_3$ (3.47 µg) was added and incorporation into the cell was monitored using a titanium(III)-citrate-EDTA (Table 5a) rinse prior to scintillation counting. The titanium wash provides for the rapid reduction and removal of any surface bound or superficially associated iron, thereby giving an accurate account of the iron incorporation into the cell (Hudson and Morel 1989). Incorporation was followed for 30 minutes in the dark followed by a one hour at 85 µE m^{-2} s^{-1}. Preliminary experiments established that this level of iron was saturating for transport, yet presented the miniumum level for detection with this system.

TABLE 5a. Composition of Titanium-citrate-EDTA wash for resolution of extracellular and intracellular iron.

COMPONENTS	AMOUNT
Na_2EDTA	4.65 g
NaCitrate	3.68 g
KCl	.187 g
NaCl	3.00 g
$TiCl_3$	7.5 mL of 1.9M (in 2 N HCl)
NaOH	Titrate to pH 7.8
H_20	***final volume 250 mL

Table 5b. Composition of saline-EDTA wash for iron-surface association analysis.

COMPONENTS	AMOUNT
Na_2EDTA	8.50×10^{-5} M
TRIS (pH 7.8)	8.76×10^{-3} M
NaCl	0.31 M
KCl	0.08 M
$MgSO_4$	0.02 M
$CaCl_2$	0.0245 M

Analysis of cell surface associations utilized the same protocol, except that cells were rinsed with a saline-EDTA rinse (Table 5b), which removes free ^{55}Fe from the surface, but not dissociate iron complexed to surface sites.

2.15 Energetics of Iron Transport

The energy requirements of iron transport were investigated in iron-replete and iron-deficient cultures by challenging cells with a variety of photosynthetic inhibitors and determining the affect on the rate of iron uptake. Comparison of light and dark rates of uptake was utilized to estimate the control (uninhibited) light driven rates of iron uptake.

Arsenate (supplied as sodium arsenate heptahydrate), 3-(3'4'-dichlorophenyl)-1,1-dimethylurea (DCMU), and triphenyl tin were utilized as chemical inhibitors of cellular energetics. Arsenate (100 µM) functions as a phosphate analog, and thus competes with phosphate during ADP→ATP photophosphorylation. Arsenate has been demonstrated to function as an inhibitor of *fur/tonB* dependant high-affinity iron and vitamin B_{12} transport in *E. coli* (Reynolds et al. 1980; Kadner 1990).

DCMU (10 µM; Sigma) functions to reduce ATP production by binding near the D_1 peptide site of photosystem II, ultimately reducing ATP production as well as decreasing the membrane potential generated by the translocation of protons. Experiments in a *Synechococcus* sp. as well as other cyanobacteria

have demonstrated that DCMU functions in a manner analagous to its effects in higher plants (Golden and Sherman 1984; Sherman et al. 1987).

Triphenyl tin (5 μM; a gift of W.G. Hopkins) functions to inhibit CF_0-CF_1 proton transfer in higher plants (Cole et al. 1981). While no literature exists on its efficiency in cyanobacteria, the conservation of the structure of the photosynthetic machinery within the cyanobacterial (in comparison to higher plants) suggests that this compound should inhibit electron transfer in a similar manner (W.G. Hopkins, pers. comm.).

Iron transport into pFe 17 and pFe 21 grown cells was monitored as above, with photosynthetic inhibitors added 30 min prior to the ^{55}Fe. Cells were rinsed with titanium(III)-citrate-EDTA to remove superficially associated iron from the surface.

Temperature was also investigated as a potential iron uptake inhibitor. Cells were harvested by centrifugation and resuspended in iron free medium. Cells were incubated for 1.5 hours at 37°C and 85 μE m^{-2} s^{-1}. The temperature of the refrigeration unit (Frigomix U-1, Johns Scientific) was then changed to 4°C and the rate of change monitored. After 50 min the temperature had stabilized at 4°C and the cells were incubated for 30 min more prior to iron uptake analysis using the titanium(III)-citrate-EDTA technique.

2.16 Determination of Cellular Iron Levels

Cellular iron quotas were determined as described by Sunda et al. (1991). In order to determine the true cellular iron quota, *Synechococcus* sp. PCC 7002 cells were precultured in appropriate iron levels, then batch cultured with $^{55}FeCl_3$ over a range of pFe values (pFe 17-21). Total iron content within the cells was monitored with the titanium-citrate technique. This allows for an establishment of the amount of iron in the cell with respect to the concentration of available iron in the growth medium. Cultures were sampled over time, and iron cell^{-1} values determined based on changes in cell number and iron content.

3. RESULTS

3.1 Speciation of Iron

In order to ascertain the availability of Fe^{3+} in the system, the concentration of different Fe-containing components within the medium was calculated over the range of iron concentrations utilized for the chemostat cultures. In all, 31 different Fe-containing components exist at concentrations greater than 10^{-100}M (Appendix I). The majority of the iron appears to be tied up in $FePO_4$ and $FeEDTA^{-4}$ complexes.

The exact changes in Fe^{3+} availability in the A$^+$ and modified BG11 media are plotted in Figure 8. Precise values at specific iron concentrations are represented by symbols, with the connecting lines representing the computer modelled functions. Results demonstrate the differences in Fe^{3+} availabilty with respect to total iron in the freshwater and marine media.

3.2 Iron-Regulated Chemostat Yields

Steady state cell densities for each iron level in chemostats are presented in Figure 9. Chemostats supplemented with iron to pFe 18, pFe 19, pFe 20, and pFe 21 demonstrated a control of cell density by the level of iron.

Figure 8. Availability of Fe^{3+} in A^* and BG11 media. Ferric iron levels (in pFe values) are presented with respect to total iron (moles L^{-1}) in the system. The speciation of all the components of the two media were utilized to calculate the pFe values at constant pH's (A^* pH = 7.8; BG 11 pH = 7.4). The complete speciation of iron appears in Appendix I. Results demonstrate that changes in iron availability with respect to total iron concentration vary between BG11 and A^* medium.

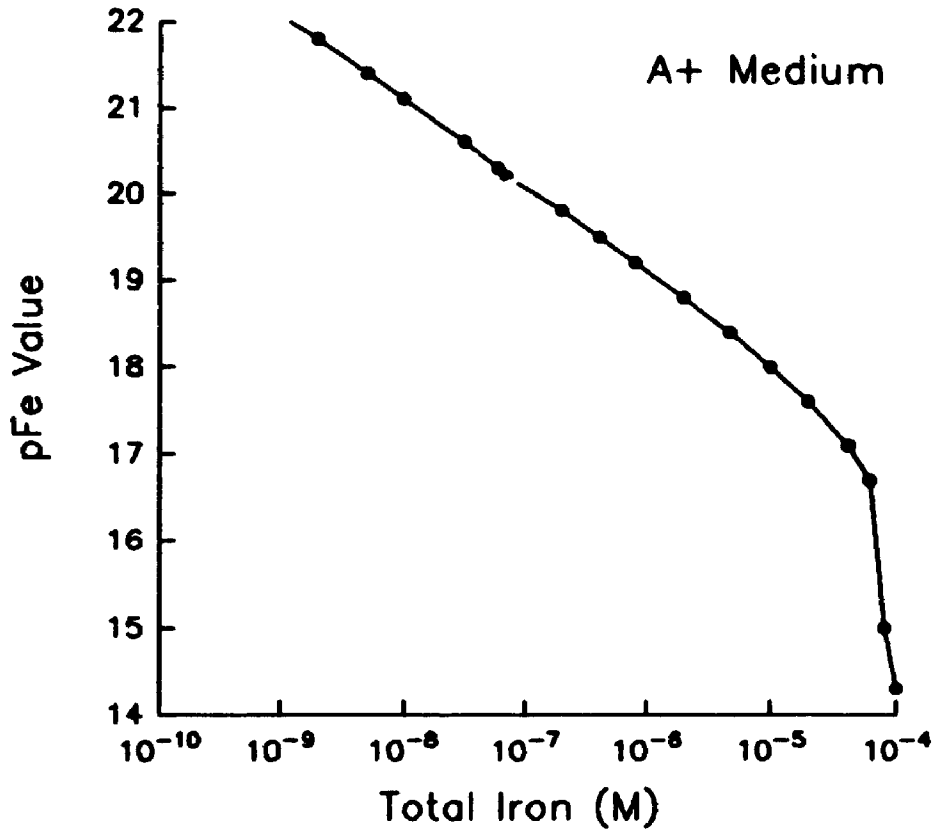
A+ Medium
pFe Value
22
21
20
19
18
17
16
15
14
10^{-10} 10^{-9} 10^{-8} 10^{-7} 10^{-6} 10^{-5} 10^{-4}
Total Iron (M)

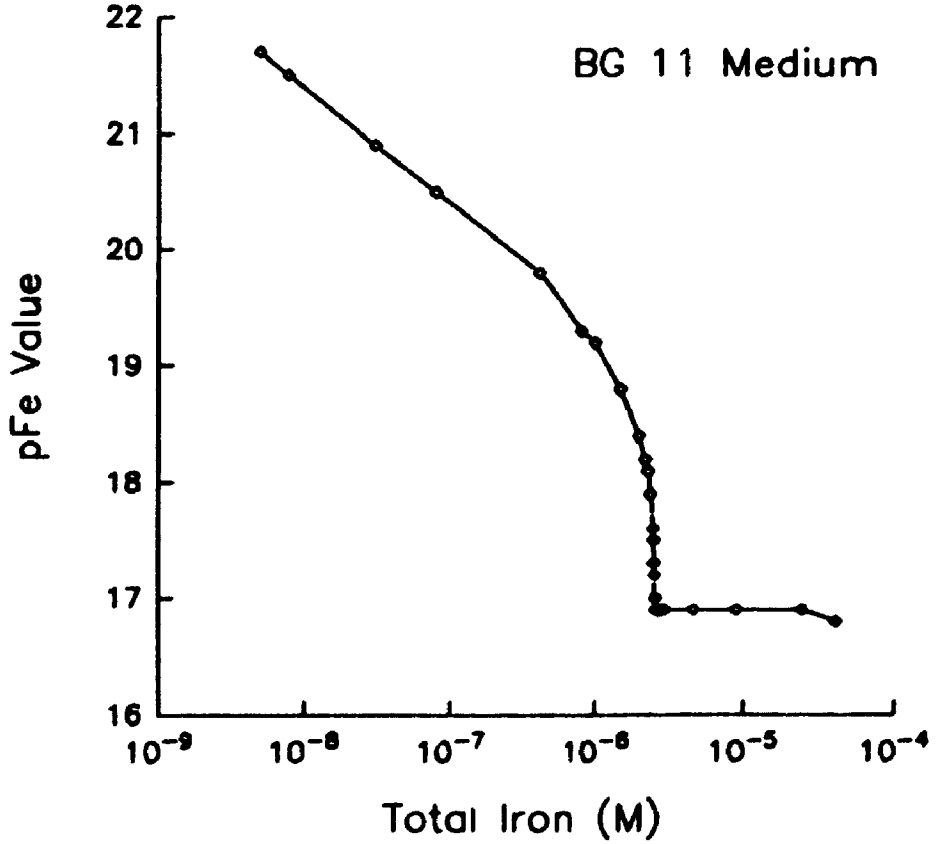
BG 11 Medium
pFe Value
22
21
20
19
18
17
16
10^{-9} 10^{-8} 10^{-7} 10^{-6} 10^{-5} 10^{-4}
Total Iron (M)

Figure 9. Steady state cell densities for iron-limited chemostats. Steady state cell densities were determined daily and are presented against the Fe^{3+} availability. Chemostats were considered to be in equilibrium after 2.5 cycles at a constant cell density. Data from chemostats where washout events were recorded (WO) is not included in the calculation of steady state (± S.D.) Results are presented in comparison to predicted cell densities based on chemostat kinetics (Section 1.9), the decrease in Fe^{3+} availability and standardized to the cell density at pFe 17.

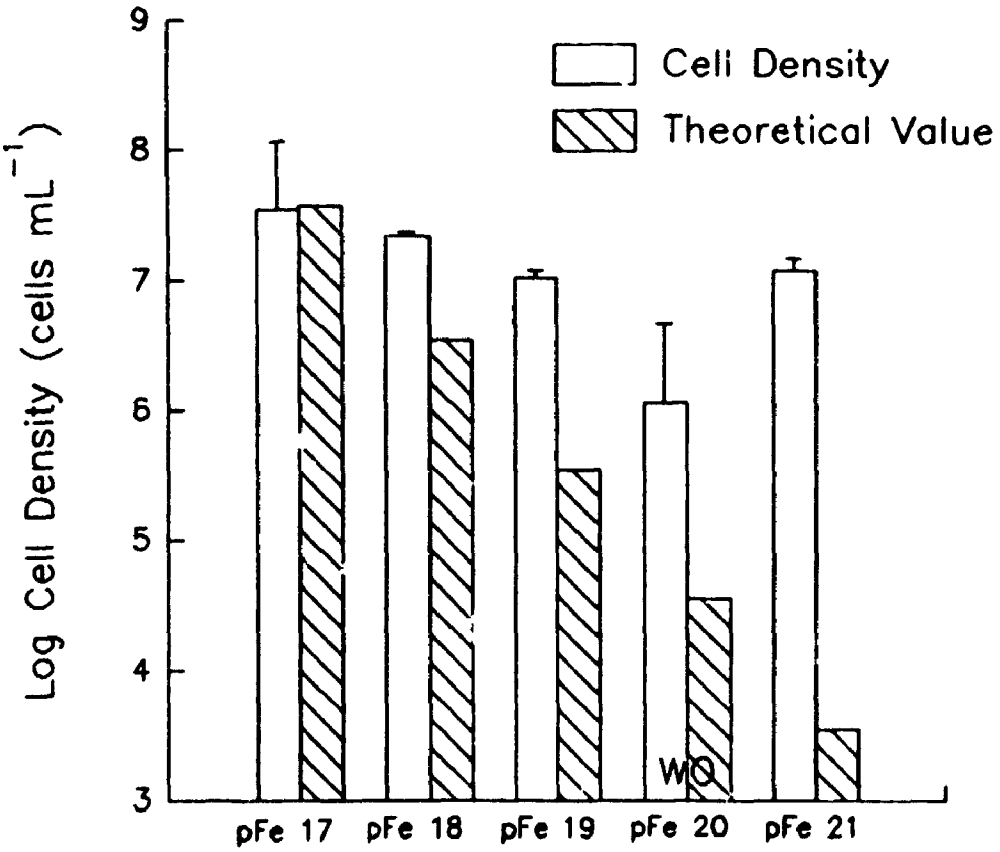
Log Cell Density (cells mL^{-1})
9
8
7
6
5
4
3
Cell Density
Theoretical Value
WO
pFe 17
pFe 18
pFe 19
pFe 20
pFe 21

In preliminary experiments (data not shown), final cell yields forthe pFe 18, 19, 20, and 21 chemostats would increase if supplemented with additional iron. Cells from the pFe 17 chemostat were saturated with iron and the cell density was controlled (limited) by the level of nitrate in the medium (11.8 mM).

The yield of the 4 iron-limited chemostats did not decrease proportional to the amount of added iron as predicted by chemostat modelling (Figure 9), suggesting that cells in the iron-limited chemostats were more efficient at utilizing the available iron pool. The pFe 17 chemostat (nitrate-limited) had a final yield only 10-fold higher than the pFe 21 $FeCl_3$ chemostat.

The cells grown in the pFe 20 iron-limited chemostat showed the greatest variability in results, suggesting that at this level of available iron cells were undergoing an iron-regulated metabolic change, such that in some cases the cyanobacteria were capable of establishing a steady state equilibrium, while at other times they were unable to maintain steady state. This variation brought about the exclusion of the pFe 20 cells from the other chemostat experiments.

3.3 Iron-Regulated Growth Rates

The effect of lower levels of available iron on maximum growth rate was determined in batch cultures and results are presented in Figure 10. Results are presented as doublings day^{-1}. The increase in growth rate at pFe 21 is suggestive of a change in iron-related physiology.

Figure 10. Effect of iron availability on maximum growth rates for *Synechococcus* sp. PCC 7002. The growth of batch cultured cyanobacteria was monitored spectrophotometrically to determine maximum growth rates with respect to specific iron availabilities. Linear regression of cell doubling during exponential phase was utilized to predict rates. Cells grown at pFe 21 demonstrate a level of recovery of growth with respect to cells grown under higher levels of iron availability. (± S.D.)

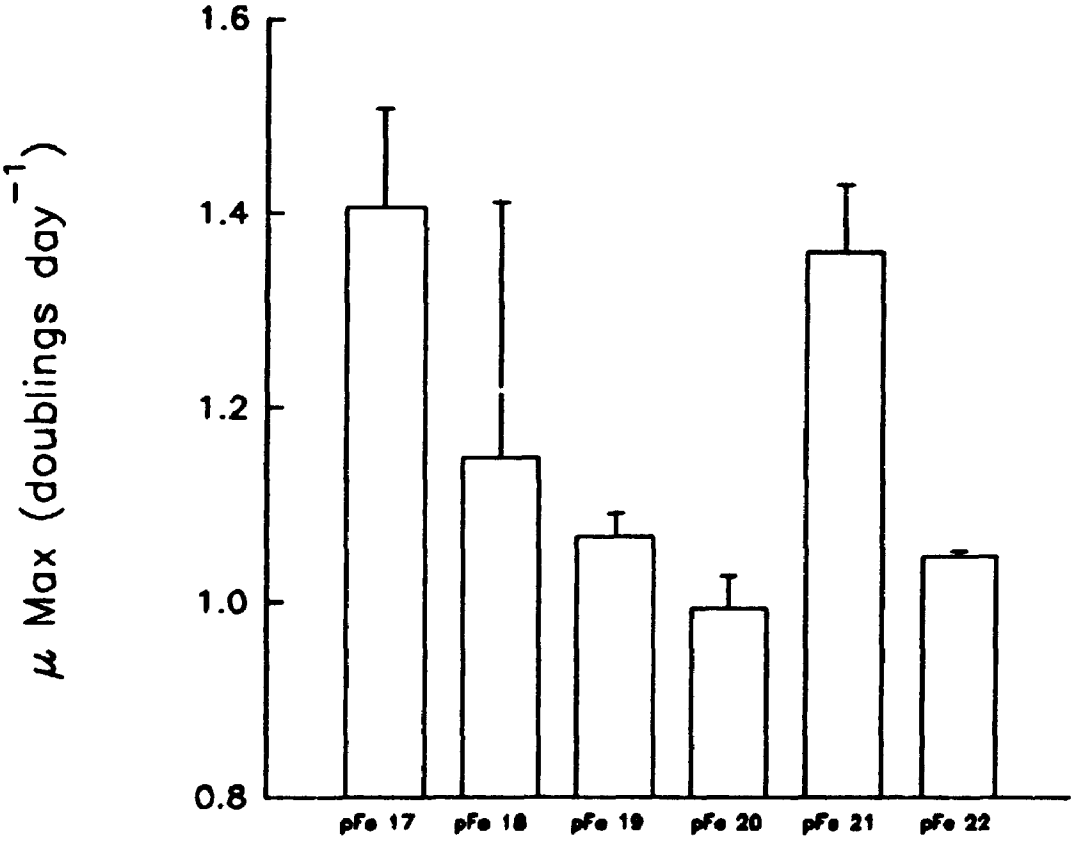
1.6
1.4
1.2
1.0
0.8
μ Max (doublings day^{-1})
pFe 17
pFe 18
pFe 19
pFe 20
pFe 21
pFe 22

Figure 11. Pigment levels in steady state cultures of *Synechococcus* sp. PCC 7002. **A)** Spectrally estimated chlorophyll levels in chemostat grown cyanobacteria. Steady state levels of chlorophyll were estimated daily and averages of individual chemostat trials are presented for chemostat cultures over the range of iron availabilities (± S.D; pFe 17, 21 n = 34; pFe 18, 19 n = 3.). **B).** Variations in the photosynthetic pigment ratio over a range of iron availabilities. Values are presented as μM Phycocyanin : μM Chlorophyll for steady state cultures (± S.D; pFe 17, 21 n = 34; pFe 18, 19 n = 3.).

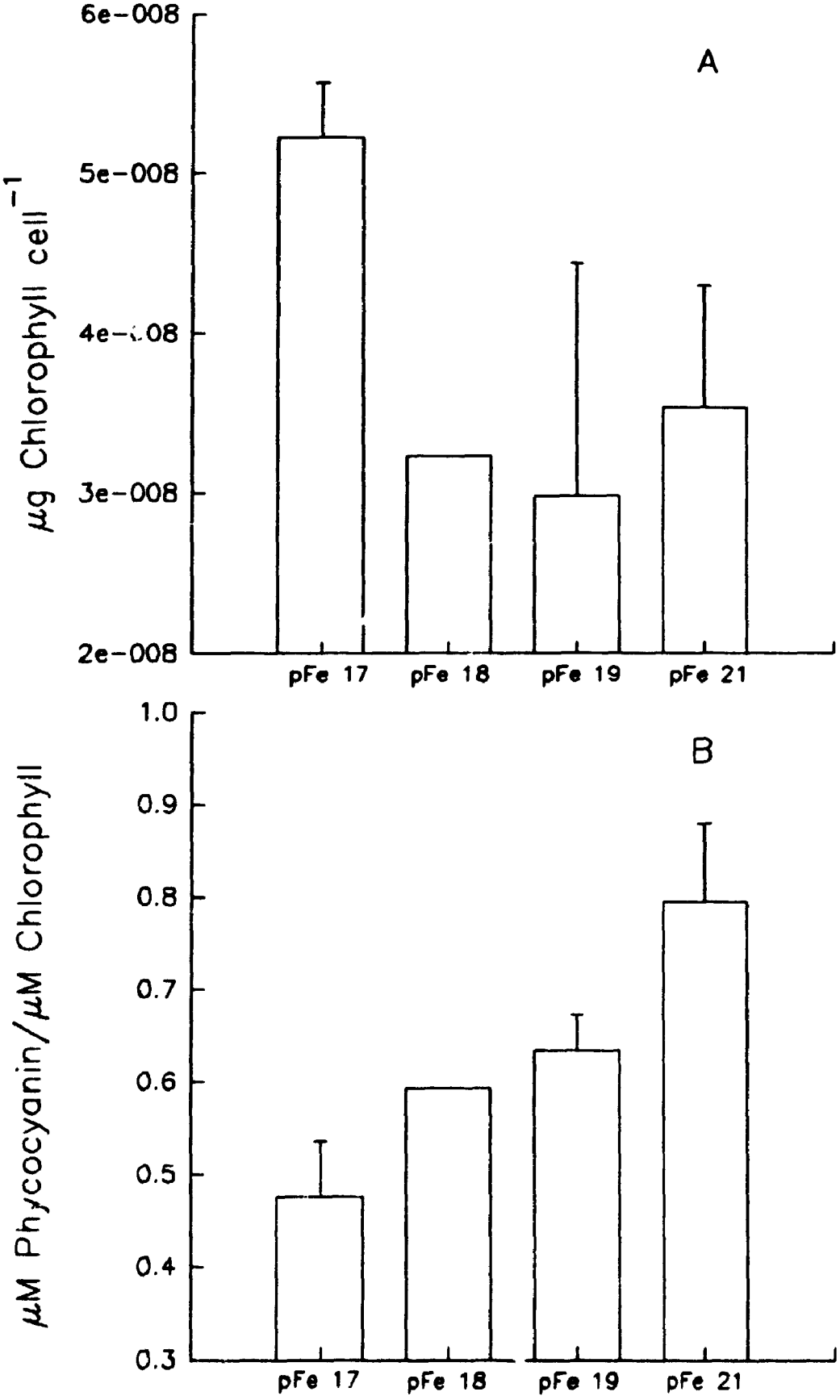
A
6e-008
5e-008
4e-008
3e-008
2e-008
μg Chlorophyll cell^{-1}
pFe 17
pFe 18
pFe 19
pFe 21
B
1.0
0.9
0.8
0.7
0.6
0.5
0.4
0.3
μM Phycocyanin/μM Chlorophyll
pFe 17
pFe 18
pFe 19
pFe 21

3.4 Cellular Pigment Production

Production of photosynthetic pigments was regulated by the amount of available iron in the chemostat medium (Figures 11). A comparison of nitrate-limited cells with iron-limited cells shows a dramatic drop in the amount of chl*a* per cell. The iron-limited cells maintained a low but relatively constant cellular chl*a* concentration. Similarly, phycocyanin per cell was altered with a shift from iron sufficient to iron-deficient growth status. A comparison of phycocyanin to chl*a* ratios (Figure 11) demonstrates an increase in the ratio at pFe 21 relative to the other iron-limited (pFe 18, pFe 19) as well as nitrate-limited (pFe 17) cells. It is important to to point out that the sample size for the pFe 17 and pFe 21 chemostats is significantly larger. Changes in the localized absorbance maxima were also noted for chl*a*. The chl*a* peak for pFe 17 grown cells was significantly higher (681.8 nm ± 2.37) in comparison to the pFe 21 chl*a* peak (674.4 nm ± 2.43).

3.5 Levels of Extracellular Siderophores

The amount of extracellular organics that would react to the Czaky test was dependant upon the amount of available iron in the medium (Figure 12) Chemostat grown cells in medium containing the highest amount of iron (pFe 17) produced no measurable amounts of extracellular hydroxamate-type siderophore reactive in the Czaky test, and only low amounts of material reactive to the two tests for the catechol-type organics.

In contrast, cells from the iron-limited chemostats provided high amounts of reactive material. Maximum levels were obtained from chemostats supplemented with pFe 19. Similar results were seen in both the Arnow and Rioux tests for the production of catechol-type siderophores (Figure 13). No appreciable reactive compounds were detected in the nitrate-limited chemostat while significant amounts were detected in all the iron-limited chemostats.

The production of extracellular siderophores in *Synechococcus* sp. PCC 7002 is accompanied by a pH shift in the reactor medium. The pH within the pFe 17 reactor is maintained at 7.83 (S.D. = 0.045) while the pH of the medium in the pFe 21 reactors was depressed to 7.59 (S.D. = 0.055).

3.6 Photosynthetic Capacity and Efficiency

Rates of light driven net cellular carbon fixation are given in Table 6. Cells from the nitrate-limited pFe 17 chemostat appear to fix CO_2 at a rate one order of magnitude faster than cells from the pFe 21 culture. To determine total turnover rates, cellular carbon was estimated at 125 *f*g cell^{-1}, based on cell size (1 μm^3), and approximate dry density (125 kg C m^{-3}), a value which was later confirmed to be in the range of natural populations (Waterbury et al. 1987). Results demonstrate that iron-limited cells lower carbon incorporation rates to approximate growth requirements. Cellular carbon appears to be turned over every 39.0 h in pFe 21 chemostats, while turnover takes only 5.58 h in pFe 17 chemostats.

Figure 12. Hydroxamate-type siderophore production in iron-limited chemostats. Results from Czaky test demonstrate an increase in siderophore levels with a decrease in iron availablity. Results are standardized to hydroxylamine equivalents ($n \geq 2$).

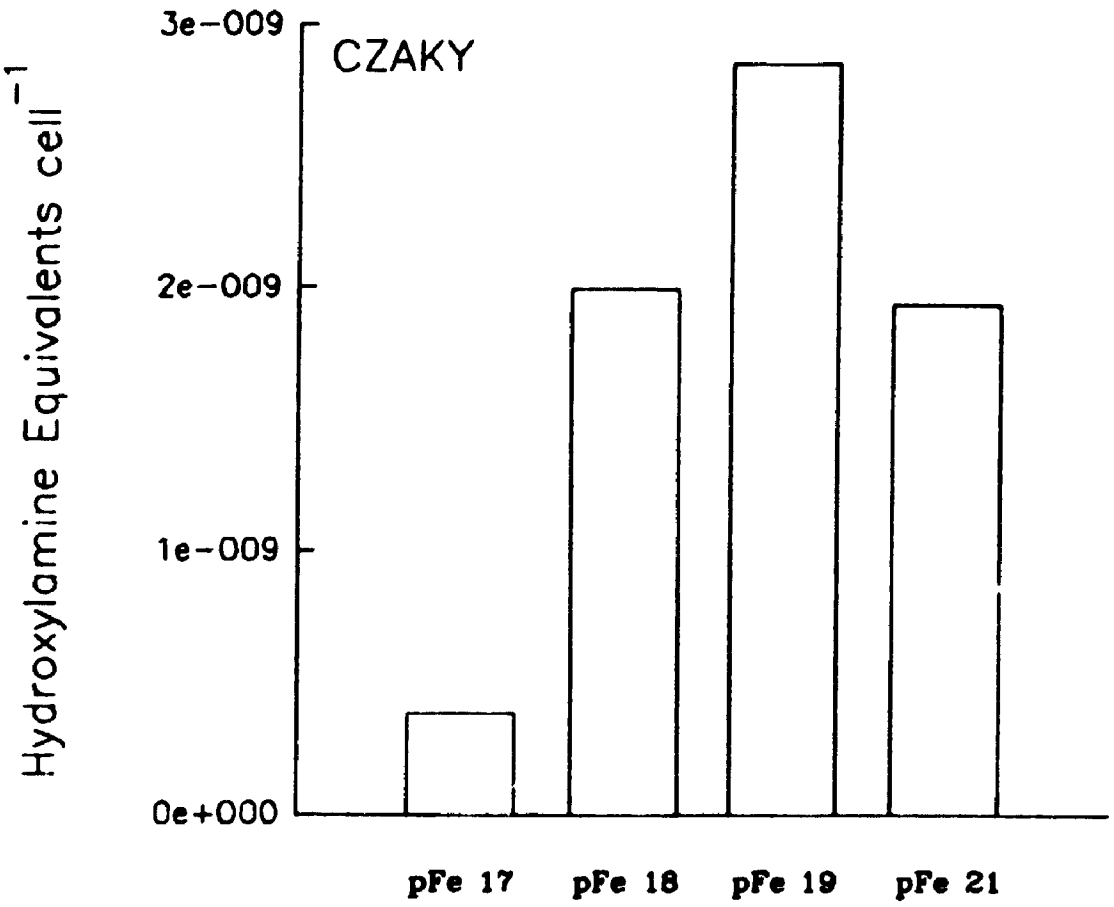
CZAKY
Hydroxylamine Equivalents cell^{-1}
3e-009
2e-009
1e-009
0e+000
pFe 17
pFe 18
pFe 19
pFe 21

Figure 13. Catechol-type siderophore production in iron-limited chemostats. Results from Arnow and Rioux tests for catecholate-type siderophore production by chemostat grown cyanobacteria. Results are standardized to DHBA equivalents ($n \geq 2$). **ND**- none detected .

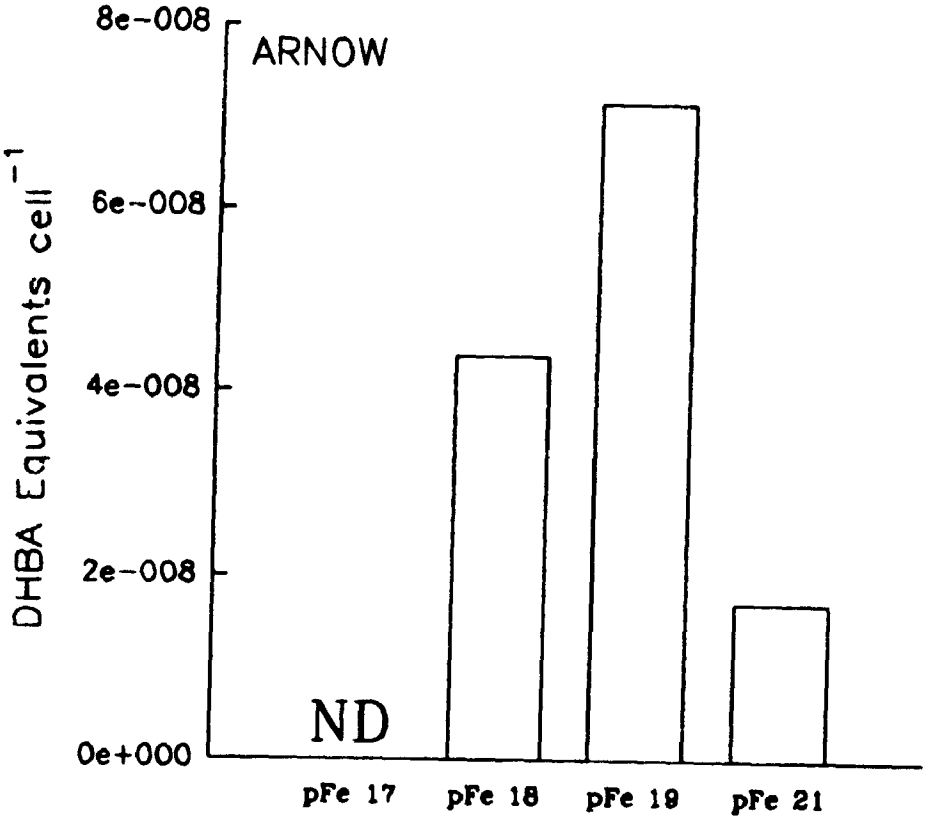
ARNOW
8e-008
6e-008
4e-008
2e-008
0e+000
DHBA Equivalents cell^{-1}
ND
pFe 17
pFe 18
pFe 19
pFe 21

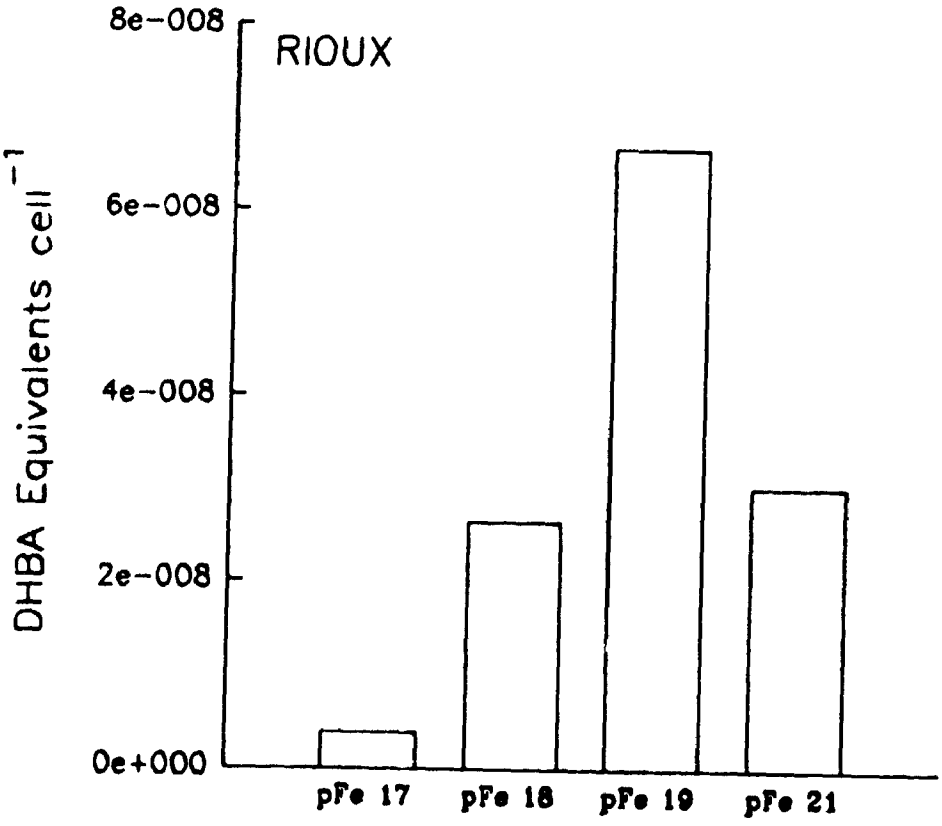
RIOUX
8e-008
6e-008
4e-008
2e-008
0e+000
DHBA Equivalents cell^{-1}
pFe 17
pFe 18
pFe 19
pFe 21

Table 6. Carbon fixation rates in chemostat grown *Synechococcus* sp. PCC 7002. Chemostat grown cyanobacteria were harvested and carbon fixation monitored with $H^{14}CO_3^-$. Cellular carbon turnover was calculated based on carbon uptake rates and estimated cellular carbon content. Turnover time was calculated based on the rate of carbon incorporation into the cell and the growth rate in the chemostats. Results suggest that iron-limited cells (pFe 21) down-regulate carbon fixation rates to approximate that of the cellular growth rate (≈40 hours) while iron-replete cultures (pFe 17) experience luxury carbon fixation. Coefficients of variation (r^2): pFe 17 = 0.0991; pFe 21 = 0.9896.

	pFe 17	**pFe 21**
Carbon Uptake $\mu mol\ min^{-1}\ cell^{-1}$	3.11×10^{-11}	4.45×10^{-12}
**assuming 125 *f*g C $cell^{-1}$		
turnover time	5.58 hrs	39.0 hrs

Figure 14. Net oxygen evolution in iron-limited *Synechococcus* sp. PCC 7002. Profiles of O_2 evolution vs. photosynthetic photon flux density for iron-replete (pFe 17) and deficient (pFe 19, pFe 21) cultures of *Synechococcus* sp. PCC 7002 from chemostats. Results are standardized to per cell (A) and per chl*a* (B) levels (± S.D. n= 5). The difference in oxygen evolution rates between cells maintained at pFe 19 and pFe 21 is highlighted by a comparison of the two graphs.

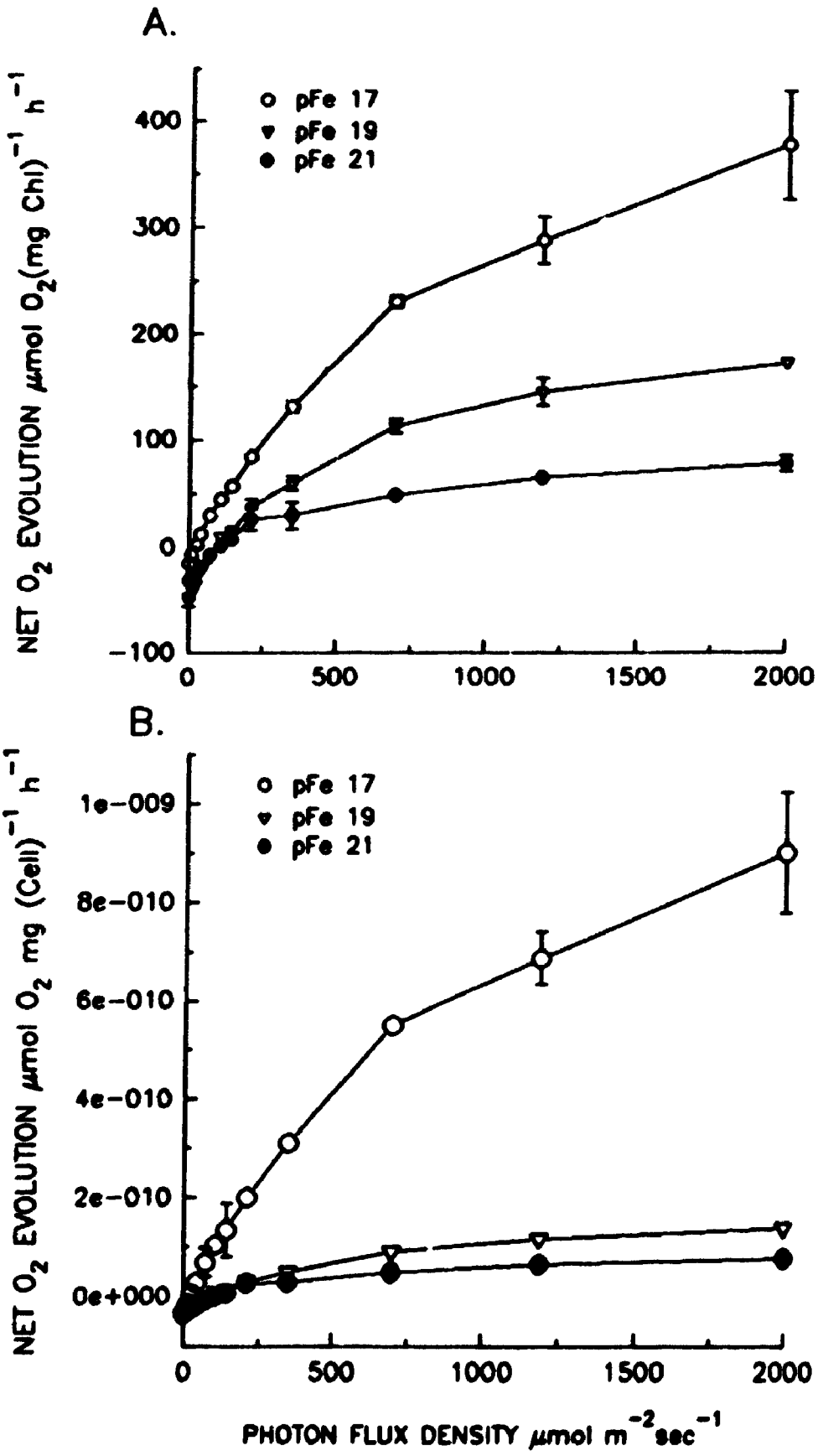
A.
pFe 17
pFe 19
pFe 21
NET O_2 EVOLUTION μmol O_2(mg Chl)$^{-1}$ h^{-1}
400
300
200
100
0
−100
0
500
1000
1500
2000
B.
pFe 17
pFe 19
pFe 21
NET O_2 EVOLUTION μmol O_2 mg (Cell)$^{-1}$ h^{-1}
1e−009
8e−010
6e−010
4e−010
2e−010
0e+000
0
500
1000
1500
2000
PHOTON FLUX DENSITY μmol m^{-2} sec^{-1}

Net oxygen evolution values are reported in Figure 14. Cells from pFe 17 chemostats demonstrated higher rates of light-satured O_2 evolution and a greater apparent quantum efficiency in comparison to those grown at pFe 19 and pFe 21 levels. A comparison of the cells from pFe 19 and pFe 21 cultures demonstrates as well a significant difference in light dependant levels oxygen evolution.

Values are reported both as a function of cellular biomass (μmol O_2 $cell^{-1}$ h^{-1}) and cellular chla levels (μmol O_2 (μg $chl^a)^{-1}$ h^{-1}) in order to emphasize these differences. Variations in the Φ_{app} of these cyanobacteria demonstrate the highest Φ_{app} for pFe 17 grown cells (Φ_{app}= 0.414 ± 0.032) and lower values for pFe 19 (Φ_{app}= 0.269 ± 0.054) and pFe 21 (Φ_{app}= 0.180 ± 0.032) populations.

3.7 Ultrastructural Variation

Transmission electron micrographs of iron-limited pFe 21 cultures of *Synechococcus* sp. PCC 7002 demonstrate that a number of ultrastructural variations are evident during iron-limited growth. Thylakoid membranes in pFe 21 grown cells appear to lose their integrity in comparison to pFe 17 grown cells (Figure 15). A comparison of these with batch grown pFe 17 cells confirms that cellular physiology is not influenced by culturing technique. Further examination also reveals a decrease in carboxysome number, but a relative increase in size of the remaining carboxysomes. As well, a decrease in intracellular polyphosphate bodies is seen in pFe 21 cells.

Figure 15. Ultrastructural differences between iron-replete and iron-deficient cultures of *Synechococcus* sp. PCC 7002. Electron micrographs demonstrating the typical ultrastructure of cyanobacteria grown under different conditions (minimum of 5 sections examined), with emphasis on changes in thylakoid structure (**T**), carboxysome size and number (**C**), and the size of polyphosphates bodies within the cell (**P**). Identification of intracellular components was based on Hardie et al. 1983b. **A).** Cells maintained in a chemostat at pFe 17. **B).** Cells maintained in a chemostat at pFe 21. **C).** Exponentially growing cells from a pFe 17 batch culture. Bar = 1 μm.

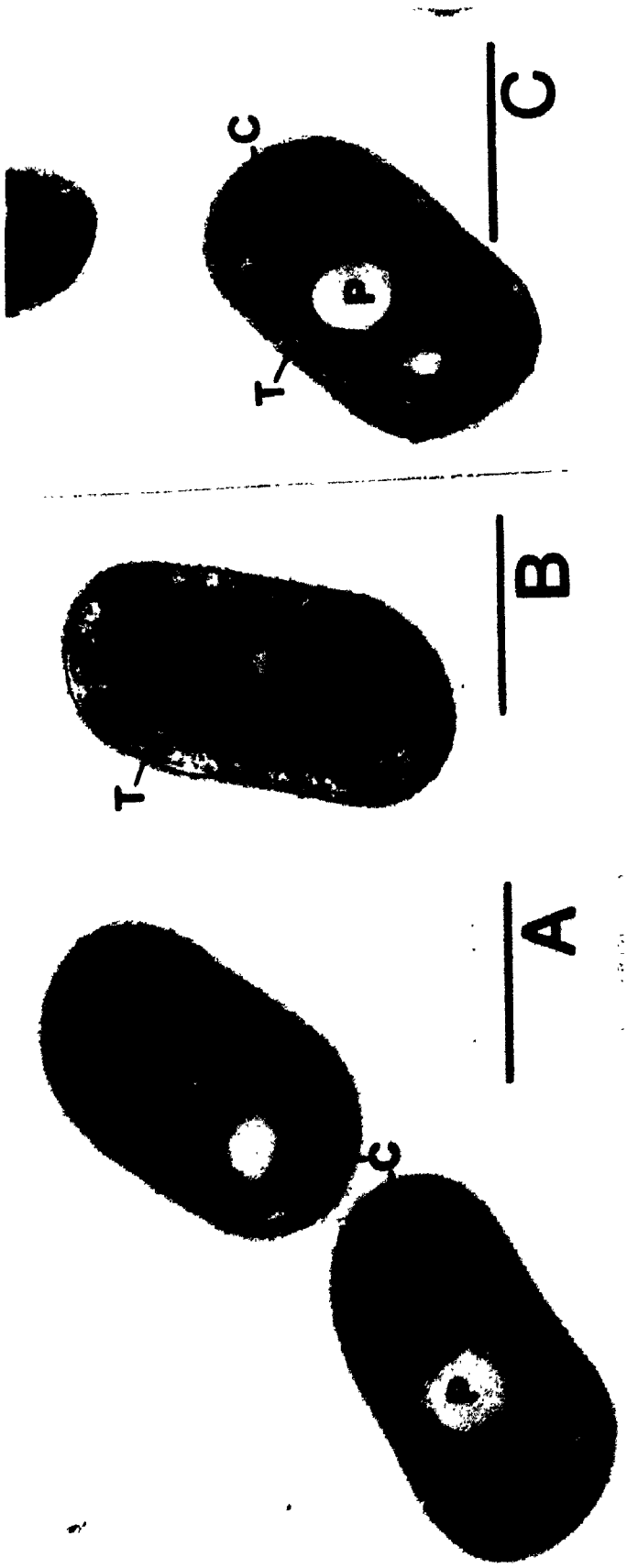
C
C
T
B
T
A
C

3.8 Effect of Iron-Limitation on Membrane Polypeptide Profiles

Synechococcus sp. PCC 7002, grown under iron-deficient (pFe 21) conditions, demonstrated marked changes in the polypeptide profiles of the thylakoid, cytoplasmic and outer membranes in comparison to cyanobacteria grown under iron-replete conditions. Proteins of 70.0, 59.0, 39.0, and 32.5 kDa were consistently identified in thylakoid membranes of pFe 21 grown cells that were not detectable in pFe 17 grown cyanobacteria (Figure 16). Similarly, a protein of 23.5 kDa was consistently identified in the cytoplasmic membrane fraction of pFe 21 grown *Synechococcus* sp. PCC 7002 (Figure 17).

Proteins of 72.0, 61.5, 59.0, 54.5, 35.0, and 29.0 kDa were consistently identified in the outer membrane of pFe 21 grown cells that were not seen in the outer membrane of pFe 17 grown cells (Figure 18). These proteins are in the same size range as those reported in other iron-limited cyanobacterial (Table 7) and eubacterial species (Neilands 1982). While the presence of proteins of 59.0 kDa in both the outer membrane and thylakoid fraction suggests some cross contamination of the samples, the lack of any other common proteins suggests that these may be either ubiquitous stress proteins, or the coincidental production of different proteins of similar size.

Analysis of periplasmic proteins components from pFe 17 and pFe 21 grown chemostats demonstrated no consistent differences when analyzed by PAGE. Transiently evoked peptides were seen in the range of 50.0 kDa, but this could not be consistently and positively confirmed.

Figure 16. Polypeptide profile of thylakoid membranes from pFe 17 and pFe 21 grown *Synechococcus* sp. PCC 7002. Silver stained polyacrylamide gel preparation of thylakoid proteins (75 µg lane^{-1}), demonstrating 4 proteins whose expression appears enhanced during iron-limited culturing.

Lane 1: pFe 17 thylakoids. **Lane 2**: pFe 21 thylakoids.

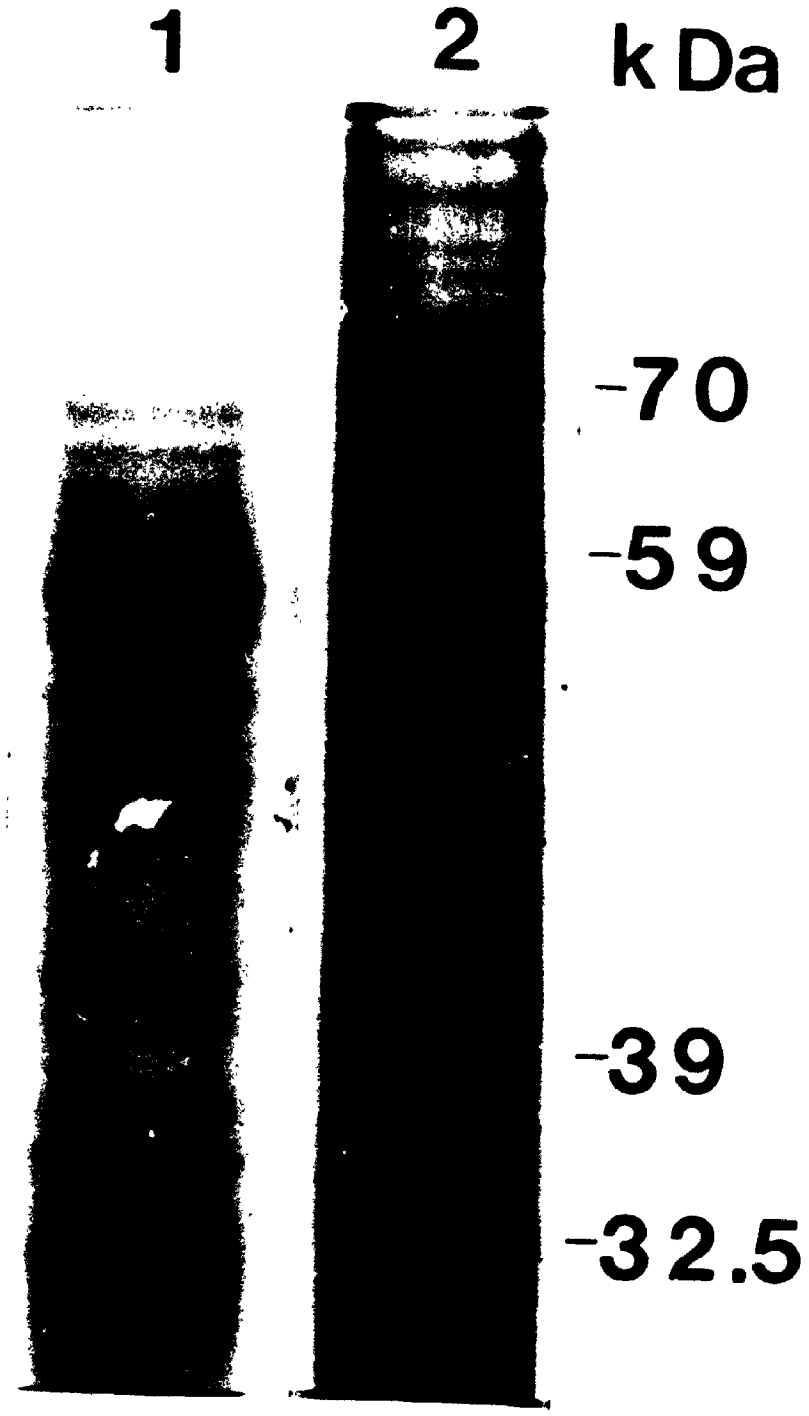
1
2
kDa
70
59
39
32.5

Figure 17. Polypeptide profile of cytoplasmic membranes from pFe 17 and pFe 21 grown *Synechococcus* sp. PCC 7002. Coomassie blue stained polyacrylamide gel preparation (75 µg lane^{-1}) demonstrating a protein at 23.5 kDa in the pFe 21 fraction. **Lane 1**: pFe 17 cytoplasmic membranes. **Lane 2**: pFe 21 cytoplasmic membranes.

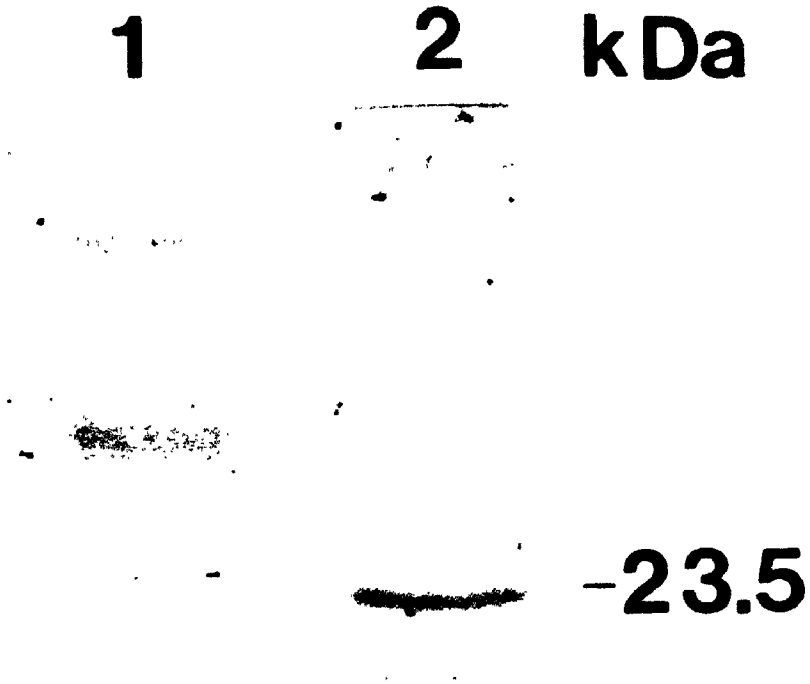
1
2
kDa
23.5

Figure 18. Polypeptide profile of outer membrane fractions from pFe 17 and pFe 21 grown *Synechococcus* sp. PCC 7002. Silver stained polyacrylamide gel preparation (75 µg protein $lane^{-1}$) demonstrating a number of enhanced proteins in the pFe 21 fraction. **Lane 1**: Outer membranes from pFe 17 cultured cells. **Lane 2**: Outer membranes from pFe 21 cultured cells.

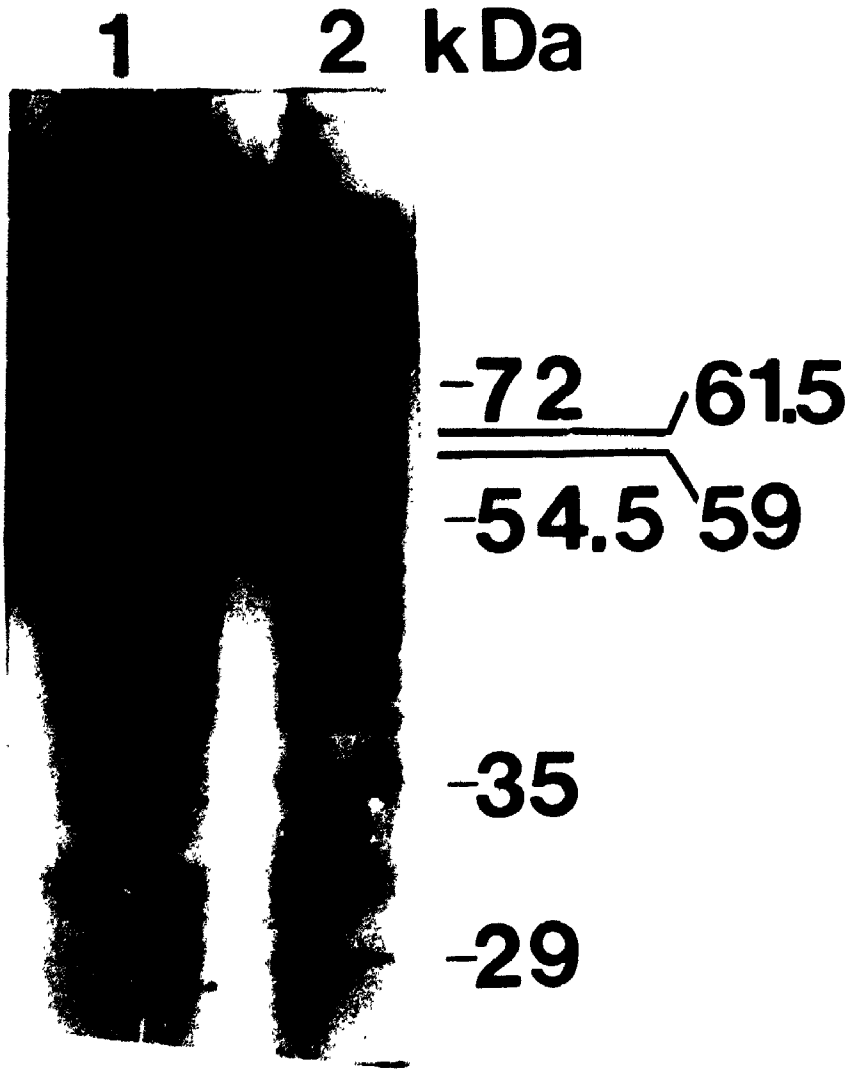
1
2
kDa
72
61.5
54.5
59
35
29

Table 7. Iron-regulated outer membrane proteins (kDa). Proteins were identified by polyacrylamide gel electrophoresis. In all cases, proteins are expressed at iron-limiting levels and not detected under iron-replete conditions.

		Reference
Oscillatoria tenuis	200, 158, 81, 53, 51	Brown, 1991
Synechococcus sp. PCC 7942	92, 48-50, 35	Scanlan et al. 1989
Synechococcus sp. PCC 7002	72, 61.5, 59, 54.5, 35, 29	**This study**
Synechocystis sp. PCC 6803	52, 36	Scanlan et al. 1989

3.9 Identification of Siderophores in *Synechococcus* sp. PCC 7002

Cell-free, spent medium from all of the chemostats was examined by TLC for the presence of iron-binding organic compounds. Using the ferric chloride spray to detect iron-chelating compounds, it was determined that the concentrated cell-free spent medium from pFe 17 chemostat did not contain sufficient iron-binding material for observation. In contrast, spent medium for all of the cultures examined under iron-limiting conditions (pFe 18 or less), contained four iron-reactive compounds recognizable by thin layer chromatography (Table 8). R_f values for these compounds, determined using a variety of solvents, allowed for a comparison between them. At all levels of iron availability, the iron-reactive properties of these compounds appear to be constant.

Fractionation of the siderophores from pFe 21 chemostats on Sephadex LH-20 columns, and subsequent analysis with the CAS assay, confirmed that four different iron-binding compounds were produced (Figure 19). LH-20 fractionation of the extracellular, organic compounds produced in pFe 21 batch cultures demonstrates a slightly different profile (Figure 20). Two major CAS peaks are visible in these fractions, suggesting a change in comparative production levels of the iron chelators. Comparison of the absorbance values at 280 nm (proteins and phenolics) and 405 nm (putative siderophore absorbance maxima) suggests that at least two compounds are responsible for this profile (Figure 20). Thin layer chromatography confirmed that the four

chelators found in iron-limited batch cultures are the same as those found in iron-limited chemostat cultures (based on R_f values), but the production of each individual siderophore varies between different culturing protocols (Table 8).

Of the two siderophores isolated, only sufficiently pure quantities of 2 compounds (Chelators #1 and #3) were retrieved to allow for further chemical analysis. Particle ionization mass spectrometry (Figure 21) allowed for a determination of the precise mass of these compounds, from which appropriate chemical formulae were estimated (Table 9).

3.10 Siderophore Production In Different Species

Siderophore production was monitored in a number of different cyanobacteria (Table 10). Thin layer chromatography was combined with the tests of Arnow, Rioux and Czaky to determine the numbers and types of siderophores produced by the different species cultured at pFe 21. Results suggest that all of the cyanobacteria tested in this study were able to produce at least one siderophore, with some producing multiple iron-sequestering compounds. Chemical analysis of the siderophore isolates allowed for a determination of hydroxamate- and catechol-type siderophore production. In situations when a compound provided a positive result in none of the reactions, it was considered to be of the atypical-type (Table 10).

Table 8. Siderophores produced by iron-limited *Synechococcus* sp. PCC 7002. The four siderophores produced by this cyanobacterium are presented with their R_f values for three solvents utilized to separate them. Also presented is the relative proportion of their production in batch and chemostat culture systems, which was determined by a visual analysis of the relative ratio of I_2 and $FeCl_3$ reactive material on TLC plates, as well as the CAS data for LH-20 fractions. The numbers assigned to chelators represent the order of their isolation.

Siderophore	Pro:But:H_2O 1:1:1	But:HAc:H_2O 60:25:15	Isoprop:H_2O 7:3	Batch	Chem
Chelator#1	.638	.804	.877	++++	+++
Chelator#2	.725	.593	.100	+++	+
Chelator#3	.833	.741	.820	++	++++
Chelator#4	.880	ND	.900	+	+

Figure 19. LH-20 profiles of siderophores from iron-limited *Synechococcus* sp. PCC 7002 chemostat cultures. Analysis of extracellular organic fractions, isolated with Amberlie XAD-16, for iron-chelating compounds from pFe 21cultures with the CAS assay. Results demonstrate that four different peaks of iron-chelating compounds were resolved by LH-20 fractionation (37.5 x 1 cm column with a methanol:chloroform (50:50) solvent system, fraction volumes of 1 mL).

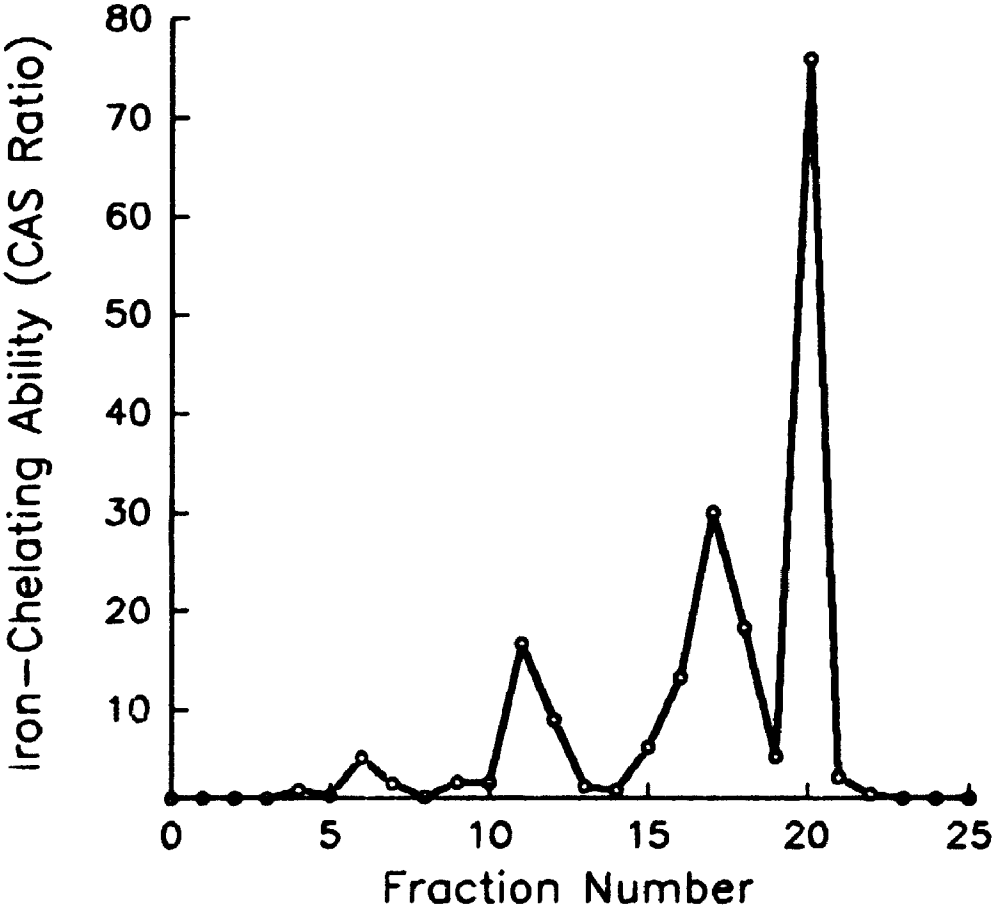
Iron-Chelating Ability (CAS Ratio)
80
70
60
50
40
30
20
10
0
5
10
15
20
25
Fraction Number

Figure 20. LH-20 profiles of siderophores from iron-limited *Synechococcus* sp. PCC 7002 batch cultures. Analysis of the extracellular organic fractions, isolated with Amberlie XAD-16, for iron-chelating compounds from pFe 21 batch cultures of *Synechococcus* sp. PCC 7002. After fractionation through an LH-20 column (conditions the same as Figure 19), extracellular organic fractions from *Synechococcus* sp. PCC 7002 were analyzed for iron binding capability (CAS assay), putative siderophore levels (ABS_{405nm}) and potential phenolic and protein content (ABS_{280nm}). Differences between the ABS_{280nm} and ABS_{405nm} profiles confirm the CAS data in demonstrating that at least two different iron chelators are present.

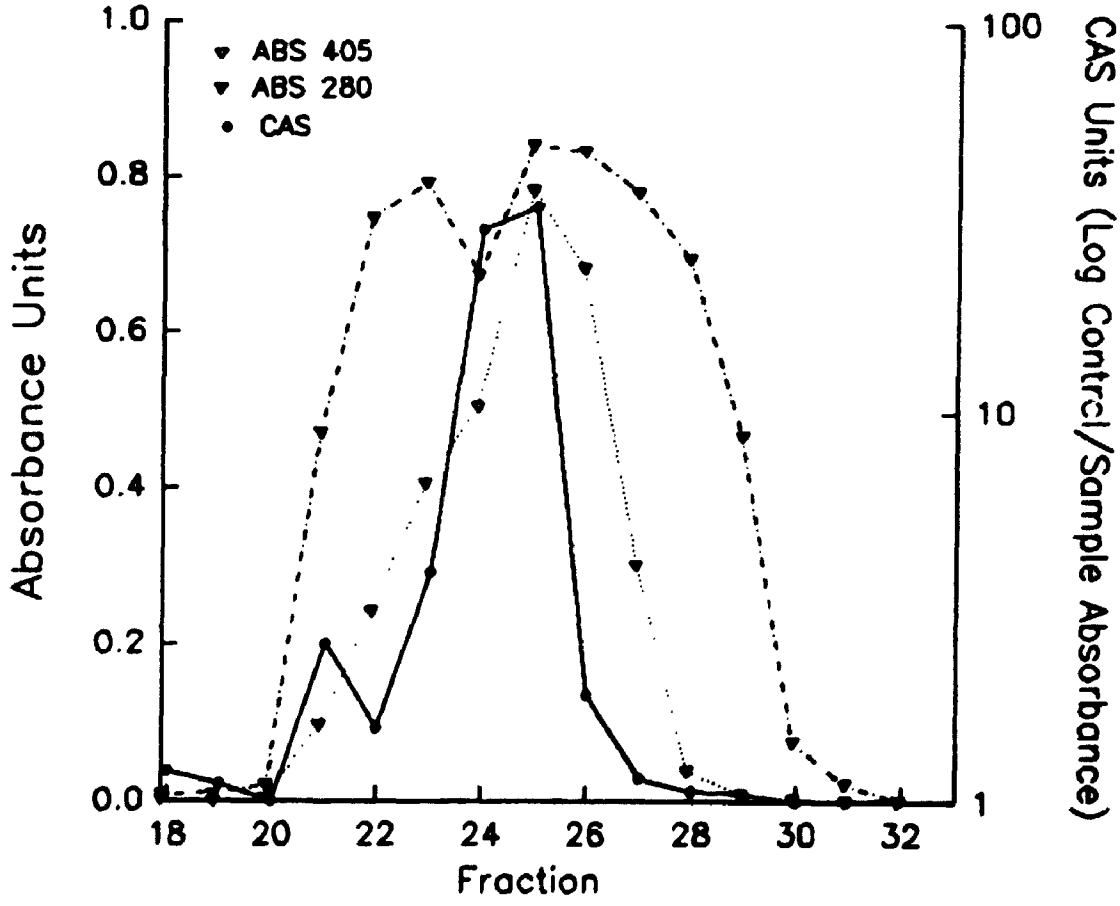
ABS 405
ABS 280
CAS
Absorbance Units
1.0
0.8
0.6
0.4
0.2
0.0
100
10
1
CAS Units (Log Control/Sample Absorbance)
18
20
22
24
26
28
30
32
Fraction

Figure 21. Particle ionization mass spectra of siderophores. Mass spectra of *Synechococcus* sp. PCC 7002 Chelators #1 and #3 was accomplished utilizing isobutane as the chemical ionization agent. Spectra were determined in methanol solubilized samples, with precise masses being determined by the addition of a known standard. **A.** Spectrum for Chelator #1. Siderophore mass (452.3378) is reflected in the 453 peak with the peak at 493 derived from a siderophore-isobutane fusion product. **B.** Spectrum for Chelator #3. Siderophore mass (391.2824) reflected in the 391 peak, with the peak at 443 reflective of a siderophore-isobutane fusion product.

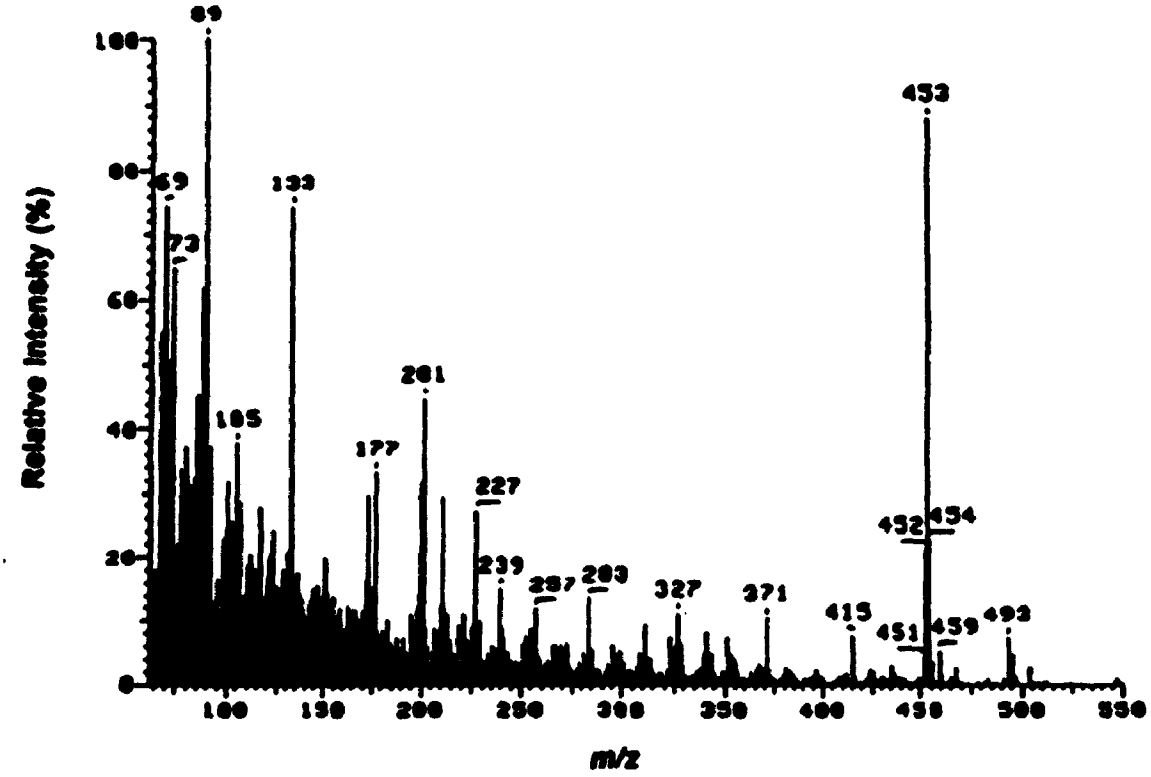
Relative Intensity (%)
m/z
69
453
133
73
201
185
177
227
452
454
239
287
283
327
371
415
451
459
493

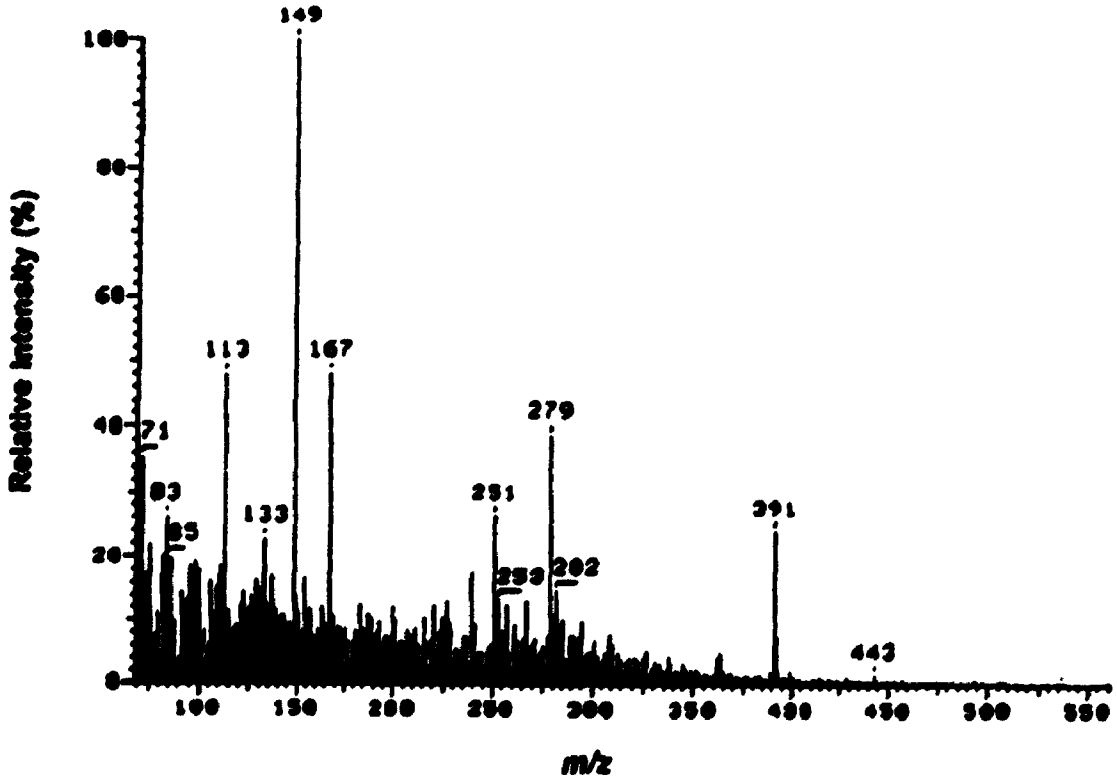
Relative Intensity (%)
m/z
149
113
167
279
71
83
85
133
251
291
259
282
443

Table 9. Precise mass and predicted chemical formulae for two novel cyanobacterial siderophores. Formulae are best fit predictions based on precise mass measurements from particle ionization mass spectrometry for compounds isolated from *Synechococcus* sp. PCC 7002. Formulae are calculated from accepted precise mass values for the elements. Results are presented with a comparison to Schizokinen, the only completely characterized cyanobacterial siderophore (* Matzanke 1991).

Siderophore	Precise Mass (Mass spectrometry)	Chemical Formulae (Predicted)
Synechococcus **PCC 7002**		
Chelator #1	452.3378	$C_{24}H_{48}N_4O_4$ (452.3362)
Chelator #3	391.2824	$C_{22}H_{37}N_3O_3$ (391.2838)
Anabaena **sp.***		
Schizokinen	-------	$C_{16}H_{28}N_4O_9$ (420.1856)

Table 10. Siderophore production by freshwater and marine species of cyanobacteria. Chemical tests were utilized to determine the number of hydroxomate and catechol-type siderophores.

STRAIN	SIDEROPHORES	HYDROXAMATE	CATECHOLS
FRESHWATER			
Synechococcus sp. PCC 6301	3	2	1
Synechococcus sp. PCC 6908	2	1	1
Synechococcus sp. PCC 7942	1	1	-
Synechocystis sp. PCC 6803	1	-	-
Oscillatoria tenuis Ag. UTEX 428	3	1	2
Anabaena catenula UTEX 375	2	1	1
MARINE			
Synechococcus sp. PCC 7002	4	1	2
Synechococcus sp. WH 8101	2	1	1
Synechococcus sp. WH 7805	1-2	ND	ND
Synechococcus sp. BBC2A	2	ND	ND

ND. Not Determined

N.B. Discrepencies in total siderophore number may represent the presence of atypical-type siderophores in some species.

In order to compare interspecies production of siderophores among coccoid cyanobacteria, thin layer chromatography of siderophores from each cyanobacterium was carried out (Table 11). In all but one instance (PCC 7002 #1 and PCC 6301 #1), the compounds appear to be unique. PCC 7002 #1 and PCC 6301 #1 co-migrated on TLC plates when mixed and resolved in isopropanol:water (data not shown). The slight difference in their R_f's in other solvent systems suggests that they may not be identical.

Analysis of surface associated iron-chelators from *Synechococcus* sp. PCC 7002 and *Synechococcus* sp. PCC 6301 demonstrated that, during periods of iron-limited growth, both cells produced chloroform soluble iron-chelators which remained associated with the cell surface after rinsing with iron-free growth medium, but were liberated by chloroform from the cell surface. While the compound produced by *Synechococcus* sp. PCC 6301 was confirmed to be catechol-type (positive Rioux reaction), no confirmed determination of the *Synechococcus* sp. PCC 7002 chelator type was accomplished.

3.11 Iron Uptake by *Synechococcus* PCC 7002

The titanium-citrate EDTA wash proved to differentiate between iron superficially associated with the surface of the cell, and iron actually incorporated into the cell (Figure 22). Rates for iron uptake in pFe 17 and pFe 21 chemostat grown cells demonstrate only minor differences between the rates of iron uptake in cyanobacteria grown under these two conditions (Table 12).

Table 11. Relative mobility function of iron chelators by thin layer chromatography. Siderophores from coccoid cyanobacteria were resolved in propanol:butanol:water (1:1:1) or isopropanol:water (7:3) and iron chelators visualized using 1% $FeCl_3$ in ethanol. Chelator names reflect the species from which they were isolated and the order of their isolation within that species.

Chelator	Prop:But:H_2O 1 : 1 : 1	Isoprop:H_2O 7 : 3
PCC 6301 #1	.579	.880
PCC 6301 #2	.761	.079
PCC 6301 #3	.796	.237
PCC 6803 #1	.777	.800
PCC 6908 #1	.741	.857
PCC 7002 #1	.638	.877
PCC 7002 #2	.725	.100
PCC 7002 #3	.833	.820
PCC 7002 #4	.880	.900
BBC2A #1	.127	.871
BBC2A #2	.192	.077
WH 7805 #1	.190	.920
WH 8101 #1	.561	.184
WH 8101 #2	.283	.526

Figure 22. Efficacy of titanium-citrate EDTA wash. The distinction between extracellular and intracellular iron utilizing the titanium-citrate-EDTA and saline-EDTA washes. Results demonstrate the effect of rinsing pFe 21 grown cells, presented with $^{55}FeCl_3$, with titanium citrate wash. **A)**. Cells were rinsed with titanium citrate or the saline EDTA wash and iron levels determined by scintillation analysis. Results show that the surface of the cell is quickly saturated with iron (saline-EDTA wash). **B)**. Data for two trials of pFe 21 grown cyanobacteria showing the linearity of iron uptake as determined with titanium citrate wash.

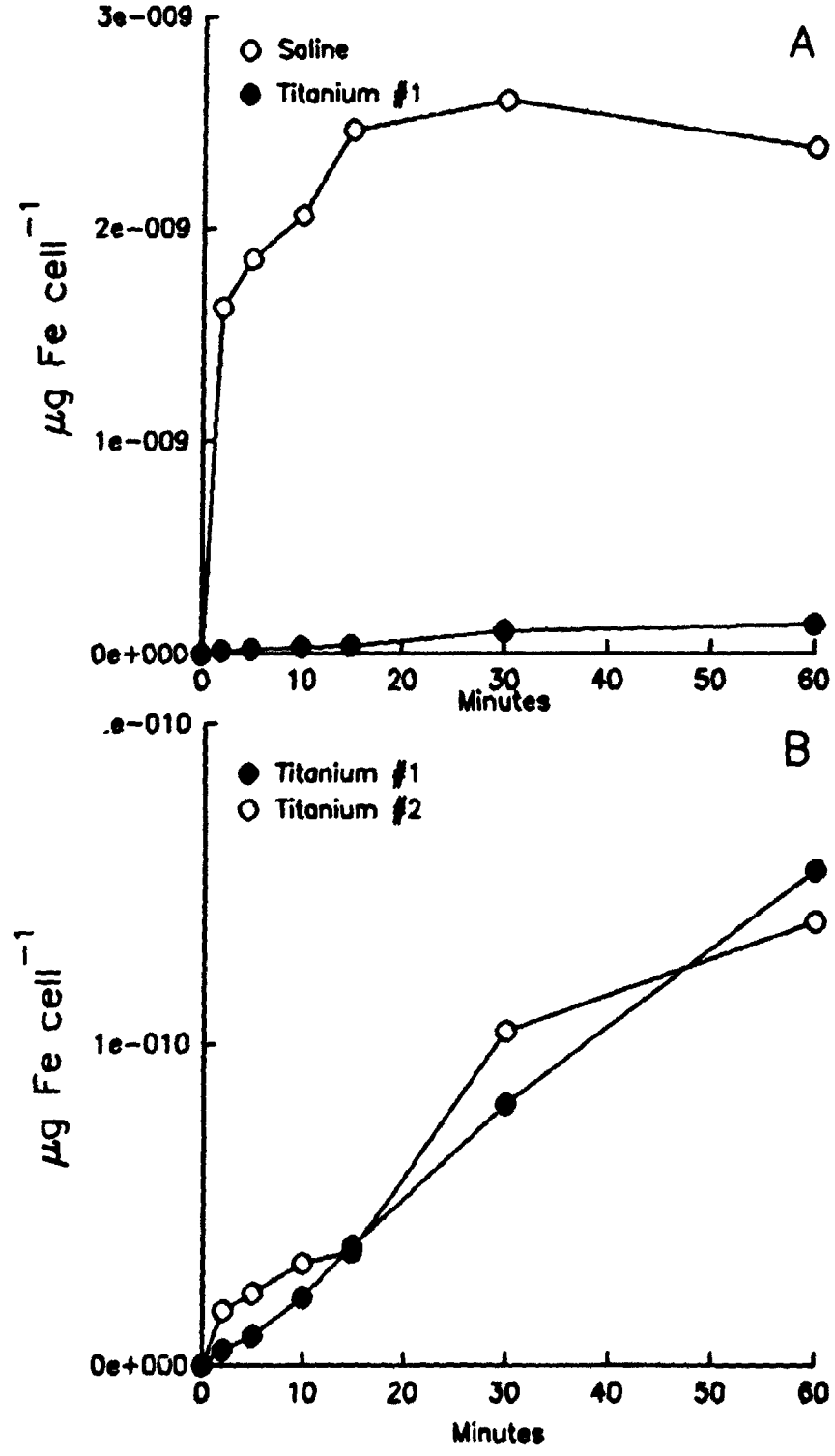
3e-009
2e-009
1e-009
0e+000
μg Fe cell⁻¹
Saline
Titanium #1
A
0
10
20
30
40
50
60
Minutes
.e-010
1e-010
0e+000
μg Fe cell⁻¹
Titanium #1
Titanium #2
B
0
10
20
30
40
50
60
Minutes

Table 12. Iron uptake rates and surface associations in iron-deficient and iron-replete cultures of *Synechococcus* sp. PCC 7002. **A).** A crude extract of siderophore containing all four siderophores produced by *Synechococcus* sp. PCC 7002 was utilized to test the effect of siderophores on iron uptake in *Synechococcus* sp. PCC 7002 with different iron growth histories. Chemostat grown cells were harvested and iron uptake monitored using the titanium-citrate-EDTA wash. Results are indicated as rate (with coefficient of variance) as well as per cent control. **B).** Surface associated iron was monitored by exposing cells to ^{55}Fe for 5 minutes then rinsing with the saline-EDTA wash. Results (± S.D.) suggest that the presence of siderophores decreases the surface associations of pFe 17 grown cells with iron while increasing the surface association of iron with pFe 21 grown cells.

A.		**pFe 17**	**pFe 21**
Uptake of ^{55}Fe $\mu g\ cell^{-1}\ min^{-1}$	Control (no added siderophore)	2.09×10^{-12} ($r^2 = 0.833$)	2.22×10^{-12} ($r^2 = 0.937$)
	With Siderophore	3.44×10^{-12} ($r^2 = 0.805$) (166%)	1.8×10^{-11} ($r^2 = 0.720$) (811%)
B.			
Surface Association $\mu g\ cell^{-1}$	Control (no added siderophore)	1.41×10^{-9} ($\pm 4.9 \times 10^{-11}$)	1.82×10^{-9} ($\pm 9.1 \times 10^{-13}$)
	With Siderophore	8.17×10^{-10} (58%)	2.76×10^{-9} (152%)

Increases in the level of $^{55}FeCl_3$ demonstrated no increase in uptake, suggesting that the transport systems were saturated for substrate. The amount of iron associated with the surface of pFe 21 grown cells was only 29% higher than that associated with pFe 17 grown cells. These values markedly change, however, when isolated, crude siderophore extract was added back to the systems. The iron uptake rate of pFe 17 grown cells increased to 166%, while the rate of iron uptake in pFe 21 grown cells increased to 811% of the control (no siderophore added) value. The increase in the uptake rate in the pFe 21 cyanobacteria was parallelled by an increase in the association of iron with the cell surface (Table 12). This was in contrast to the pFe 17 grown cells, where the presence of siderophores decrease the iron on the surface.

3.12 Effect of Photosynthetic Inhibitors on Iron Uptake

To determine if iron acquisition iron requires photosynthetic energy, inhibitors of photosynthesis were introduced to cells prior to an analyses of uptake. In all cases (sodium arsenate, triphenyl tin, and DCMU), the inhibitors were successful at reducing iron uptake rates to levels which were comparable to the rates of iron incorporation in cells which were monitored in the dark with no inhibitors added (Table 13). As demonstrated by the arsenate trials (Figure 23), the titanium-citrate-EDTA procedure allowed for an easy differentiation of light and dark rates in the control, and demonstrated that a low background rate of uptake continued in the inhibited cells. The results indicate

Table 13. Effect of photosynthetic inhibitors on iron transport in *Synechococcus* sp. PCC 7002. Titanium citrate results for iron uptake from iron-replete and iron-deficient cyanobacteria (in μg $cell^{-1}$ min^{-1} with coefficient of variance r^2). Results are presented as a percent of control for the specific iron level in order to highlight the differences.

	pFe 17	pFe 21
Control	2.09×10^{-12} ($r^2 = 0.833$)	2.22×10^{-12} ($r^2 = 0.937$)
Dark	4.6×10^{-13} (22.4%) ($r^2 = 0.939$)	1.8×10^{-13} (8.1%) ($r^2 = 0.854$)
4°C	3.0×10^{-15} (0.1%) ($r^2 = 0.024$)	7.0×10^{-14} (3.2%) ($r^2 = 0.083$)
Photosynthetic inhibitors		
DCMU (10 μM)	1.5×10^{-13} (7.3%) ($r^2 = 0.532$)	1.9×10^{-13} (8.6%) ($r^2 = 0.322$)
Triphenyl Tin (5 μM)	2.7×10^{-13} (13.2%) ($r^2 = 0.899$)	4.0×10^{-14} (1.8%) ($r^2 = 0.641$)
Arsenate (100 μM)	2.4×10^{-13} (11.7%) ($r^2 = 0.973$)	1.1×10^{-13} (5.0%) ($r^2 = 0.729$)

Figure 23. Affect of arsenate on iron uptake in *Synechococcus* sp. PCC 7002. Results for an iron uptake trial with pFe 21 grown cyanobacteria challenged with sodium arsenate. Both control and arsenate trials show similar rates of iron uptake (using the titanium-citrate-EDTA wash) during the dark period, but substantially different rates during light driven iron acquisition.

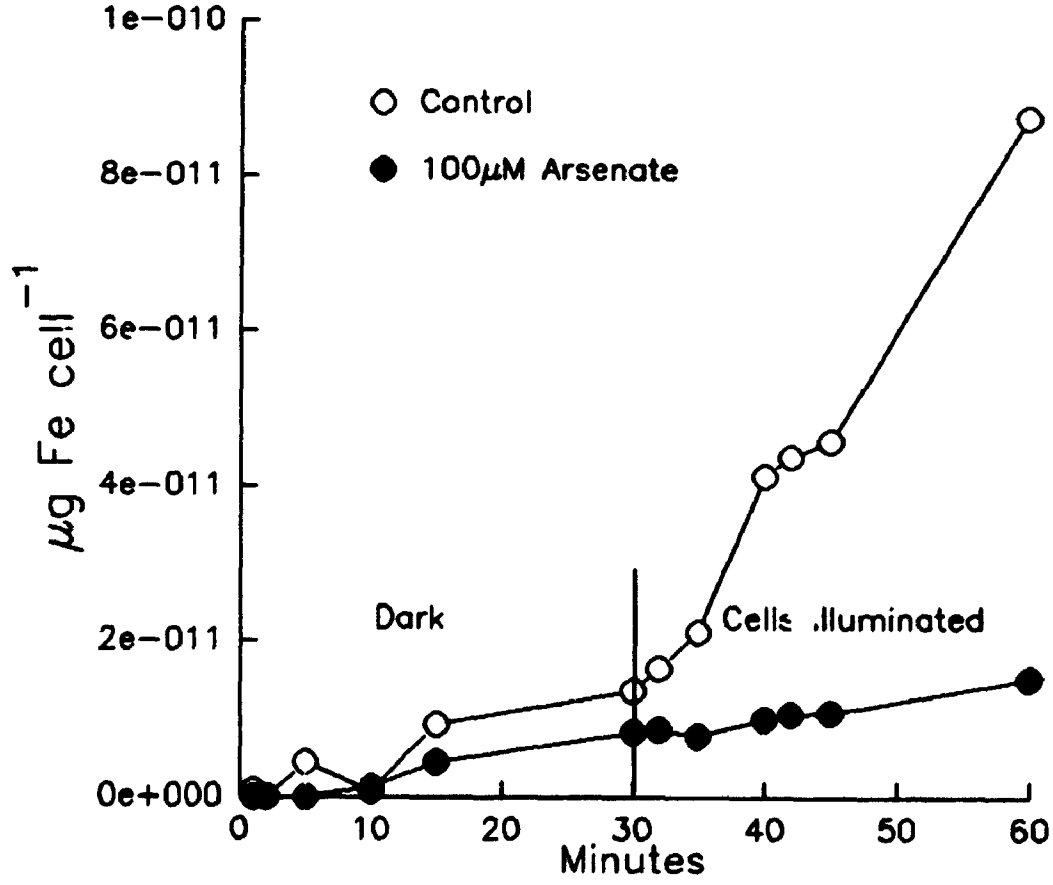
1e−010
8e−011
6e−011
4e−011
2e−011
0e+000
μg Fe cell⁻¹
Control
100μM Arsenate
Dark
Cells Illuminated
0
10
20
30
40
50
60
Minutes

that photosynthetic energy (production of which is inhibited by all these compounds) appears to be required for the acquisition of iron not only by pFe 21 grown cells but also by pFe 17 grown cells.

Acquisition of iron by cells was also analyzed at 4°C (Table 13). In both cases, the reduction in temperature dramatically reduced the rate of uptake. Upon returning the temperature to 37°C, the rate returned to normal.

3.13 Iron-Protein Associations

The association of $^{55}FeCl_3$ with isolated outer membrane and periplasmic fractions was examined in order to determine if iron status brings about changes in polypeptide iron-binding characteristics. The pFe 17 grown fractions consistently bound more iron than the pFe 21 grown fractions (Table 14). When compared to the control values, however, the presence of crude siderophores consistently increased the iron-binding capacity of pFe 21 periplasmic fractions while decreasing the iron/protein associations in the pFe 17 fractions. In outer membrane fractions, siderophores appeared to have no significant effect on the pFe 21 iron/protein interaction, but decreased this interaction (to 22.3%) in pFe 17 fractions. The presence of ß-mercaptoethanol decreased the iron/protein associations in the periplasmic samples as well as in the pFe 21 outer membrane sample (Table 14). There was, however, a slight increase in the iron protein association with siderophore when ß-mercaptoethanol was added to the pFe 17 outer membrane fraction.

3.14 Iron Content of *Synechococcus* sp. PCC 7002

The iron content of iron-limited *Synechococcus* sp. PCC 7002 was determined and is presented in Figure 24. Results demonstrate that cellular iron levels decrease proportionally with the availabilty of iron. Regression analysis of the log-log data yielded the following relationship:

$$[Fe_{internal}] = - 0.3482\ [pFe] - 2.6982$$

$$r^2 = 0.9758$$

Results are determined from ^{55}Fe incorporation, and have been corrected for iron introduced from the inocula.

Table 14. Iron-protein associations in isolated membrane fractions. Outer membrane and periplasmic components from pFe 17 and pFe 21 grown cells were examined for iron-chelating ability with and without the addition of siderophores ($n \geq 2$). "Sid & ß-mer" represents the addition of siderophore and ß-mercaptoethanol.

Outer Membrane	µg Fe (µg protein)$^{-1}$	Percent Control
pFe 17	3.86×10^{-5}	100
with siderophore	8.60×10^{-6}	22.3
with sid & ß-mer	1.19×10^{-5}	30.7
pFe 21	7.99×10^{-6}	100
with siderophore	8.11×10^{-6}	101.5
with sid & ß-mer	2.29×10^{-6}	28.7
Periplasmic Protein		
pFe 17	7.87×10^{-5}	100
with siderophore	6.29×10^{-5}	79.9
with sid & ß-mer	1.04×10^{-5}	13.2
pFe 21	3.77×10^{-6}	100
with siderophore	1.88×10^{-5}	498.4
with sid & ß-mer	1.66×10^{-5}	441.5

Figure 24. Iron content of *Synechococcus* sp. PCC 7002. Internal iron levels, as determined by the titanium-citrate method, are given (± S.D.). Values are presented in relation to predictions based on a diffusion mediated control of internal iron concentrations. Results are presented as a function of pFe value. (pFe 17 - pFe 20, n = 9; pFe 21, n = 12).

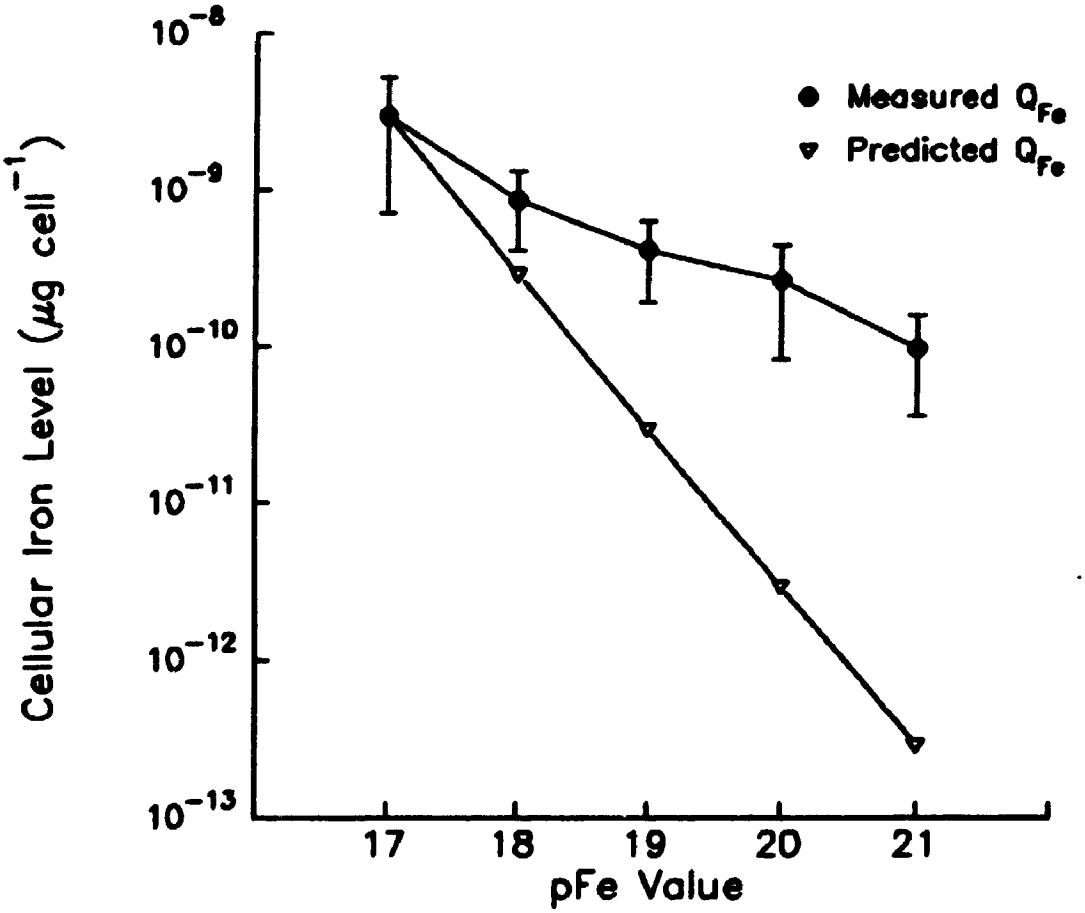
Cellular Iron Level (μg cell^{-1})
10^{-8}
10^{-9}
10^{-10}
10^{-11}
10^{-12}
10^{-13}
17
18
19
20
21
pFe Value
Measured Q_{Fe}
Predicted Q_{Fe}

4. Discussion

It has been established that cyanobacteria play an important role in the regulation of the biological and biogeochemical cycles in many aquatic systems (Section 1.1). It remains to be determined, however, which factors within these systems function to regulate cyanobacterial productivity. Many members of the scientific community now believe that the availability of iron may regulate production in certain aquatic systems. It was of preeminent interest, therefore, to determine how cyanobacteria respond to growth-limiting levels of iron availability, and to determine if they are capable of high-affinity iron acquisition.

4.1 Iron-Dependant Physiology

Cell densities in chemostat cultures demonstrate a level of recovery at pFe 21 values (Figure 9), suggesting that the cells are somehow able to compensate for the lower availability of iron. To accomplish this, cells may either lower their requirements for iron (the cellular iron quotient, Q_{Fe}), or increase their ability to scavenge iron from their environment. Work in batch culture (Rueter and Unsworth 1991) has demonstrated that some cyanobacteria maintain a non-linear relationship between iron availability and growth, while no siderophore production was detected. They did not, however, show any recovery in growth rate, unlike the results from either the equilibrated chemostats or the batch cultures of *Synechococcus* sp. PCC 7002. Growth recovery at low iron levels in *Oscillatoria tenuis* (Brown 1991), *Anacystis*

nidulans and *Anabaena variablis* (Kerry 1988) has been correlated to the ability to scavenge iron with a high-affinity system (Figure 3).

From the chemostat data the Q_{Fe} values can be calculated, but due to the non-linear cell yield with respect to iron concentration, one can only consider these values to be concentration specific (Table 15). These values reflect the requirement for iron in the medium in order to maintain cell density at a growth rate of 0.6 day^{-1}. Q_{Fe} is affected not only by the physiological variation within the cyanobacteria, but also by the changes in the iron scavenging ability of the cells. Brand (1991) utilized final cell density levels in batch culture in order to determine cellular quotients for 22 species of pelagic marine plankton. Brand (1991) rationalized that maximum cell yield in cultures shown to be iron-limited would be predictive of Q_{Fe} values for cells. He neglected to consider, however, the remobilization of iron during the lysis of cells, the exudation of organically complexed iron and the kinetic conversion of iron from a biologically unavailable form to a biologically available form as available iron levels are reduced. Brand also fails to consider that cyanobacteria, in stationary growth phase, differ physiologically from those in exponential growth phase (ie. natural populations). Results of this nature, therefore, bring into question their validity in extrapolations to natural populations.

Changes in cellular pigmentation have commonly been utilized as markers for cyanobacterial nutritional stress . Rueter and Unsworth (1991) concluded that it is unwise to use chla levels as normalization factors when

Table 15. Predicted cellular iron quotients from chemostat grown *Synechococcus* sp. PCC 7002. Cellular iron quotients based on mean steady state cultures within chemostats at specific iron availabilities. Results are expressed in terms of total iron (Q_{Fe}: M Fe cell^{-1}) as well as available iron (Q_{Fe3+}: M Fe $^{3+}$ cell^{-1}).

Chemostat pFe Value	Q_{Fe}	Q_{Fe3+}
17	1.20×10^{-12}	2.27×10^{-25}
18	2.14×10^{-13}	1.82×10^{-26}
19	3.88×10^{-14}	2.99×10^{-27}
20	2.70×10^{-14}	2.22×10^{-27}
21	4.21×10^{-16}	3.29×10^{-29}

varying iron status. Similar reductions in chl*a* with iron status were demonstrated in *Anacystis nidulans* (Öquist 1971, 1974a,b; Sherman and Sherman 1983; Guikema and Sherman 1984). This work supports these findings as well as demonstrates that changes in PC and PC/chl*a* ratio occur (Figure 11). For these reasons, most values have been normalized to per cell.

Ultrastructural changes have been noted in batch cultured *Synechococcus* sp. PCC 7002 (Hardie et al. 1983a). Examination of chemostat grown cells demonstrates that iron-limited growth brings about a reduction in thylakoid integrity (Figure 15). Other reports of *Synechococcus* spp. have confirmed that iron-regulated thylakoid disassociations do occur (Boyer et al. 1987). These changes are perhaps associated with a loss of structural components (proteins, lipids) brought about by nutrient deficiency. Low-iron grown cells also show a reduction in the number of cellular carboxysomes. This was not previously demonstrated in electron micrographs of batch cultured *Synechococcus* sp. PCC 7002 (Hardie et al. 1983a). Limitation of *Synechococcus* sp. PCC 7002 for other nutrients (i.e., vitamin B_{12}) has demonstrated both phenomena (see Appendix II).

The extrusion of protons has been associated with the strategies for iron acquisition of some organisms during periods of iron-limited growth. Here, the pFe 21 shift in pH would require the generation of 228 H^+ $cell^{-1}$ min^{-1}. This considers only the direct shift, and not the buffering capacity of the medium, which drives it significantly higher (8.6×10^5 H^+ $cell^{-1}$ min^{-1}). This shift in pH,

however, appears to have a neglible effect on the availability of Fe^{3+} to the cyanobacteria: the decrease in pH causes the concentration of Fe^{3+} to shift from 4.57×10^{-22} M (pFe 21.34) to 4.32×10^{-22} M (pFe 21.37) (calculated with Mineql* ver 2.1), slightly decreasing the availability of iron. The program is, however, unable to account for natural organic chelators (siderophores), and thus the effect of the pH shift on these compounds remains undetermined.

The extrusion of H^+ into the extracellular environment by higher plants occurs in several iron acquisition systems, including the Turbo Reductase system; this system leads to the reduction of organically complexed Fe^{3+} and its subsequent transport into the roots of certain plants (Bienfait 1987). Other organisms, such as yeast (e.g., *Sacchromyces cerevisiae*) exude protons to the medium to provide a simple and effective method of increasing the availability of iron in the environment (Neilands et al. 1987). The flux of protons here, however, may be associated with other parameters relating to changes in cellular physiology, and thus not a direct consequence of iron-limitation.

The transport of iron in eubacteria requires energy (ATP) for the translocation of the iron from the iron-siderophore complex into the cell (Braun et al. 1987). Such transport systems often involve proton-ATPases to generate ATP for iron transport and consequently translocate H^+ across the membrane (Figure 25). While cation-transport ATPases have been shown to exist in a *Synechococcus* sp. (Kanamura et al. 1993), it remains to be determined if such

Figure 25. Proton extrusion and ATPase involvement in iron acquisition. Illustration of the potential involvement of membrane associated ATPases in iron acquisition in cyanobacteria. During high-affinity iron transport, proton ATPases, intimately associated with ferrisiderophore transport proteins, would extrude protons to the environment while iron was assimilated. This process would utilize cellular ATP: the excess requirements of ATP to be met by cyclic photophosphorylation at photosystem I. A switch to cyclic photophosphorylation would result in a reduction in cellular carbon fixation and oxygen evolution. The net results demonstrate an internalization of Fe^{3+} (eventually converted to Fe^{2+} at some point), and the extrusion of H^+ to the extracellular environment.

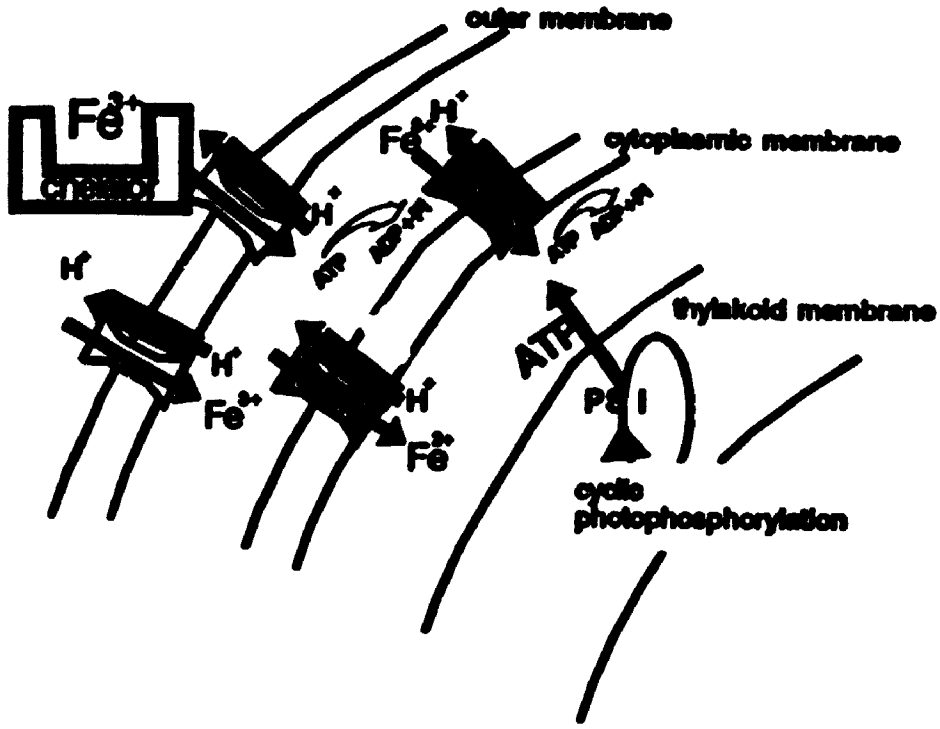
outer membrane
cytoplasmic membrane
thylakoid membrane
ATP
cyclic
photophosphorylation

a system is functional here. If an ATPase dependant system is involved in this cyanobacterium, it would partially explain the increase in the extracellular levels of H^+. This system would, however, create an increased ATP requirement within the cell; this increased supply of ATP must ultimately be accounted for.

The photosynthetic efficacy of iron-limited cells is of unique interest as it is of direct consequence of and to their physiological state. The reduction in carbon fixation rates to the level of the cellular carbon turnover rate (μ = doubling time of ≈ 40 hours) suggests that the luxury fixation of carbon (i.e., incorporation of carbon at a rate in excess of basic growth requirements) in the pFe 17 chemostat requires excess iron (Table 6). The carbon fixation rates of the pFe 17 grown cells are similar to those of natural populations of marine *Synechococcus* spp. (Table 15), with the pFe 21 rates being significantly less. It is important to note, in comparison, that the natural populations are under pressures of grazing, light intensity fluctuations, and nutrient fluctuations that do not affect the chemostat grown cyanobacteria.

The decrease in carbon fixation levels is paralleled by changes in the oxygen evolution profiles (vs. light intensity) of cells under iron-limitation (Figure 14). A relative decrease in the maximum oxygen evolution rate as well as the apparent quantum efficiency (Φ_{app}) occurs in both the pFe 19 and pFe 21 grown cells in comparison to the pFe 17 cultures. This supports the carbon data in suggesting that an alteration in physiological parameters has occurred. Oxygen evolution in pFe 19 cells, in comparison to the pFe 21 attests to this variation

Table 16. Carbon fixation rates in natural populations. A comparison of laboratory results (this study) for pFe 17 and pFe 21 grown *Synechococcus* sp. PCC 7002 and *in situ* measurements of carbon fixation rates in natural populations of *Synechococcus* spp. (Waterbury et al. 1987).

	Carbon Fixation
***Synechococcus* sp.**	(*f*g cell^{-1} h^{-1})
PCC 7002	
pFe 17 chemostat	22.38
pFe 21 chemostat	3.2
Natural Populations	
Surface measurements	40
80m below surface	16

in their iron physiology. It is possible that the decrease in oxygen evolution may be the result of a proportional increase in cyclic photophosphorylation in photosystem I; this process decreases cellular rates of carbon fixation and oxygen evolution while maximizing ATP production (Lawlor 1987). This shift would be cued by an increased cellular ATP demand resulting from the energetic requirements of ferrisiderophore translocation (Figure 25). The differences in carbon fixation and oxygen evolution between pFe 17 and pFe 21 cultures not only demonstrate that variations in cellular metabolism exist. They also support the concept that an increase in the cyclic photophosphorylation of ADP to ATP by photosystem I is occurring. This actual shift is, however, is not (and was not intended to be) demonstrated by these experiments.

While changes in the cellular utilization of iron are obvious from the data, the main purpose here was to identify components of, and demonstrate evidence for the activity of a high-affinity iron transport systems (should such a system have been found). Reports of siderophores and iron-regulated proteins do exist in the literature (see Sections 1.4 - 1.7), but the complete characterization of a system within a single coccoid cyanobacterium remains to be accomplished. Accomplishment of this task would establish a potential bioassay organism for iron-limited environments. The components which were searched for were based on the systems of *Escherichia coli*, which are now well documented (Neilands 1977, 1982; Winkelmann et al. 1987; Winkelmann 1991).

4.2 Siderophore Production By Cyanobacteria

The prevalence of siderophore production and utilization of high-affinity transport schemes in cyanobacteria has been of some debate (Rueter and Unsworth 1991). Ten species of cyanobacteria were examined here, all of which produced detectable iron-chelating compounds by these techniques (Table 10). Of the ten, seven were shown to produce multiple siderophores, and six were shown to produce catechol-type siderophores. Other low iron compensation mechanisms, including reductions in cellular Q_{Fe} (Reuter and Unsworth 1991) and the use of surface reductases (Boyer and Morse 1992), have been proposed for cyanobacterial species. These results suggest that siderophore excretion may be a common response by *Synechococcus* spp., as well as other species of cyanobacteria, to growth-limiting iron levels. The frequent identification of catechol-type siderophores further suggests that catechol-type siderophores may play an integral role, not previously examined, in cyanbacterial high-affinity iron transport. Previous characterizations of siderophore production by cyanobacteria have focussed on the hydroxamate-type siderophores, utilizing the test of Czaky (1948) and bioassays with hydroxamate-type siderophore auxotrophs (Boyer et al. 1987). This description of catechol-type siderophore production and evidence suggests that cyanobacteria may be utilizing a variant of eubacterial high-affinity iron transport systems (Section 4.7).

4.3 Siderophore Production In Continuous Culture

The ability of some cyanobacteria to produce siderophores, under iron-limiting conditions, has been widely accepted for some time (Boyer et al. 1987). The actual effect of siderophores on cyanobacterial iron physiology, however, is still of some debate. Analysis of siderophore production here has shown that hydroxamate-, catechol-, and atypical-type siderophores are produced by *Synechococcus* spp. during periods of iron-limitation. *Synechococcus* sp. PCC 7002 produces catechol- and hydroxamate-type siderophores maximally at pFe 19, but a recovery in growth does not occur until pFe 21. This suggests that the presence of siderophores alone is not sufficient to remove the constraints of iron-limitation from these cyanobacteria . The decrease in detectable levels of siderophore production at pFe 21 further suggests that there is either a physiologically-controlled decrease in the level of siderophore production, or an increase in utilization (and subsequent removal from the medium) of the siderophores by the cyanobacteria. This last possibility is consistent with the increase in cellular proliferation within the chemostat reactors and the increase in growth rate seen in pFe 21 batch cultures.

The presence of siderophores in natural environments is expected to function to increase the total availability of iron in these systems. The siderophores scavenge iron to such an extent that biologically unavailable iron becomes biologically available, thereby increasing the total available iron in the system. The amount of "new" iron becoming available would be dependant not

only on the rate of siderophore production, but also on the release of organically complexed iron from the cyanobacteria and the ability of other organisms to utilize ferrisiderophore and organically complexed iron sources.

4.4 Iron-Regulated Membrane Proteins

If the production of siderophores is not the limiting factor in the uptake of iron from the environment, then the production of the components of uptake (e.g., membrane proteins) may be. Freshwater cyanobacteria do not assimilate S^{35}-methionine or other amino acids well (Scanlan et al. 1993). Proteins are thus presented in silver or Coomassie stained form. Results here demonstrate that the concentration of a number of specific proteins is altered during periods of iron-limitation. Similar results in *Oscillatoria tenuis* (Brown, 1991) and *Synechococcus* sp. PCC 7942 (Scanlan et al. 1987) suggest that some of these proteins may indeed be ferrisiderophore transport proteins. Proteins detected in *Synechococcus* sp. PCC 7002 all appear to be of a size similar to those produced in fungal and eubacterial iron transport systems (Braun et al. 1987).

The isolated membrane fractions from pFe 17 grown cells have a higher affinity for unchelated ^{55}Fe (from $^{55}FeCl_3$) in comparison to the pFe 21 fractions. The presence of siderophores, however, decreases the capacity for iron of the pFe 17 fractions, while increasing the affinity for iron of the pFe 21 fractions (Table 14). This demonstrates that the iron-binding capacity of pFe 17 proteins may not be transport related. Cytochromes, ferredoxins, carbohydrates and

acidic peptides in the pFe 17 fractions may add to the overall iron-binding capabilities. In pFe 21 cells, a switch to non-iron integral components (ie. from ferredoxin to flavodoxin) combined with a reduction in the level of iron-containing enzymes, results in the apparent decrease in affinity for the unchelated iron in the controls. The production of ferrisiderophore specific proteins by pFe 21 cells brings about an increase in the apparent affinity of fractions containing these proteins for iron. Without these proteins (pFe 17 fractions), the iron is chelated away from the membrane fractions by the siderophores. Thus it appears that the pFe 21 periplasmic proteins do contain some form of ferrisiderophore receptor proteins.

The minimal increase in the pFe 21 outer membrane iron associations in the absence of siderophores suggests that either the sites are already saturated with iron, or that the association of the proteins with ferrisiderophore complexes requires interactions or conformations not possible with the isolated protein fractions. In *Escherichia coli*, proteins traversing the periplasmic space from the cytoplasmic membrane to the outer membrane are required for ferrisiderophore mediated iron acquisition; they allow for conformational changes and energy translocation events (Braun et al. 1987). The protein in the isolated membrane fractions may not be able to associate with the ferrisiderophore complexes due to inability to attain the proper conformation.

4.5 Iron-Binding and Transport in *Synechococcus* PCC 7002

Analysis of the iron bound to the surface of pFe 17 and pFe 21 cells confirms that the pFe 21 cells are producing ferrisiderophore specific proteins (Table 12). The increase in surface association of $^{55}FeCl_3$ with pFe 21 grown cells, when siderophore is added, illustrates that there are ferrisiderophore receptors on the surface of the cells. The absence of these receptors in the outer membrane of pFe 17 grown cyanobacteria brings about a reduction in iron surface associations as the siderophore chelates the iron away from the cell.

The activity of a high-affinity iron transport system is illustrated by the titanium-citrate-EDTA data for whole cell iron uptake (Table 12). Addition of crude siderophore increases the iron uptake rates in pFe 17 and pFe 21 grown cultures. The small increase in iron uptake rates by the pFe 17 grown cells is most probably due to an increase in the availability of Fe^{3+} in the microenvironment around the cells, as the addition of chelators (in this case the siderophores) will alter the iron equilibria (ie. pFe level) within the medium. The marked increase in iron uptake rate of pFe 21 cells, taken with the other evidence, is testimony to the activity of a high-affinity iron transport system.

These rates of iron transport into the cyanobacteria represent subtrate saturated levels, and thus may not represent normal rates. Iron-deficient *Synechococcus* sp. PCC 7002 appear to scavenge iron maximally at a rate of 3.20×10^{-15} g Fe cell^{-1} d^{-1} without added siderophore and at 2.59×10^{-14} g Fe cell^{-1} d^{-1} with added siderophore. This is similar to predictions for other marine

phytoplankton grown under iron-limiting conditions. In *Pleurochrysis carterae* a marine coccolithophorid, iron uptake rates have been estimated in similar experiments to be 2.9 x 10^{-14} g Fe $cell^{-1}$ d^{-1} (Hudson and Morel 1990), while the diatom *Thalassiosira weissflogii* assimilates iron at 2.4 x 10^{-13} g Fe $cell^{-1}$ d^{-1} (Harrison and Morel 1986). Dark rates for *T. weissflogii* iron assimilation (in iron-deficient cultures), estimated to be 2.00 x 10^{-13} g Fe $cell^{-1}$ d^{-1} (Anderson and Morel 1982), are more rapid than the dark rate (no siderophore added) for *Synechococcus* PCC 7002 (2.64 x 10^{-16} g Fe $cell^{-1}$ d^{-1}). It is difficult, however, to compare these rates due to the contrast in cell size. Expression of iron uptake rates in terms of cell volume shows that *Synechococcus* PCC 7002 assimilaties iron at a higher rate than the eukaryotic phytoplankton (Table 17).

Similar normalization of the chemostat predicted Q_{Fe} values for *Synechococcus* sp. PCC 7002 demonstrates that, for iron-limited cultures, this cyanobacterium has a higher iron requirement per unit volume (μm^3) in comparison to the eukaryotic phytoplankton (Table 18). This is expected for two reasons. The larger size and structural organization of the eukaryotic phytoplankton, in comparison to the cyanobacterium, intrinsically suggests that the eukaryotes require a greater proportionality of structural material. This manifests itself as an increase in the C:Fe of the cell, as the carbon based structural components (eg. cellulose, sugars) generally require little iron. Similar results are seen in comparisons of the nitrate requirements of prokaryotic and eukaryotic phytoplankton (Whitton 1992). *Synechococcus* sp.

Table 17. Normalization of iron assimilation rates (pFe 21) and a comparison with other phytoplankton. Iron uptake rate are normalized to cell volume (* adapted from Hudson and Morel 1990).

	***Synechococcus* PCC 7002**	***Pleurochrysis carterae****	***Thalassiosira weissflogii***
Fe Uptake$_{max}$ (g Fe cell^{-1} d^{-1})	3.2×10^{-15}	2.9×10^{-14}	2.4×10^{-13}
cell volume (μm^3)	2	407	736.6
Normalized Rate (g Fe μm^{-3} d^{-1})	1.6×10^{-15}	7.13×10^{-17}	3.26×10^{-16}

Table 18. Normalization of Q_{Fe} and comparison to other phytoplankton.

A) Q_{Fe} for phytoplankton grown under iron-deficient conditions and normalized to cell volume (* adapted from Hudson and Morel 1990). Values for *Synechococcus* (pFe 21) were converted from Table 15. **B)** Normalization of values to intracellular carbon based on batch culture levels and 125 fg C cell^{-1}. Values are compared to those for *Thalassiosira oceanica* and a total algal sample from sub-Arctic Pacific station T-6 (Sunda et al. 1991).

A.

	***Synechococcus* PCC 7002**	***Pleurochrysis carterae*** *	***Thalassiosira weissflogii*** *
Cell Quotient (at μ) amol cell^{-1} d^{-1}	4.2	50 - 100	100 - 200
μ (div d^{-1})	0.6	1.0	2.0
cell vol (μm^3)	2	407	736.6
Q_{Fe} μm^{-3}	2.1	0.123 - 0.246	0.136 - 0.272

B.

	***Synechococcus* PCC 7002**						
	pFe 17	**pFe 18**	**pFe 19**	**pFe 20**	**pFe 21**	***T. oceanica***	**Sta. T-6**
Fe:C (*m*mol:mol)	5.10	1.480	0.708	0.455	0.150	2.0×10^{-3}	2.6×10^{-3}

PCC 7002 also represents a coastal species of cyanobacteria (Van Baalen, 1968). Coastal phytoplankton typically have higher Q_{Fe} values than the open ocean species (Brand 1991). This may explain the higher Q_{Fe} μm^{-3} of the cyanobacterium.

4.6 Energetics of Iron Acquisition

The titanium-citrate procedure, combined with the photosynthetic inhibitors, was utilized to determine if cellular energy was required for iron acquisition. Results demonstrate reductions in iron acquisition rates in the presence of these photosynthetic inhibitors in both pFe 17 and pFe 21 grown cyanobacterial species (Table 13). The rates, in the presence of these inhibitors, are similar to the rate of iron uptake in cells maintained under no illumination. While this suggests that energy may be required for iron transport at all times, the reduction may also be due to a reduction in the overall cellular physiology, creating a buildup of free Fe in the cell as cellular requirements are satiated. The current dogma suggests that iron acquisition under iron-replete conditions is diffusion mediated (Neilands 1977; Section 1.7), and reduction in cellular metabolism would reduce the iron concentration gradient and subsequent assimilation rate. It may also be interpreted, however, that energy (ATP) is required for Fe acquisition at all levels, perhaps in the form of a low level surface reductase or low-affinity transport system. The presence of reductase-type components has been suggested to be involved in iron

assimilation in some *Anabaena* spp., where siderophores are not produced (Boyer and Morse 1992).

The utilization of photosynthetic inhibitors was also investigated by Hudson (1989). His work demonstrated that some uncouplers are successful at reducing iron transport in the coccolithophorid *Pleurochrysis carterae* (CCCP inhibits iron uptake rates by 80.0%) while others were less successful (DNP inhibits iron uptake by only 15.0%). Hudson reasoned that the pKa of the unsuccessful uncoupler (4.1 for DNP) was responsible for their lack of efficacy under these conditions (pH 8.1). It is important to note though that *P. carterae* does not produce any extracellular siderophores (Hudson 1989), thus it is difficult to compare these systems.

4.7 High-Affinity Iron Acquisition

In this thesis, I recognize and determine two iron-uptake velocities for what I describe as the low (free ferric iron) and high-affinity (siderophore-mediated ferric ion) transport. High-affinity iron transport systems in microorganisms are typically identified by the presence of the mechanistic components of these systems, and the subsequent regulation of these systems by the availablity of iron. Since the concept of "affinity" of iron transport has a significantly different meaning than in the context of nutrient transport, the description of affinity within iron-transport requires explanation.

Macro-nutrients such as nitrate and phosphate have low solubilities in lipids and very slow diffusion rates through cell membranes. Transport into an algal cell is usually modelled after the two-step enzymatic reaction (*a*): 1) chemical binding to the uptake site and 2) transfer through the cell membrane and delivery to the inside of the cell. The kinetics of this type of transport are described through the traditional Michaelis-Menten reaction kinetics. For the transport reaction (*b*), the uptake rate is described as (*c*).

a. $[E] + [S] \underset{K_{-1}}{\overset{K_1}{\rightleftharpoons}} [ES] \xrightarrow[K_{cat}]{} \{EP\} \rightarrow [P] + [E]$

Where E is the enzyme, S is the substrate, and P is the product of the reaction.

b. $S \underset{K_{-L}}{\overset{K_L}{\rightleftharpoons}} SL \xrightarrow{K_{cat}} Cell$

Where S is the nutrient, L is the surface bound nutrient transporter.

c. $\rho = [S] / (K_m + [S])$, where $K_m = (K_{-1} + K_{cat}) / K_1$

From the two step model, two important parameters of transport can be determined: the maximum uptake rate (ρ) and the half-saturation constant (K_m). These two parameters provide information on the concentration of the uptake sites and the reaction rate constants, respectively. In most reactions the

slowest step is the catabolism step (K_{cat}), allowing K_m to approximate $\{K_{-1}/K_1\}$, the binding constant of the substrate to the cell. The smaller the value of K_m the larger the avidity- or the higher the affinity of the transport system for the nutrient S. However, the attractiveness of S to L is a thermodynamically-fixed property of L. Defining a transport system as a "high" or "low" affinity system can only be done through a comparison of two systems with comparable L. In this situation, the affinity of the substrate can be experimentally determined and, through comparison, the system expressing the lowest K_m is declared the "high(er) affinity" system.

Direct incorporation of Michaelis-Menten type nutrient transport into an iron transport model is not acceptable since the basic formulation of the model can not be met. We must consider the model of the transport system to include an external reactive pool of "biologically unavailable" iron. Iron added to the environment is involved in a competitive equilibrium between cellular transport and kinetic incorporation onto the external pool ($\underline{d}$). It is experimentally clear (Hudson 1989) that the level of iron denoted as biologically available (Fe*) contrc's the transport velocities. Thus, at low concentrations of Fe (where [Fe*] < Km) transport is linearly related to [Fe*]. However, if the concentration of iron were to be elevated to increase [Fe*] to a point where [Fe*] > K_m, the reaction to form biologically unavailable iron is sufficiently fast that the cell ligands (L) that bind Fe are undersaturated for the desired [Fe*] and the transport becomes independent of [Fe*]. In this case the relationship between velocity

and concentration cannot be determined since the stable level of Fe* is controlled by the relative rates of formation (K_p) and dissociation (K_{-p}) of the competing complexes of iron in the chemical environment and the Fe-L complex at the cell surface.

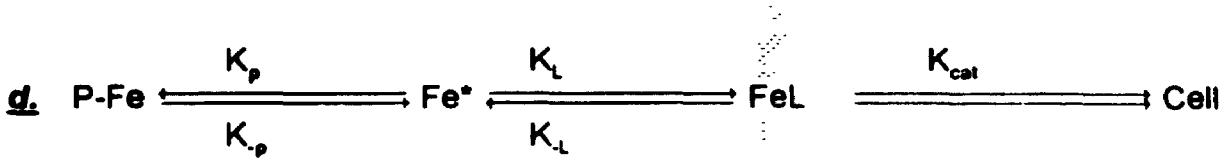

Where P is the pool of biologically unavailable iron, L is the cell surface ligand, and Fe* is the fraction of biologically available iron.

In conclusion, Michaelis-Menten kinetics cannot be used to describe the affinity of the transport of iron (or to verify the high- or low-affinity characteristics of the system) since no relationship can be established (at the scale of the velocity of iron transport) between the concentration of externally available iron and the velocity of the transport of the substrate to tne product. It is also impractical, as my uptake for pFe 21 cells is substrate saturated, and contamination makes studies below pFe 21 suspect as the level iron contamination, even with Chelex-100 treated reagents, often is of the same order of magintude as the introduced iron (D. Muggli, pers. comm.).

While it is clear that uptake velocities cannot be utilized to describe affinity of the transport system to the level of iron in the medium, the growth rates of cells at different levels of iron indicate the relative "affinities" of the cells to the limiting nutrient. I have been able to consider the growth rate of cells at

steady-state (chemostats) and in batch culture where the level of available iron [Fe*] has been established by varying the total pool of iron and by using an external chelator (EDTA). In these experiments, the velocity of iron transport is a function of the cellular requirements of the limiting nutrient (Q) and the specific growth rate of the cells ($\rho = \mu Q$). Since I have shown that the cellular quota decreases less than the level of the total available iron when the cells are limited by iron ($\Delta Q_{Fe} = -0.34$ when Δ pFe = -1.00), and yet the growth rates are maintained, then the transport rate of iron into the cell must be modified to compensate for the decreasing [Fe*] concentration. This transport system can be viewed as (*d*), where for the higher iron concentrations a pseudoequilibrium can be considered. That is, the rate of uptake (ρ) is dependant on a calculated [Fe*] until a critically low [Fe*] is obtained and the siderophore mediated transport system is induced. The presence of this system is verified by the determination of extracellular and cell-bound components, but the affinity of this system is established through the recovery of the growth rates of the cells at very low calculated [Fe*] levels. To achieve these growth rates the induced system must supply iron to the cells at a relatively fast rate (to match the growth rate) by increasing the affinity of the system for iron from the "biologically unavailable" pool of reactive iron (*e*). Thus the "affinity" of the iron transport system has little to do with the velocities of the transport and more to do with the modification of the relative availabilities of the iron pool to the cell.

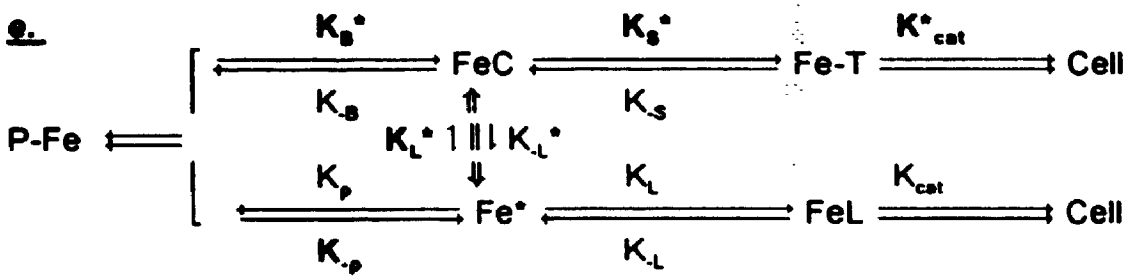

$$\rho = 1/Q\ [K_L + K_S]\ [Fe^* + FeC]\ [L_{Tot} + T_{Tot}]$$

Where:
C is the external siderophore or siderophore complex.
T is the siderophore-iron membrane transporter.

The increased ability of the cells to effectively draw on the external pool of iron is experimentally demonstrated by an analysis of chemostat Q_{Fe} values with respect to the total cellular iron content over a range of iron concentrations (Figure 26). These results provide an insight into the size of the external iron pool required for cells to assimilate a single unit of iron. For pFe 17, 18, 19 and 20 grown cells, high levels of iron are required for cells to assimilate a single unit of iron. For pFe 21 grown cells the level of iron required to assimilate a single unit is more than an order of magnitude less than for the other iron concentrations, suggesting that these cells are capable of utilizing a smaller pool to saturate a given iron requirement. The only explanation for this is an increased ability of the cells to utilize the previously biologically unavailable iron in the system. Thus, by increasing their ability

Figure 26. External iron pool requirements for *Synechococcus* sp. PCC 7002. Q_{F_e} predictions from chemostat data (Table 15) are normalized to cellular iron requirements (Figure 24). Results reflect the envirnmmental pool size of external iron for cells at a specific pFe value relative to the incorporation one unit of iron.

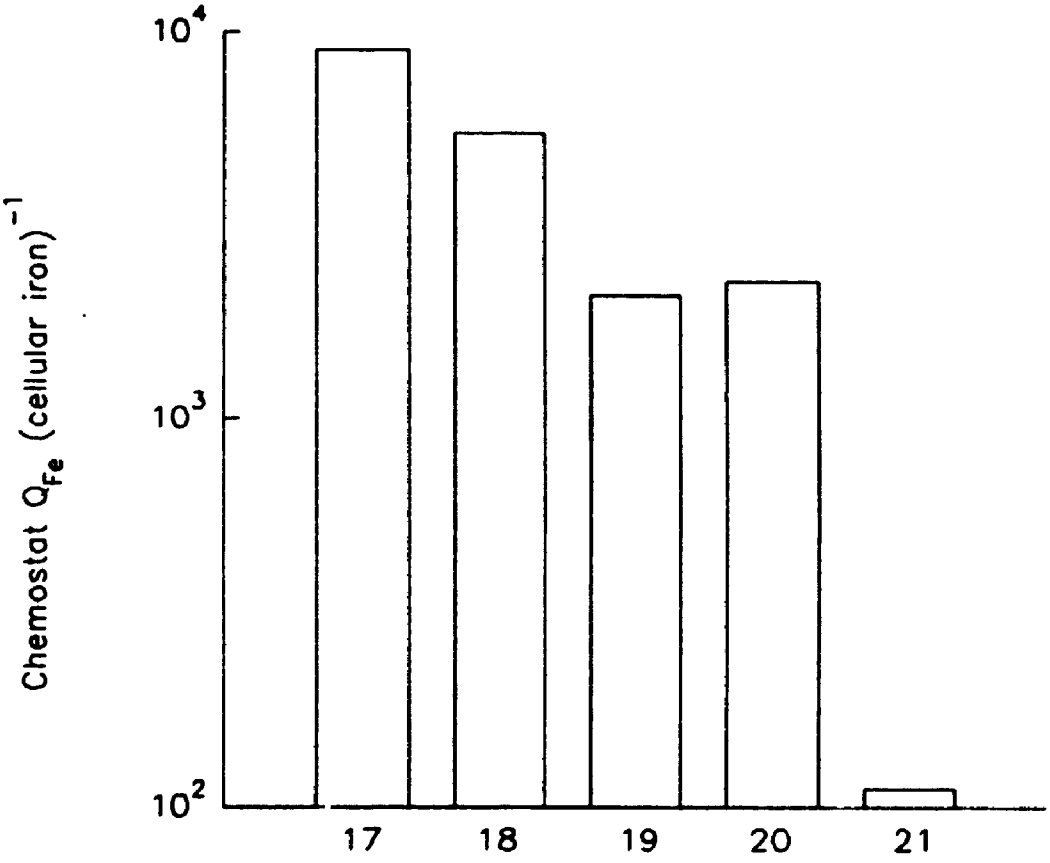
Chemostat Q_{Fe} (cellular iron)$^{-1}$
10^4
10^3
10^2
17
18
19
20
21

to utilize more of the environmental iron pool, the cells have increased their "affinity" for iron in the system.

It is important to note that increased affinity may not manifest itself as an increase in the rate of iron assimlation in comparison with uptake systems of other affinities. Normalization of the batch culture iron quotas to growth rate demonstrates that pFe 17 cells maintain a higher net uptake rate (3.78×10^{-17} moles cell^{-1} d^{-1}) than pFe 21 cells utilizing high-affinity iron transport (1.1×10^{-18} moles cell^{-1} d^{-1}). This highlights the important distinction between the velocity of uptake and the affinity of a system for a substrate.

4.8 Cyanobacterial Strategies For Iron Acquisition

Most cyanobacteria, unlike many fungi and eubacteria, are forced to deal with the acquisition of nutrients in aquatic environments where the diffusion of organics released from the cell, in a combination with a positional flux of the organism due to mixing events in the water column, would decrease the probability of ferrisiderophore association with the cell. In most aquatic systems, microbial acquisition of nutrients is carried out by "finesse" transport systems; systems commonly associated with Gram-negative bacteria involving membrane associated components and energy driven transport (Neilands 1977; Kadner 1990). Exo-enzyme activity, such as utilized by many Gram-positive organisms is intrinsically unsuccessful due to the dilution effect that occurs in

open aquatic environments. It is thus a curiosity that cyanobacteria would secrete extracellular organics in an attempt to increase cellular iron levels.

The results of these experiments suggest that cyanobacterial high-affinity iron transport involves the serial utilization of multiple siderophores (Figure 27). When initially challenged by low levels of iron, cyanobacteria excrete hydroxamate-type siderophores to the environment in order to increase the solubility of iron in the microenvironment around the cell. These siderophores are hydrophilic in nature and freely diffuse through the aquatic environment.

Iron-limited cells also release hydrophobic catechol-type siderophores, which concomitantly associate with the surface of the cell due to their hydrophobicity. The identification of chloroform soluble compounds associated with the surface of *Synechococcus* sp. PCC 6301 (Section 3.10) confirms suspicions about the localization of hydrophobic catechols on the surface of cyanobacteria. When a hydroxamate-type siderophore, complexed to Fe^{3+}, comes within proximity of the cell, the catechol-type siderophores strip ferrihydroxamate complex of its iron. The iron transfer is facilitated by the catechol-siderophores higher affinity for iron in comparison to the hydroxamate-type siderophore (Mantzanke 1991). This suggests that the true "high-affinity" part of the system is based on the kinetics of catechol-type siderophore transport and/or the hydroxamate-catecholate iron transfer event.

This system may also explain the relationship between the production of iron chelators by cyanobacteria, and a reduced susceptibility to toxic levels of

Figure 27. Acquisition of iron by cyanobacteria. During periods of iron-limited growth, the release of siderophores on the cell may be accompanied by the expression of ferrisiderophore specific proteins of the cell surface. **A)** Iron acquisition involving only the production of hydroxamate-type (**H**) siderophores functions similar to eubacterial systems. **B)**. Production and subsequent expression of catechol-type (**C**) siderophores on the surface of the cell estabilishes a serial iron transfer; iron is transferred from the ferrihydroxamate complex to the catecholate siderophore prior to its internalization into the cell.

A.

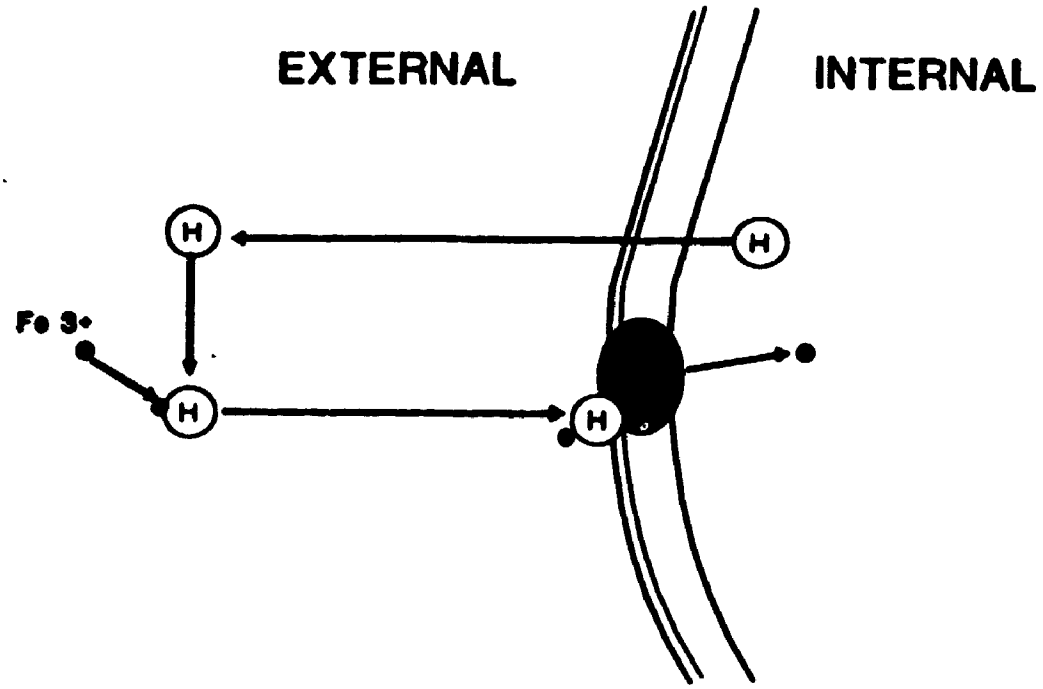

B.

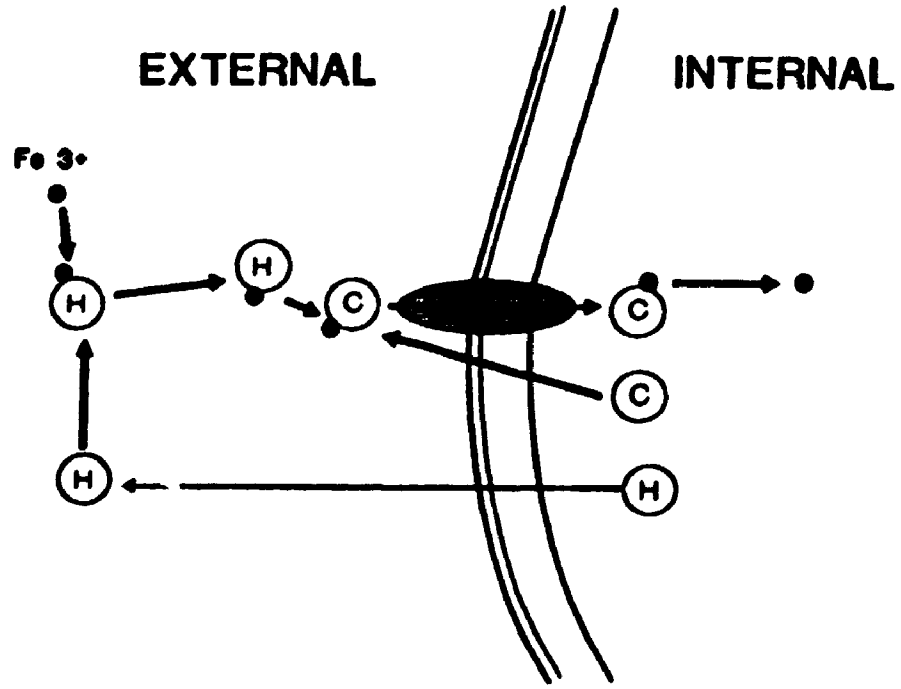

trace metals. Copper toxicity, in cyanobacteria, has been shown to be offset by the presence of extracellular iron chelators (McKnight and Morel 1979, 1980; Clarke et al. 1987). Addition of the hydroxamate-type siderophore schizokinen to iron-replete and iron-deficient cultures of *Anabaena* sp. strain 7120 (a cyanobacterium which produces schizokinen) has been shown to alleviate copper toxicity (Clarke et al. 1987). It is thought that the chelation of the copper by the siderophore prevents the assimilation of the copper into the cell. The question remains, however, as to why the copper-siderophore complex is not transported into the cell by the iron high-affinity transport machinery. While this may be an effect of the conformational requirements of the metallosiderophore complexes for transport, selectivity, at the surface of the cell by catechol-type siderophores, may in part explain this phenomenom. When the catecholate compounds are presented with ferric-hydroxamate complexes at the surface, they remove the iron from the complex, and the iron is subsequently transported into the cell. In situations where the hydroxamate-type siderophore is associated with copper, the greater selectivity of the catechol prevents it from assimilating the copper. This functions to impart a degree of resistance to toxic levels of copper while in turn scavenging iron. The affinities of the catechol-type siderophores for copper remain to be determined.

This suggests that it would have been interesting to look at the effect of copper on iron uptake rates. If copper associates with the siderophores produced by

Synechococcus sp. PCC 7002, then it would affect the rate of iron assimilation during high-affinity iron transport.

4.9 Implications for the Global Aquatic Environment

It is difficult to infer from these results the complete implications of iron-limitation on aquatic systems. The dynamics of these environments is multidimensional; nutrient flux, primary productivity, grazing rate, microbial nutrient remobilization and the physical events of mixing and light penetration all interact intimately. If primary productivity is limited by the availabiltiy of Fe^{3+}, then altering this may have dramatic consequences. Shifts in species composition, brought about by iron fertilization, have already been demonstrated during on-ship experiments in the Pacific (Martin and Gordon 1988). These fluctuations increased the relative abundance of diatom populations, at the expense of other planktonic algae. Experiments with iron-limited natural populations from the sub-Arctic Pacific Ocean have further demonstrated that the addition of iron markedly increases diatom population, while indigenous populations of coccoid cyanobacteria remain unaffected (P.J. Harrison, pers.comm.). Repression of high-affinity transport in cyanobacteria, if such systems are active in the natural population may function to decrease their productivity (as a pFe 21 to pFe 20 shift in a chemostat system would). The implications of such an event are numerous.

The ability of cyanobacteria have to utilize iron which is biologically unavailable to other organisms also presents interesting implications for the pelagic iron cycle. If open ocean cyanobacteria respond to iron-limitation in a manner similar to *Synechococcus* sp. PCC 7002, then models for an oceanic iron cycle would require that the conversion of iron from biologically unavailable to available must be considered. This is definitely an area that future research must consider.

These results do demonstrate, however, that iron may play an integral role in the phytoplankton driven aspects of carbon flux in aquatic systems. Carbon flux into the oceans is an important part of the global carbon cycle (Chisholm and Morel 1991). Understanding the role of the picoplankton in this process will lead an increased ability to predict the affects of anthropomorphic perturbations on the aquatic systems on our planet.

5. Conclusions

In this thesis, I have demonstrated that *Synechococcus* has a defined physiology when confronted with a low iron environment. The cell's physiology shifts in such a manner as to actively scavenge iron from the environment by producing siderophores and membrane proteins that have a high affinity for iron. Siderophore production involves the release of multiple siderophores in the genus *Synechococcus*, including hydroxamate-, catechol-, and atypical-type compounds. These scavenge iron to such an extent that previously unavailable iron becomes available to the organism, and therefore to the biological system in general. The result of siderophore release in cyanobacteria is an increase in the overall ability of the cell to assimilate iron, which manifests itself in a greater level of surface affinity of the cell for iron as well as an increase in the rate of iron uptake. Concurrent to this is a decrease in the cells overall requirement for iron, although the decrease in iron requirements alone is not sufficient for this cyanobacterium to survive in the absence of ferrisiderophore acquisition.

When confronted with a low iron environment, the physiology of the cell shifts to a more efficient state; carbon fixation is reduced to minimum growth requirements. Iron transport during iron-limited growth is an energy dependant process, with that energy being derived from photosynthesis.

The results of this thesis will allow for *Synechococcus* sp. PCC 7002 to be established as an ecological indicator organism for iron-limited environments. By culturing this cyanobacteria in cell-free, natural water

samples, and observing the associated physiology we will now be able to determine if a sample of water is truly iron-limited.

6. References

Andersen MA, Morel FMM 1982. The influence of aqueous iron chemistry on the uptake of iron by the coastal diatom *Thalassiosira weissflogii*. Limnol. Oceanogr. 27:789-813.

Apte SK, Bhagwat AA 1989. Salinity-stress induced proteins in two nitrogen-fixing *Anabaena* strains differentially tolerant to salt. J. Bacteriol. 171:909-915.

Armstrong JE, Van Baalen C 1979. Iron transport in microalgae: the isolation and biological activity of a hydroxamate siderophore from the blue-green alga *Agmenellum quadruplicatum*. J. Gen. Micro. 111:253-262.

Arnow LE 1937. Colorimetric determination of components of 3,4-dihydroxyphenylalanine-tyrosine mixtures. J. Biol. Chem. 118:531-537.

Averell BA, Orme-Johnson WH 1978. Iron sulfur proteins and their synthetic analogs. In: Siegel H (ed). Metal Ions in Biological Systems. Vol. 7, Marcel Dekker, New York, pp:127-183.

Bertaux O, Valencia R 1973. Blocage de la division cellulaire et malformations induites par carence B_{12} chez les cellules synchrones de *Euglena gracilis* Z. C.R. Séances Acad. Sci. Paris 276:753-756.

Bertaux O, Mederic O, Valencia O 1991. Amplification of ribosomal DNA in the nucleolus of vitamin B_{12}-deficient *Euglena* cells. Exp. Cell Res. 195:112-128.

Bienfait F 1987. Biochemical basis of iron efficiency reactions in higher plants. In: Winkelmann G, van der Helm D, Neilands JB (eds). Iron Transport in Microbes, Plants and Animals. VCH, New York, pp. 3-34.

Biederman G, Schindler P 1957. On the solubility product of precipitated iron (III) hydroxide. Acta. Chem. Scand. 11:731-740.

Borbely G, Suranyi G and Korcz A 1985. Effect of heat shock on protein synthesis in the cyanobacterium *Synechococcus* sp. strain PCC 6301. J. Bacteriol. 161:1125-1130.

Boussiba S, Richmond AE 1980. C-phycocyanin as a storage protein in the blue-green alga *Spirulina platensis*. Arch. Micro. 125:143-147.

Bowen HJM 1966. Trace Elements in Biochemistry. Academic Press, New York, pp. 60-84.

Boyer GL, Gillam AH and Trick CG 1987. Iron chelation and uptake. In: Fay P, Van Baalen C (eds). The Cyanobacteria. Elsevier, New York, pp. 415-436.

Boyer GL, Morse PD. Are siderophores important in supporting blue-green algae blooms; the Murphy hypothesis revisited. Northeast Algal Symposium, Woods Hole, MA. April 25-26, 1992.

Brand LE 1991. Minimum iron requirements of marine phytoplankton and the implications of biogeochemical control of new production. Limnol. Oceangr. 36:1756- 1771.

Brandt K, Raben E 1922. Zur kenntuiss der chemischen zusammensetzung des plankton. Wiss. Meerest ntersuchungen, Kiel, 19:177-210.

Braun V, Hantke K, Eick-Helmerich K, Koster W, Preßler U, Sauer M, Schaffer H, Staudenmaier H and Zimmermann L 1987. Iron transport systems in *Escherichia coli*. In: Winkelmann G, van der Helm D, Neilands JB (eds). Iron Transport in Microbes, Plants and Animals. VCH, New York, pp. 35-52.

Brown CM 1991. Iron deprivation in the filamentous cyanobacterium *Oscillatoria tenuis*. M.Sc. Thesis. The University of Western Ontario, London, Ontario.

Brown CM, Trick CG 1992. Response of the cyanobacterium, *Oscillatoria tenuis*, to low iron environments: the effect on growth rate and evidence for siderophore production. Arch. Microbiol. 157:349-354.

Bruland KW, Franks RP, Knauer GA and Martin JH 1979. Sampling and analytical methods for the determination of copper, cadmium, zinc, and nickel at the nanogram per liter level in seawater. Anal. Chem. Acta. 105:233-245.

Bruland KW, Donat JR and Hutchins DA 1991. Interactive influences of bioactive trace metals on biological production in oceanic waters. Limnol. Oceanogr. 36:1555-1577.

Burdett IDJ, Murray RGE 1974. Electron microscope study of septum formation in *Escherichia coli* strains B and B/r during synchronous growth. J. Bacteriol. 119:1039-1056.

Capone DG, Carpenter EJ 1982. Nitrogen fixation in the marine environment. Science (Wash. D.C.) 21:1140-1142.

Carell EF 1969. Studies on chloroplast development and replication in *Euglena*. I. Vitamin B_{12} and chloroplast replication. J. Cell Biol. 41: 431-440.

Carell EF, Johnston PL and Christopher AR 1970. Vitamin B_{12} and the macromolecular composition of *Euglena*. J. Cell Biol. 47:525-530.

Carlucci AF, Bowes PM 1972. Vitamin B_{12}, thiamine, and biotin contents of marine phytoplankton. J. Phycol. 8:133-137.

Carlucci AF, Sibernagel SB 1966. Bioassay of seawater III. Distribution of vitamin B_{12} in the northeast Pacific Ocean. Limnol. Oceanogr. 11:642-646.

Carlucci AF, Sibernagel SB 1969. Effect of vitamin concentrations on growth and development of vitamin-requiring algae. J. Phycol. 5:63-67.

Carpenter EJ 1983. Nitrogen fixation by marine *Oscillatoria* (*Trichodesmium*) in the world's oceans. In: Carpenter EJ, Capone DG (eds). Nitrogen in the Marine Environment. Academic, New York, pp.65-103.

Chisholm SW, Morel FMM (eds) 1991. What controls phytoplankton production in nutrient-rich areas of the open sea? Limnol.Ocenaogr. 36:1507-1970.

Clarke SE, Stuart J and Sanders-Loehr J 1987. Induction of siderophore activity in *Anabaena* spp. and its moderation of copper toxicity. Appl. Environ. Microbiol. 53:917-922.

Cole RM, MacPeek WA and Cohen WS 1981. The coupling of electron flow to ATP synthesis in pea and maize mesophyll chloroplasts. Plant. Physiol. 68:610-615.

Czaky TZ 1948. On the estimation of bound hydroxylamine in biological materials. Acta. Chemica. Scandinavia. 2:450-454.

Ditullio GR, Hutchins DA and Bruland KW 1993. Interaction of iron and major nutrients controls phytoplankton growth and species composition in the tropical North Pacific Ocean. Limnol. Oceanogr. 38:495-508.

Dolphin D (ed) 1982. B 12. Vols. 1,2. Wiley-Interscience, Toronto.

Douglas D, Peat A and Whitton BA 1986. Influence of iron status on structure of the cyanobacterium (blue-green alga) *Calothrix parientina*. Cytobios 47:155-165.

Droop MR 1966. Vitamin B_{12} and marine ecology. III. An experiment with a chemostat. J. Mar. Biol. Assoc. U.K. 46:659-671.

Droop MR 1968. Vitamin B_{12} and marine ecology. IV. The kinetics of uptake, growth and inhibition in *Monochrysis lutheri*. J. Mar. Biol. Assoc. U.K. 48:689-733.

Duce RA, Tindale NW 1991. Atmospheric transport of iron and its deposition in the ocean. Limnol. Oceangr. 36:1715-1726.

Emery TF, Neilands JB 1961. Structure of ferrichrome compounds. J. Am. Chem. Soc. 83:1626.

Eppley RW, Renger EH, Venrick EL and Mullin MM 1973. A study of plankton dynamics and nutrient cycling in the central gyre of the Nonn Pacific Ocean. Limnol. Oceanogr. 18:534-551.

Estep M, Armstrong JE and Van Baalen C 1975. Evidence for the occurence of specific iron (III)-binding compounds in near-shore marine ecosystems. Appl'ed Micro. 30:186-188.

Filip C, FLetcher G, Wulff JL and Earhart CR 1973. Solubilization of the cytoplasmic membrane of *Escherichia coli* by the ionic detergent Sodium-lauryl sarcosinate. J. Bacteriol. 115:717-722.

Fogg GE 1973. In: Carr NG, Whitton BA (eds). The Biology of Blue-Green Algae. San Francisco, University of California, Berkeley, pp. 368-387.

Fogg GE 1987. Marine planktonic cyanobacteria. In: The Cyanobacteria. Fay P, Van Baalen C, (eds). Elsevier, New York, pp. 415-436.

Gillam AH, Lewis AG and Andersen RJ 1981. Quantitative determination of hydroxamic acids. Anal. Chem. 53:841-844.

Golden SS, Sherman LA 1984. Biochemical and biophysical characterization of herbicide-resistant mutants of the unicellular cyanobacterium, *Anacystis nidulans* R2. Biochim. Biophys. Acta 764:239-246.

Goldman SJ, Lammers PJ, Berman MS and Sanders-Loehr J 1983. Siderophore-mediated iron uptake in different strains of *Anabaena* sp. J. Bacteriol. 156:1144-1150.

Gorham PR, McLachlan JL, Hammer UT and Kim UK 1964. Isolation and culture of toxic strains of *Anabaena flos-aquae* (Lyngb.). Verh. Int. Verein. Theor. Angew. Limnol. 15:796-804.

Gran H 1931. On the conditions for the production of phytoplankton in the sea. Rapp. et Proc. Verb. 75:37-46.

Guikema JA, Sherman LA 1983. Organization and function of chlorophyll in membranes of cyanobacteria during iron starvation. Plant. Physiol. 73:250-256.

Guikema JA, Sherman LA 1984. Influence of iron deprivation on the membrane composition of *Anacytis nidulans*. Plant Physiol. 74:90-95.

Guillard RL 1968. B_{12} specificity in marine centric diatoms. J. Phycol. 4:59-64.

Guillard RRL, Cassie V 1963. Minimum cyanocobalamin requirements of some marine centric diatoms. Limnol. Oceanogr. 8:161-165.

Haines KC, Guillard RRL 1974. Growth of vitamin B_{12}-requiring marine diatoms in mixed laboratory cultures with vitamin B_{12}-producing marine bacteria. J. Phycol. 10:245-252.

Hall JL, Flowers TJ and Roberts RM: Plant Cell Structure and Metabolism. London, Longman, 1982. pp. 543.

Hardie LP, Balkwill DL and Stevens Jr SE 1983a. Effects of iron starvation on the physiology of the cyanobacterium *Agmenellum quadruplicatum*. Appl. Environ. Microbiol. 45:999-1006.

Hardie LP, Balkwill DL, and Stevens Jr SE 1983b. Effects of iron starvation on the ultrastructure of the cyanobacterium *Agmenellum quadruplicatum*. Appl. Environ. Microbiol. 45:1007-1017.

Harrison GI, Morel FMM 1986. Response of the marine diatom *Thalassiosira weissflogii* to iron stress. Limnol. Oceanogr. 35:1002-1020.

Hart TJ 1941. Phytoplankton periodicity in Antarctic surface waters. Discovery Rep. 21:261-356.

Hartee EF 1972. Determination of protein: a modification of the Lowry method that gives linear photometric response. Anal. Biochem. 48:422-427.

Harvey HW 1933. On the rate of diatom growth. J. Mar. Biol. Assoc. U.K. 19:253-277.

Harvey HW 1937. The supply of iron to diatoms. J. Mar. Biol. Assoc. U.K. 22:205-219.

Harvey HW 1947. Manganese and the growth of phytoplankton. J. Mar. Biol. Assoc. U.K. 26:562-579.

Hudson RJM 1989. The chemical kinetics of iron uptake by marine phytoplantkon. Ph.D. Thesis, Massachusettes Institute of Technology, Cambridge, MA.

Hudson RJM, Morel FMM 1989. Distinguishing between extra- and intracellular iron in marine phytoplankton. Limnol. Oceanogr. 36:1113-1120.

Hudson RJM, Morel FMM 1990. Iron transport in marine phytoplankton: kinetics of cellular and medium coordination reactions. Limnol. Oceanogr. 35:1002-1020.

Hutchins DA, Rueter JG and Fish W 1991. Siderophore production and nitrogen fixation are mutually exclusive strategies in *Anabaena* 7120. Limnol. Oceanogr. 36:1-12.

Hutchins DA, DiTullio GR and Bruland KW 1993. Iron and regenrated production: evidence for biological iron recycling in two marine environments. Limnol. Oceanogr. 38:1242-1255.

Johnson PW, Sieburth JM 1979. Chroococcoid cyanobacteria in the sea: a ubiquitous and diverse phototrophic biomass. Limnol. Oceanogr. 24:928-935.

Kadner RJ 1990. Vitamin B_{12} transport in *Escherichia coli*: energy coupling between membranes. Mol. Micobiol. 4:2027-2033.

Kanamura K, Kashiwagi S and Mizuno T 1993. The cyanobacterium, *Synechococcus* PCC 7942, possesses two distinct genes encoding cation transporting P-type ATPases. FEBS Letters 220:99-104.

Kerry A 1988. The effect of iron availability on the growth and physiology of *Anabaena variablis*, *Anacystis nidulans* and related microorganisms. M.Sc. Thesis, University of Toronto, Toronto, Ontario.

Kerry A. Laudenbach DL and Trick CG 1988. Influence of iron limitation and nitrogen source on growth and siderophore production by cyanobacteria. J. Phycol. 24:566-571.

Kroll H, Knell M, Powers J and Simonian J 1957. A phenolic analog of ethylenediamine-tetraacetic acid. J. Am. Chem. Soc. 79:2024-2025.

Laemmeli UK 1970. Cleavage of structural proteins during assembly of the head of bacteriophage T_4. Nature 222:680-685.

Lammers PJ, Sanders-Loehr J 1982. Active transport of ferric schizokinen in *Anabaena* sp. J. Bacteriol. 151:288-294.

Laudenbach DL, Trick CG and Straus NA 1989. Cloning and characterization of an *Anacystis nidulans* R2 superoxide dismutase gene. Mol. Gen. Genet. 216:455-461.

Lawler, DW 1987. Photosynthesis: Metabolism, Control and Physiology. Wiley & Sons, New York, pp. 116-117.

Li, WKW, Subba Rao DV, Harrison WG, Smith JC, Cullen JJ, Irwin B and Platt T 1983. Autotrophic picoplankton in the tropical ocean. Science 219:292-295.

Luckey M, Pollack JR, Wayne R, Ames BN and Neilands JB 1972. Iron uptake in *Salmonella typhimurium*: utilization of exogenous siderochromes as iron carriers. J. Bacteriol. 111:731-738.

Mahasneh IA 1991. Siderophore production in the *Rivulariaceae*, blue-green alga (cyanobacteria). Microbios 65:97-103.

Matzanke BF 1991. Structures, coordination chemistry and functions of microbial iron chelates. In: Winkelmann G (ed). Handbook of Microbial Chelates. CRC Press, Boston, pp.15-64.

Martin JH, Fitzwater SE 1988. Iron deficiency limits phytoplankton growth in the north-east pacific subarctic. Nature 331:341-343.

Martin JH, Fitzwater SE, Gordon RM, Hunter CN and Tanner SJ 1993. Iron, primary production and carbon nitrogen flux studies during the JGOFS North Atlantic bloom experiment. Deep-Sea Res. Pt. II-Top. St. Oce. 40:115-134.

Martin JH, Gordon RM and Fitzwater SE 1990. Iron in Antarctic waters. Nature 345:156-158.

Martin JH, Gordon RM, Fitzwater SE and Broenkow WW 1989. VERTEX: phytoplankton/iron studies in the Gulf of Alaska. Deep-Sea Res. 36:649-680.

Maxwell DP, Falk S, Trick CG and Huner NPA 1993. Growth at low temperatures mimics high light acclimation in *Chlorella vulgaris*. Plant Physiol. (in press).

McKnight DM, Morel FMM 1979. Release of weak and strong copper-complexing agents by algae. Limnol. Oceanogr. 24:823-837.

McKnight DM, Morel FMM 1980. Copper complexation by siderophores from filamentous blue-green algae. Limnol. Oceanogr. 25:62-71.

Menzel DW, Ryther JH 1961. Nutrients limiting the production of phytoplankton in the Sargasso Sea, with special reference to iron. Deep Sea Res. 7:276-281.

Menzel DW, Speath JP 1962. Occurence of vitamin B_{12} in the Sargasso sea. Limnol.Cceanogr. 7:151-158.

Merril CR, Switzer RC and Van Keuren ML 1979. Trace polypeptides in cellular and human body fluids detected by two-dimensional electrophoresis and a highly sensitive silver stain. Proc. Nat. Acad. Sci. (USA) 76:4335-4339.

Miller AG, Turpin DH and Canvin DT 1984. Growth and photosynthesis of the cyanobacterium *Synechococcus leopoliensis* in HCO_3-limited chemostats. Plant. Physiol. 75:1064-1070.

Mitchell BG, Brody EA, Holm-Hansen O, McClain C and Bishop J 1991. Light limitation of phytoplankton biomass and macronutrient utilization in the Southern Ocean. Limnol. Oceanogr. 36:1662-1677.

Mittler R, Tel-Or E 1991. Oxidative stress responses and shock proteins in the unicellular cyanobacterium *Synechococcus* R2 (PCC 7942) Arch. Microbiol .155:19203-130.

Monod, J 1950. La technique de la culture continue: Theorie et applications. Annales d'Institut Pasteur, Lille 179:390-410.

Moore RM, Milley JE and Chatt A 1984. The potential for biological mobilization of trace elements from aeolian dust in the ocean and its importance in the case of iron. Oceanol. Acta 7:221-228.

Morel FMM, Hudson RJM 1984. The geobiological cycle of trace elements in aquatic systems: Redfield revisited. In: Stumm W (ed) Chemical Processes in Lakes. Wiley-Interscience, pp. 251-281.

Morel FMM, Hudson RJM, Price NM 1991. Limitation of productivity by trace metals in the sea. Limnol. Oceanogr. 36:1742-1755.

Murphy LS, Haugen E 198? The distribution and abundance of phototrophic picoplankton in the North Atlantic. Limnol. Oceanogr. 30:47-58

Murphy TP, Lean DRS 1975. The distribution of iron in a closed ecosystem. Verh. Internat. Verein. Limnol. 19:258-266.

Murphy TP, Lean DRS and Nalewajko C 1976 Blue-green algae: their excretion of iron-selective chelators enables them to dominate other algae. Science 192:900-902.

Murphy TP, Hall KJ and Yesaki I 1983. Biogenic regulation of iron availability in a eutrophic hard-water lake. Science of the Total Environment 28:37-50.

Myers J, Graham JR and Wang RT 1980. Light harvesting in *Anacystis nidulans* studied in pigment mutants. Plant Physiol. 66:1144-1149.

Neilands JB 1977. Siderophores: biochemistry, ecology and mechanism of iron transport in Enterobacteria. Adv. Chem. Ser. Bioinorganic Chem. II. 162:1-32.

Neilands JB 1981. Iron absorption and transport in microorganisms. Ann. Rev. Nutr. 1:27-46.

Neilands JB 1982. Microbial envelope proteins related to iron. Ann. Rev. Microbiol. 36:285-309.

Neilands JB 1984. Methodology of siderophores. Struct. Bonding 58:1-24.

Neilands JB, Konopka K, Schwyn B, Coy M, Francis RT, Paw BH and Bagg A 1987. Comparative biochemistry of microbial iron assimilation. In: Winkelmann G, van der Helm D, Neilands JB (eds) Iron Transport in Microbes, Plants and Animals. VCH, New York, pp. 3-34.

Neilands JB, Leong SA 1986 Siderophores in relation to plant growth and disease. Ann. Rev. Plant. Physiol. 37:187-208.

Neilands JB, Nakamura K 1991. Detection, determination, isolation, characterization, and regulation of microbial iron chelates. In: Winkelmann G, (ed) Handbook of Microbial Chelates. CRC Press, Boston, pp.1-14.

Neu HC, Heppel LA 1965. The release of enzymes from *Escherichia coli* by osmotic shock and during the formation of spheroplasts. J. Biol. Chem. 240:3686-3692.

Omata T, Murata N 1983. Isolation and characterization of three types of membranes from the blue-green alga (cyanobacterium) *Anacystis nidulans*. Plant Cell Physiol. 24: 1101-1112.

Öquist G 1971. Changes in plant composition and photosynthesis induced by iron-deficiency in the blue-green alga *Anacystis nidulans*. Plant Physiol. 25:188-191.

Öquist G 1974a. Iron deficiency in the blue-green alga *Anacystis nidulans*: changes in pigmentation and photosynthesis Plant Physiol. 30:30-37.

Öquist G 1974b. Iron deficiency in the blue-green alga *Anacystis nidulans*: fluorescence and absorbance spectra recorded at 77°K. Plant Physiol. 31:55-58.

O'Sullivan DW, Hanson AK, Miller WL and Kester DR 1991. Measurement of Fe(II) in surface water of the equitorial Pacific. Limnol. Oceanogr. 36:1727-1741.

Pakarasi HB, Goldberg A and Sherman LA 1985. Membrane development in the cyanobacteria, *Anacystis nidulans*, during recovery from iron starvation. Plant Physiol. 79:290-295.

Peschek GA 1979. Nitrate and nitrite reductase and hydrogenase in *Anacystis nidulans* grown in Fe- and Mo-deficient media. FEMS Microbiol. Lett. 6:371-374.

Pintner IJ, Altmeyer VL 1979. Vitamin B_{12}-binder and other algal inhibitors. J. Phycol. 15:391-398.

Platt T, Subba Rao DV and Irwin B 1983. Photosynthesis of picoplankton in the oligotrophic ocean. Nature (London) 301:702-703.

Pollack JR, Ames BN and Neilands JB 1970. Iron transport in *Salmonella typhimurium*: mutants blocked in the biosynthesis of enterobactin. J. Bacteriol. 104:635-639.

Price NM, Harrison GI, Hering JG, Hudson RJ, Nirel PMV, Palenik B and Morel FMM 1989. Preparation and chemistry of the artificial algal culture medium Aquil. Biol. Oceanogr. 6:443-461.

Raven JA 1988. The iron and molybdenum use efficiencies of plant growth with different energy, carbon and nitrogen sources. New Phytol. 109:279-287.

Redfield A, Ketchum BH and Richards FA 1963. The influence of organisms on the composition of sea water. In: Hill MN (ed). The Sea. Academic Press, New York, pp. 26-27.

Reynolds ES. 1963. The use of lead citrate at high pH as an electron-opaque stain in electron microscopy. J. Cell. Biol. 17:208-211.

Reynolds, P. R., Mottur GP and Bradbeer C 1980. Transport of vitamin B_{12} in *Escherichia coli*. J. Biol. Chem. 255:4313-4319.

Rhee GY, Gotham IJ and Chisholm SW 1981. Use of cyclostat cultures to study phytoplankton ecology. In: Calcott PH (ed). Continuous Culture of Cells. Boca Raton, Flordia, CRC Press, pp. 159-186.

Rich HW, Morel FMM 1990. Availability of well defined iron colloids to the marine diatom *Thalassiosira weissfolgii*. Limnol. Oceanogr. 35:652-662.

Rioux C, Jordan DC and Rattary JBM 1983. Colorimetric determination of catechol siderophores in microbial cultures. Anal. Biochem. 133:163-169.

Rioux CR, Friedrich MJ and Kadner RJ 1990. Genes on the 90-kilobase plasmid of *Salmonella typhimurium* confer low-affinity cobalamin transport: relationship to fimbria biosynthesis genes. J. Bacteriol. 172:6217-6222.

Rippka R, Deruelles J, Waterbury JB, Herdman M and Stanier RY 1979. Generic assignments, strain histories and properties of pure cultures of cyanobacteria. J. Gen. Microbiol. 111:1-61.

Rooney NM, Trick CG. Cyanobacterial blooms: which factors might advance or deter them? Northeast Algal Symposium, Woods Hole, MA, April 1993.

Rueter JG, Unsworth NL 1991. Response of marine *Synechococcus* (Cyanophyceae) cultures to iron nutrition. J. Phycol. 27:173-178.

Sandmann G, Malkin R 1983. Iron-sulfur centers and activities of the photosynthetic electron transport chain in iron-deficient cultures of the blue-green alga *Aphanocapsa*. Plant Physiol. 73:724-728.

Scanlan DJ, Mann NH and Carr NG 1989. Effect of iron and other nutrient limitations on the pattern of outer membrane proteins in the cyanobacterium *Synechococcus* PCC7942. Arch. Microbiol. 152:224-228.

Scanlan DJ, Mann NH and Carr NG 1993. The response of the picoplanktonic marine cyanobacterium *Synechococcus* species WH7803 to phosphate starvation involves a protein homologous to the periplasmic phosphate-binding protein of *Escherichia coli*. Mol. Microbiol.10:181-191.

Schindler DW 1981. Interrlationships between the cycles of elements in freshwater ecosystems. In: Likens GE (ed). Some Perspectives of the Major Biogeochemical Cycles. SCOPE, pp. 113-123.

Schwyn B, Neilands JB 1987. Universal chemical assay for the detection and determination of siderophores. Anal. Biochem. 160:47-56.

Sherman L, Bricker T, Guikema J and Pakarasi H 1987. The protein composition of the photosynthetic complexes from the cyanobacterial thylakoid membrane. In: Fay P, Van Baalen C, (eds). The Cyanobacteria. Elsevier, New York, pp. 1-34.

Sherman DM, Sherman LA 1983. Effect of iron deficiency and iron restoration on ultrastructure of *Anacystis nidulans*. J. Bacteriol. 156:393-401.

Simpson FB, Neilands JB 1976. Siderochromes in cyanophyceae: isolation and characterization of schizokinen from *Anabaena* sp J. Phycol. 12:44-48.

Stafleu FA, Bonner CEB, McVaugh R, Meikle RD, Rollins RC, Ross R, Schopf JM, Schulze GM, De Vilmorin R and Voss EG (eds) 1972 International Code of Botanical Nomenclature. Utrecht, Netherlands.

Stevens Jr SE, Balkwill DL and Paone DAM 1981a. The effects of nitrogen limitation on the ultrastructure of the cyanobacterium *Agmenellum quadruplicatum*. Arch. Microbiol. 130:204-212.

Stevens Jr SE, Paone DAM and Balkwill DL 1981b. Accumulation of cyanophycin granules as a result of phosphate limitation in *Agmenellum quadruplicatum*. Plant Physiol. 67:716-719.

Storch TA, Dunham VL 1986. Iron-mediated changes in the growth of Lake Erie phytoplankton and axenic algal cultures. J. Phycol. 22:109-117.

Speirs RJ, Boyer GL 1991. Analysis of ^{55}Fe-labeled hydroxamate siderophores by high-performance liquid chromatography. J. Chromatography 537:259-267.

Sunda WG, Swift DG and Huntsman SA 1991. Low iron requirement for growth in oceanic phytoplankton. Nature 351:55-57.

Swift DG, Taylor WR 1974. Growth of vitamin B_{12}-limited cultures: *Thalassiosira pseudonana*, *Monochrysis lutheri*, and *Isochrysis galbana*. J. Phycol. 10:385.

Swift D G 1981. Vitamin levels in the gulf of maine and ecological significance of vitamin B_{12} there. J. Mar. Res. 39:375-403.

Trick CG 1989. Hydroxamate-siderophore production and utilization by marine eubacteria. Current Micro. 18:375-378.

Trick CG, Kerry A 1992. Isolation and purification of siderophores produced by cyanobacteria, *Synechococcus* (*Anacystis nidulans* R2) sp. and *Anabaena variabilis*. Current Micro. 24:241-245.

Van Baalen, C 1962. Studies on marine blue-green algae. Botanica marina 4:129-139.

Van Baalen, C 1968. The effects of ultraviolet irradiation on a coccoid blue-green algae. Survival, photosynthesis, and photoreactivation. Plant Physiol. 43:1689-1695.

Waterbury JB, Watson SW, Guillard RRL and Brand LE 1979. Widespread occurence of a unicellular, marine, planktonic, cyanobacterium. Nature 277:293-294.

Waterbury JB, Watson SW, Valois FW and Franks DG 1987. Biological and ecological characterization of the marine unicellular cyanobacterium *Synechococcus*. In: Platt T, Li WKW (eds). Photosynthetic Picoplankton. Dept. Fisheries and Oceans,Ottawa, pp. 71-120.

Wells, ML, Zorkin NG and Lewis AG 1983. The role of colloid chemistry in providing a source of iron to phytoplankton. J. Mar. Res. 41:731-746.

Wetzel, RG 1966. Productivity and nutrient relationships in marl lakes of northern Indiana. Verh. Int. Verein. Limnol. 16:331-332.

Whitton, B. A. 1992. Diversity, ecology and taxonomy of the cyanobacteria. In: N.H. Mann, and N.G. Carr (ed.) Photosynthetic Prokaryotes, Plenum Press, New York, pp.1-52.

Winkelmann, G, van der Helm D and Neilands JB (eds). Iron Transport in Microbes, Plants and Animals. VCH, New York, 1987.

Winkelmann G, 1991. Specificity of iron transport in bacteria and fungi. In: Winkelman G, (ed). Handbook of Microbial Chelates. CRC Press, Boston, pp.65-106.

Yamamoto S, Fujita Y, Okujo N, Saito M, Yoshida T and Shinoda S 1992. Isolation and partial characterization of a compound with siderophore activity from *Vibrio parahaemolyticus*. FEMS Microbiol. Lett. 94:181-186.

Appendix I. Speciation of Iron in A* Medium.

		mFe17		mFe18		mFe19		mFe20		mFe21	
SPECIES	Log K	CONC	Log	CONC	Log	CONC	Log	CONC	Log	CONC	Log
Fe^{3+}	0	7.76e-18	-17.1	4.47e-19	-18.3	3.69e-20	-19.4	2.78e-21	-20.5	4.57e-22	-21.3
$FeOH^{+2}$	-2.19	1.58e-24	-23.8	9.10e-26	-25.0	7.52e-27	-26.1	5.66e-28	-27.2	9.30e-29	-28.0
$FeOH_2^+$	-5.67	2.65e-32	-31.7	9.51e-34	-33.0	7.85e-35	-34.1	5.91e-36	-35.2	9.72e-37	-36.0
$Fe_2(OH)_2^{+4}$	-2.95	6.72e-47	-46.1	2.23e-49	-48.6	1.52e-51	-50.8	8.62e-54	-53.0	2.33e-55	-54.6
$FeOH_3$ AQ	-13.6	6.12e-45	-44.2	3.53e-46	-45.4	2.91e-47	-46.5	2.19e-48	-47.6	3.60e-49	-48.4
$FeOH_4^-$	-21.6	1.93e-57	-56.7	1.11e-58	-57.9	9.18e-60	-59.0	6.91e-61	-60.1	1.14e-61	-60.9
$Fe_2(OH)_2^{+4}$	-6.3	1.00e-75	-75.6	1.00e-75	-79.3	1.00e-75	-82.6	1.00e-75	-85.9	1.00e-75	-88.3
FeOHEDTA^{-2}	20.9	1.67e-16	-15.7	1.87e-17	-16.7	1.63e-18	-17.7	1.23e-19	-18.9	2.03e-20	-19.7
$Fe(OH)_2EDTA^{-3}$	10.1	8.34e-32	-31.0	9.33e-33	-32.0	8.14e-34	-33.0	6.16e-35	-34.2	1.01e-35	-35.0
$FeHPO_4^+$	17.8	2.53e-19	-18.6	1.45e-20	-19.8	1.26e-21	-20.9	9.60e-23	-22.0	1.48e-23	-22.8
FeHEDTA^{-1}	29.4	2.65e-11	-10.5	2.97e-12	-11.5	2.59e-13	-12.5	1.96e-14	-13.7	3.22e-15	-14.5
$FeCl_2^+$	2.13	2.68e-16	-15.7	1.17e-17	-16.9	9.64e-19	-18.0	7.25e-20	-19.1	1.19e-20	-19.9
$FeCl_3$ AQ	1.13	8.85e-18	-17.0	5.14e-19	-18.2	4.24e-20	-19.3	3.19e-21	-20.5	5.25e-22	-21.3
$FeCl^{+2}$	1.48	1.03e-16	-15.9	5.94e-18	-17.2	4.90e-19	-18.3	3.69e-20	-19.4	6.07e-21	-20.2
$FeSO_4^+$	3.92	1.06e-16	-15.9	5.99e-18	-17.2	4.94e-19	-18.3	3.72e-20	-19.4	6.12e-21	-20.2
$Fe(SO_4)_2^-$	5.42	5.51e-18	-17.2	3.05e-19	-18.5	2.52e-20	-19.6	1.89e-21	-20.7	3.12e-22	-21.5
FeEDTA$^-$	27.8	4.20e-05	-4.38	4.70e-06	-5.33	4.10e-07	-6.39	3.10e-08	-7.51	5.10e-09	-8.29
$FeOH_2?Cl_2$	3.04	4.67e-27	-26.3	2.69e-28	-27.5	2.23e-29	-28.7	1.67e-30	-29.7	2.75e-31	-30.6
LEPIDOCROCIT	-1.37	2.07e-20	-19.6	1.19e-21	-20.9	9.86e-23	-22.0	7.42e-24	-23.1	1.22e-24	-23.9
GOETHITE	-0.5	1.54e-19	-18.8	8.88e-21	-20.0	7.33e-22	-21.1	5.52e-23	-22.2	9.07e-24	-23.0
HEMATITE	4.01	4.83e-21	-20.3	1.68e-23	-22.8	1.09e-25	-24.9	6.20e-28	-27.2	1.68e-29	-28.8
FERRIHYDRITE	-4.89	3.13e-36	-35.5	1.80e-37	-36.7	1.49e-38	-37.8	1.12e-39	-38.9	1.84e-40	-39.7
MAGHEMITE	-6.39	1.95e-31	-30.7	6.68e-34	-33.1	4.42e-36	-35.3	2.58e-38	-37.6	6.77e-40	-39.2
JAROSITE K	14.8	6.73e-71	-70.2	1.14e-74	-73.9	1.00e-75	-77.1	1.00e-75	-80.5	1.00e-75	-8.29
MAG-FERRITE	-16.8	2.44e-40	-39.6	8.15e-43	-42.0	5.55e-45	-44.2	3.15e-47	-46.5	8.51e-49	-48.1
JAROSITE NA	11.2	6.25e-74	-73.2	1.00e-75	-76.9	1.00e-75	-80.1	1.00e-75	-83.5	1.00e-75	-85.9
JAROSITE H	12.1	1.00e-75	-91.9	1.00e-75	-95.6	1.00e-75	-98.8	1.00e-75	-102.	1.00e-75	-105
STRENGITE	26.4	1.66e-27	-26.7	9.53e-29	-28.0	7.87e-30	-29.1	5.92e-31	-30.2	9.74e-32	-31.0
$FePO_4$	25.8	1.67e-03	-2.78	9.57e-05	-4.02	7.91e-06	-5.10	5.95e-07	-6.23	9.78e-08	-7.01
$FE_2(SO_4)_3$	-3.58	7.02e-47	-46.1	2.19e-49	-48.6	1.50e-51	-50.8	8.48e-54	-53.0	2.29e-55	-54.6
FeH_2PO_4	25.0	6.36e-20	-19.2	3.64e-21	-20.4	3.01e-22	-21.5	2.26e-23	-22.6	3.72e-24	-23.4

Appendix II: Physiological Profile of *Synechococcus* sp. PCC 7002 Grown in Vitamin B_{12}-Limited Continuous Culture.

Among their complex nutrient requirements, a number of cyanobacteria have an obligate requirement for vitamin B_{12}. These cyanobacteria cover a broad range of genera including *Dermocarpa*, *Synechocystis*, *Pleurocapsa*, and *Synechococcus* (Rippka et al. 1979). Vitamin B_{12} has been suggested to potentially limit the productivity of cyanobacteria and other phytoplankton in some pelagic and neritic aquatic systems (Swift 1981).

Vitamin B_{12} (cyanocobalamin) is an essential cofactor in a number of integral cellular processes, including intramolecular rearrangements, methylations, and the reduction of ribonucleotides to deoxyribonucleotides (Dolphin 1982). While studies on the effect of vitamin B_{12}-limited growth have examined biochemical and physiological variations in eukaryotic algae (Droop 1966; Carlucci and Silbernagel 1969; Swift 1981) and particularly diatoms (Haines and Guillard 1974; Guillard 1968; Carlucci and Bowes 1972), little has been done to examine the physiological or biochemical changes that occur during vitamin B_{12}-limited growth in cyanobacteria.

Under conditions of vitamin B_{12}-limitation, some eukaryotic algae have been shown to produce vitamin B_{12}-binding proteins which are released to the environment (Pintner and Altmyer 1979). These proteins bind vitamin B_{12} making it unavailable to other organisms. The Gram-negative bacterium *Escherichia coli* acquires vitamin B_{12} via an energy dependant, membrane

associated vitamin B_{12} specific transport system which is regulated by the *furItonB* regulatory system (Kadner 1990). It remains to be determined how coccoid cyanobacteria acquire vitamin B_{12} from their environment. While they do not produce vitamin B_{12}-binding proteins (Pintner and Altmyer 1979), they do appear to utilize energy dependant nutrient acquisition schemes (ie. high-affinity iron transport) similar to other Gram-negative organisms (Section 4.7). These systems require surface associated receptor proteins which identify and assist in the assimilation of specific nutrients.

Synechococcus sp. PCC 7002, a unicellular, halotolerant, cyanobacterial isolate from Puerto Rico (Van Baalen 1962), has been shown to have an obligate requirement for vitamin B_{12} (Rippka et al. 1979). Previous characterizations of the nutrient-limited physiology of this cyanobacterium have neglected vitamin B_{12} but considered iron (Hardie et al. 1983a, 1983b; Wilhelm and Trick 1993), nitrogen (Stevens et al. 1981a) and phosphorous (Stevens et al. 1981b). These studies have, however, focused on the effects of nutrient deprivation in batch culture ("starvation"). Growth at limiting levels of nutrient may be better examined in a continuous culture chemostat system (Droop 1966). In his work on the vitamin B_{12} requirements of *Monochrysis lutheri*, Droop (1968) was able to monitor the changes in cellular vitamin B_{12} quota through a series of dilution rates in vitamin B_{12}-limited chemostats.

My purpose here was to determine whether growth over a range of vitamin B_{12}-limiting conditions would induce observable physiological changes,

and document these changes and the cellular requirements ("quotient") for vitamin B_{12} in *Synechococcus* sp. PCC 7002 in chemostat systems. I have also examined the affects of vitamin B_{12} availability on outer membrane protein profiles in order to determine if specific proteins, which may be involved in vitamin B_{12} acquisition, are enhanced during vitamin B_{12}-limitation.

Methods and Materials

Strains and Media

Synechococcus sp. PCC 7002 (*Agmenellum quadruplicatum* PR6) was grown in modified A^+ medium at 37°C in chemostat cultures at a dilution rate equivalent to a turnover of 0.6 volumes d^{-1}. Filter sterilized $FeCl_3$ was added to a final concentration of 4.2×10^{-5} M. Crystalline cyanocobalamin (Sigma chemicals) was brought into aqueous solution, filter sterilized, and dispensed so as to produce a range of cyanocobalamin concentrations from 5.0×10^{2} µg L^{-1} to 5.0×10^{-4} µg L^{-1}, with each concentration differing by an order of magnitude.

Analysis of Physiological Variation

Chemostat yields, cellular pigment levels and ultrastructural variation were monitored as described (Sections 2.2 i, 2.3, and 2.6). Outer membrane fractions from steady state populations of cyanobacteria maitained in vitamin B_{12}-limited cultures were prepared utilizing the the sodium lauryl sarcosinate procedure (Section 2.11 i), and fractions resolved and visualized in linear (15%) polyacrylamide gels (Section 2.12).

RESULTS

Chemostat Yields and Pigment Production

Cell populations of equilibrated chemostats are as displayed in Figure 28. Concentrations of vitamin B_{12} above 500 µg L^{-1} are in excess and the chemostat is then limited by the available nitrate (data not shown). Chemostats were shown to establish an equilibrium over a vitamin B_{12} concentration range of 500 µg L^{-1} to 5 x 10^{-3} µg L^{-1}. Yields are expressed as an average of cell number over four days of enumeration at an equilibrium state. Cells grown in continuous culture which were switched to vitamin B_{12} concentrations of 5 x 10^{-4} µg L^{-1} were unable to maintain themselves in the culture medium and the chemostat eventually washed out (not shown). The rate of washout, however, when correlated with the rate of dilution, allows for an estimation of the growth rate at 0.005 µg L^{-1} vitamin B_{12} to be 0.237 d^{-1}.

Distinct changes in cellular chla were observed in cell cultures grown under varying vitamin B_{12} levels (Figure 29), while cellular phycocyanin levels remained relatively static. A flux in chla $cell^{-1}$ is demonstrated at 5 µg L^{-1} vitamin B_{12}, but beyond this concentration the pigment level decreases with the vitamin B_{12} concentration.

Figure 28. Influence of vitamin B_{12} concentration on steady state cell densities in chemostat cultures of *Synechococcus* sp. PCC 7002. Vitamin B_{12} concentrations in $\mu g\ L^{-1}$.

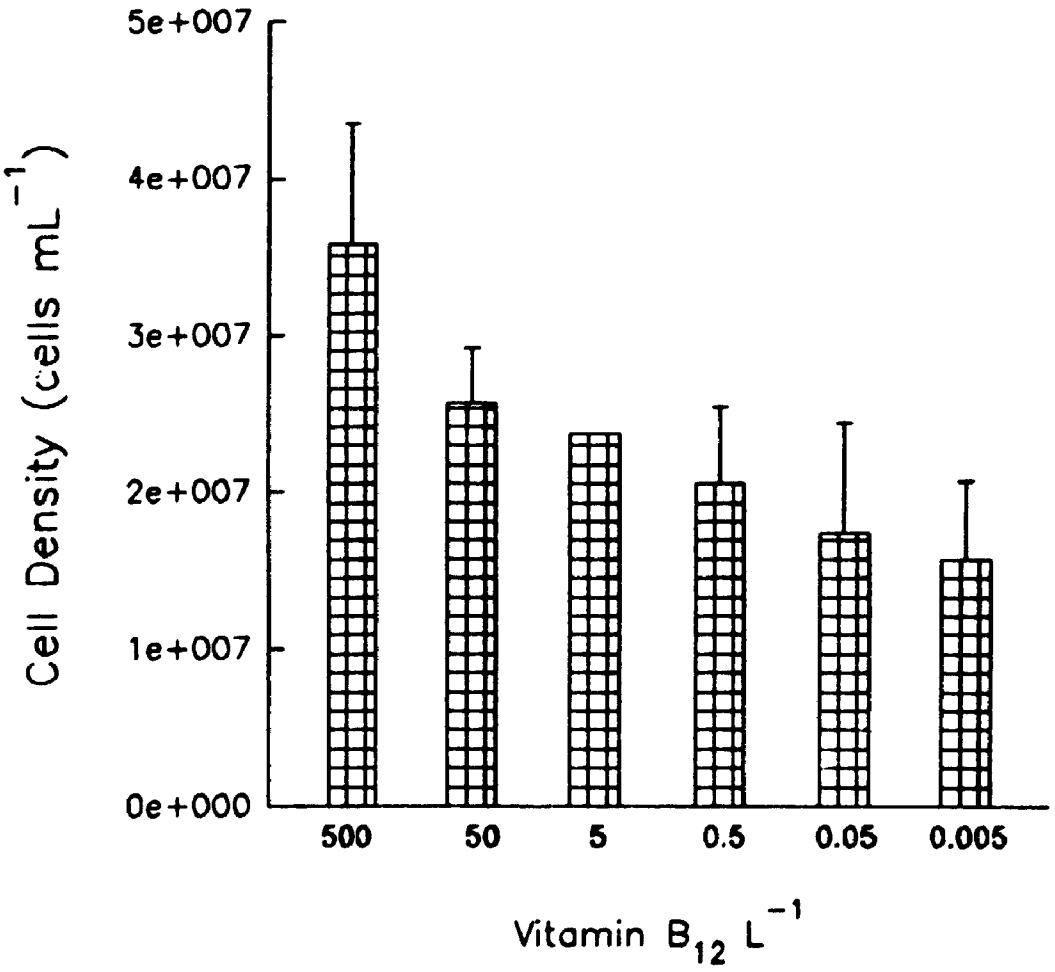
5e+007
4e+007
3e+007
2e+007
1e+007
0e+000
Cell Density (cells mL^{-1})
500
50
5
0.5
0.05
0.005
Vitamin B_{12} L^{-1}

Figure 29. Concentration of photosynthetic pigements (chlorophyll, phycocyanin) in vitamin B_{12}-limited chemostat cultures.

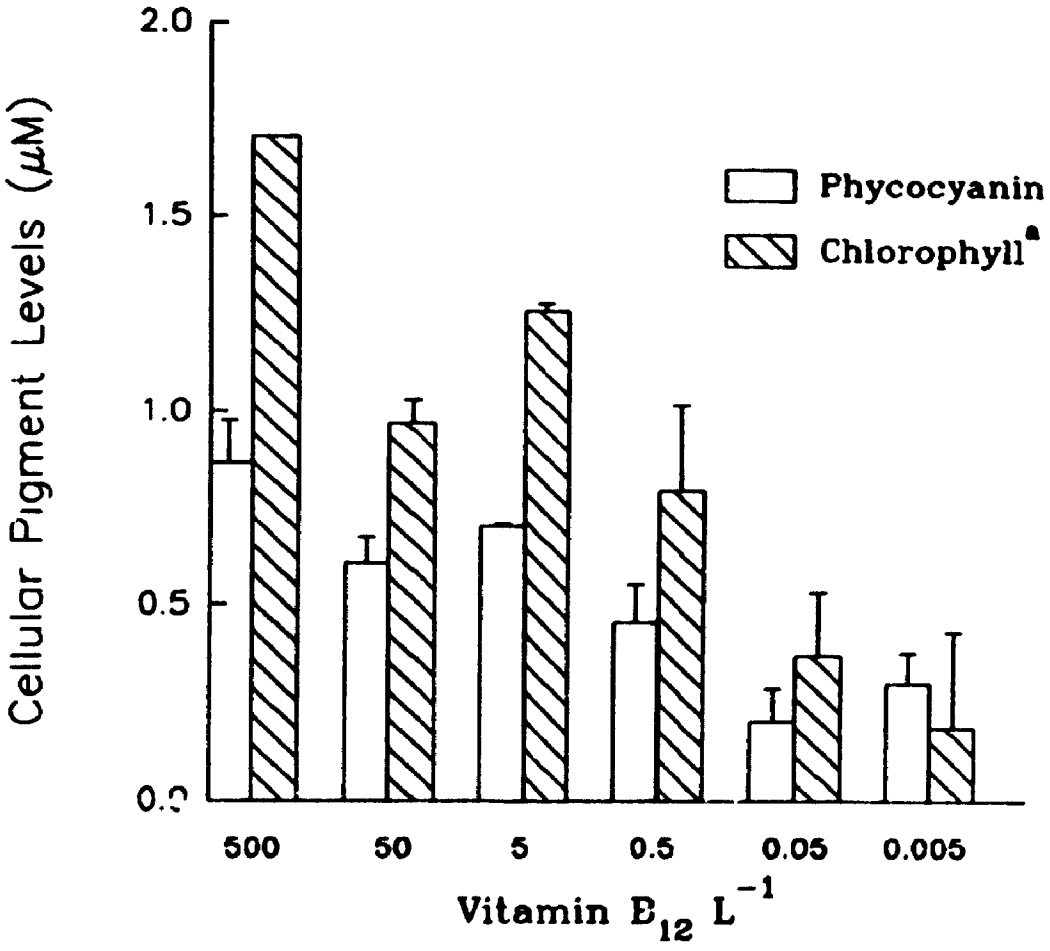
2.0
1.5
1.0
0.5
0.0
Cellular Pigment Levels (μM)
Phycocyanin
Chlorophyll a
500
50
5
0.5
0.05
0.005
Vitamin B12 L-1

Outer Membrane Proteins

Silver staining of the sarkosyl insoluble outer membrane components of cells grown at vitamin B_{12}-replete (5.0×10^{2} µg L^{-1}) and vitamin B_{12}-deficient (5.0×10^{-2} µg L^{-1}) conditions demonstrated the consistent production/enhancement of three proteins during periods of vitamin B_{12} limitation (Figure 30). A strongly expressed protein of 34.0 kDa, as well as two negatively staining proteins of 70.0 and 95.0 kDa were detected on silver-stained polyacrylamide gels. Proteins were seen as early as 48 hours after transfer of cells to vitamin B_{12}-limiting conditions (not shown), but were most prominent at 96 hours.

Electron microscopy

Changes in cellular ultrastructure were examined in cells grown in vitamin B_{12}-limiting conditions (5.0×10^{-3} µg L^{-1}) and compared to the vitamin B_{12} sufficient control cultures (Figure 31). Cyanobacteria, grown under vitamin B_{12}-replete conditions, show well structured thylakoids within the cells (Figure 31a) while cells grown at limiting levels of vitamin B_{12} demonstrate a reduction in the integrity of the thylakoid structure (Figure 31b). Some vitamin B_{12}-limited cells demonstrate decompressed or separated lamellae (Figure 31b), suggesting that vitamin B_{12}-deprivation may be leading to a breakdown in the integrity of these structures.

Figure 30. Silver stained polyacrylamide gel of isolated outer membranes from vitamin B_{12}-limited *Synechococcus* PCC 7002. Cells were maintained in chemostats at 500 µg L^{-1} vitamin B_{12} until steady state was reached and then transfered to test condition for a period of 96 h prior to analysis. **A)** 500 µg L^{-1} vitamin B_{12}. **B)** 0.05 µg L^{-1} vitamin B_{12} after 96 h.

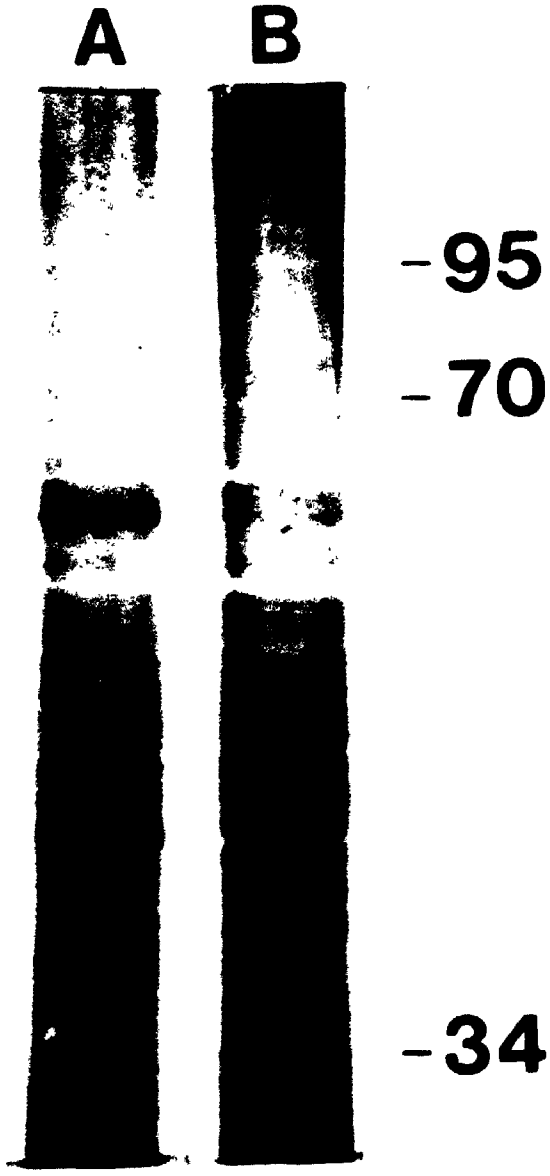
A
B
-95
-70
-34

Figure 31. Ultrastructure of vitamin B_{12}-limited *Synechococcus*. Transmission electron micrographs of *Synechococcus* sp. PCC 7002 maintained at vitamin B_{12}-replete (**A.**) and vitamin B_{12}-deficient (**B.**) conditions. **T**- thylakoids; **P**- polyphosphate bodies; **C**- carboxysomes. Bar = 1μm.

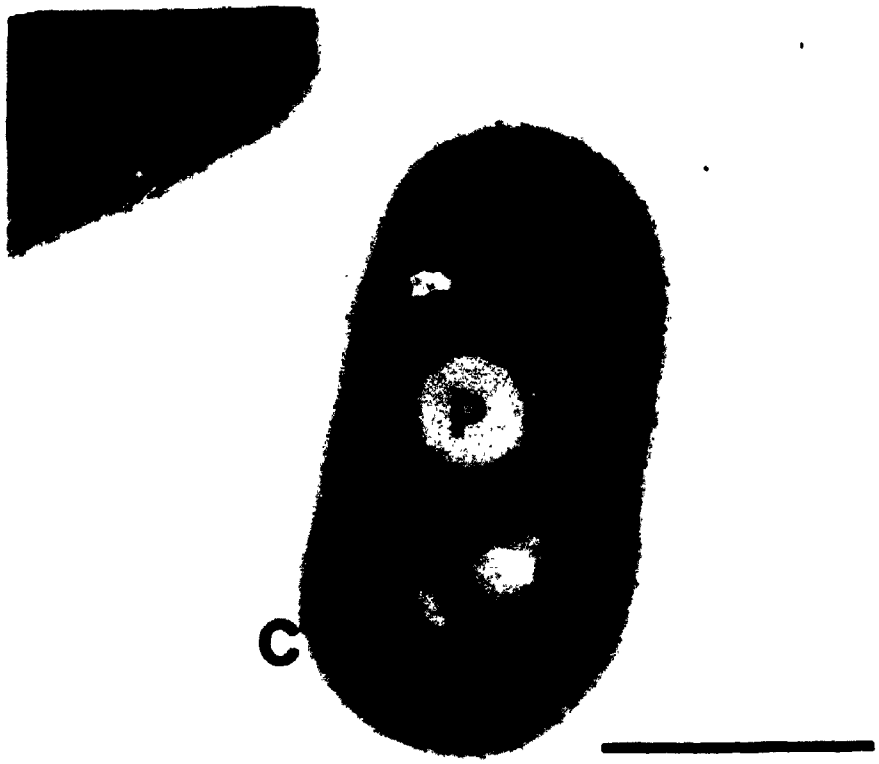

A.

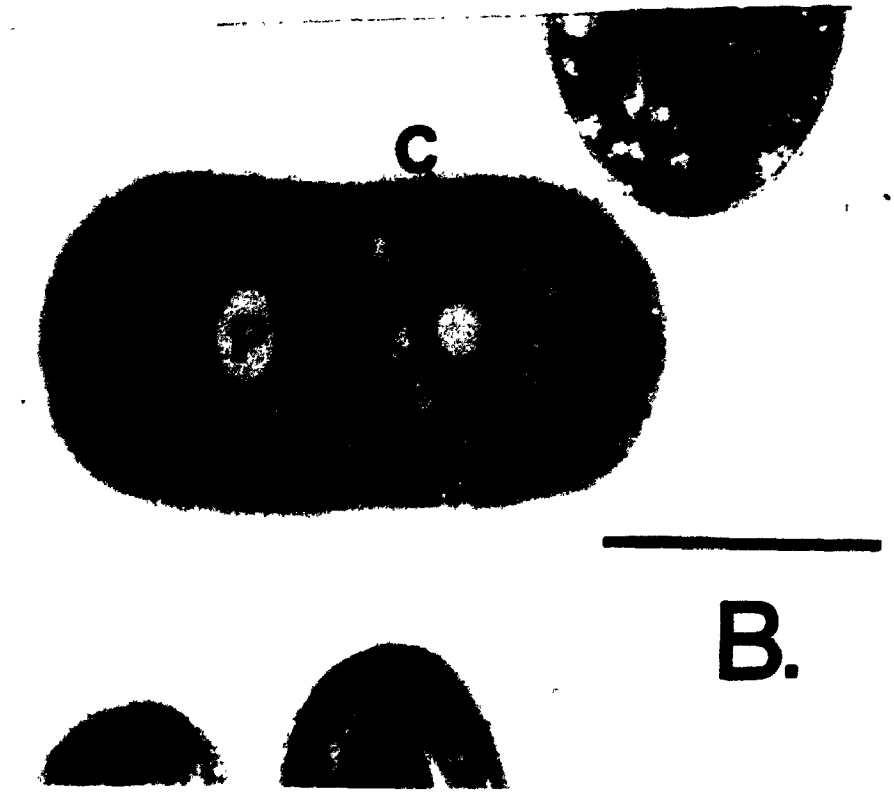

B.

Discussion

In this study, I have documented some of the physiological changes that occur in *Synechococcus* sp. PCC 7002 during periods of vitamin B_{12}-limited growth. Unlike previous characterizations of nutrient physiology in this cyanobacterium (Hardie et al. 1983a,b; Stevens et al. 1981a,b), I have analyzed these parameters under conditions of continuous culture so as to obtain data from physiologically equilibrated and exponentially growing cells.

As expected, reduction in the amount of the limiting nutrient (vitamin B_{12}) leads to a reduction in the cell density yields of the chemostats (Figure 28). This monophasic response to nutrient deprivation is predictable if the organism scavenges the specific nutrient through a constitutive transport system, as opposed to the biphasic response one sees in an inducible or high-affinity type transport system (Brown and Trick 1992; Section 3.3).

A similar response is seen in the analysis of chlorophyll per cell (Figure 29). The anomaly of the initial drop in chlorophyll per cell (50 μg mL^{-1}) is suggestive of a response due to a decrease in the luxury uptake of vitamin B_{12} and a possible utilization of this as a nitrogen source. Previous work has shown that standard A$^+$ medium at levels of 500 μg mL^{-1} vitamin B_{12} is nitrate-limited, and since the cyanocobalamin molecule contains approximately 12% N (by mass), the excess vitamin B_{12} may be acting as a source for cellular nitrogen. The increase seen in cellular chlorophyll at 5 μg mL^{-1} vitamin B_{12} may thus attributed to a slight decrease in growth rate vs. chlorophyll production in

the cells as vitamin B_{12} is no longer available as a nitrogen source. This suggests that it is at and below this level where the population begins to become "truly" vitamin B_{12}-limited. Suggestions of this sort have been made with respect to the utilization of vitamin B_{12} as a source of Co in marine organisms (Bruland et al. 1991).

The determination of the maximum growth rate at the 5.0×10^{-4} µg vitamin B_{12} L^{-1} level to be 0.237 day^{-1} is interesting as some natural concentrations have been found to be in the range of growth where it appears to be limiting. Carlucci and Silbernagel (1966) found North East Pacific concentrations of the vitamin to be in the range of 0.1 µg L^{-1} while Menzel and Speath (1962) found that vitamin B_{12} concentrations below 100 m were in the 0.08-0.2 µg L^{-1} range. While these levels were shown to be potentially limiting in chemostat cultures, this data cannot be extrapolated to actual conditions due to the complexities of vitamin B_{12} flux; natural populations being comprised of vitamin B_{12} auxotrophs as well as vitamin B_{12} over-producers (Swift 1981).

Enhancement of outer membrane proteins during growth at vitamin B_{12}-limiting levels suggests that the cyanobacteria may harbour an energy dependant, high-affinity acquisition system for vitamin B_{12} similar to that of other nutrients actively scavenged by Gram-negative bacteria (ie. iron-siderophore transport systems). In *Escherichia coli*, inducible vitamin B_{12} transport systems facilitate the energy dependant acquisition of vitamin B_{12} during periods when it is a growth-limiting factor. It is more likely, however, that a constitutive active

transport system is enhanced during periods of low vitamin B_{12} availability. Due to the size of the vitamin B_{12} molecule, it is too large to pass readily through the porin channels in the outer membrane of Gram-negative organisms (Reynolds et al. 1980).

Of particular interest here is in the production of a protein of 34 kDa by *Synechococcus* sp. PCC 7002 during periods of low vitamin B_{12} availability; proteins of similar size have also been identified in *Synechococcus* sp. PCC 7002 during periods of low iron availability (Section 3.8) as well as in *Synechococcus* sp. PCC 7942 during periods of iron-limited (35.0 kDa), and phosphate-limited (32.0 kDa) growth (Scanlan et al. 1989). While it cannot be stated that this is the same protein, it may suggest that a regulatory protein, such as those of the *fur/ton*B system of *E. coli* might be induced/enhanced in response to vitamin B_{12}-limiting conditions. The *fur/ton*B system is known to be involved in the regulation of iron and vitamin B_{12} transport in *E. coli* (Kadner 1990), and similar systems have been found in *Salmonella typhimurium* (Rioux et al. 1990).

Ultrastructural differences between nutrient-replete and -deficient batch cultures have been examined for a variety of nutrients in *Synechococcus* spp.; for iron (Hardie et al. 1983b; Sherman and Sherman 1983), phosphate (Stevens et al. 1981a) and nitrogen (Stevens et al. 1981b). As in their experiments, we find that the growth of this *Synechococcus* sp. at nutrient-limiting conditions induces a variety of structural modifications. This is particulary evident in the

deterioration of the thylakoid structures within the cells (Figure 31). The micrographs also demonstrate that growth under vitamin B_{12}-limiting seems to have no effect on the presence of inclusion bodies within *Synechococcus* sp. PCC 7002, similar to the previous reports for iron (Hardie et al. 1983b). Such thylakoid alterations during nitrate-limitation have been credited to a break down in the accessory pigment C-phycocyanin (C-PC), which accounts for some of the electron density that is associated with the thylakoids in non-limited cells (Stevens et al. 1981b). Suggestions have attributed this to the use of C-PC as a source of nitrogen during periods of nitrogen-limited growth (Boussiba and Richmond 1980), but the lack of an affect of vitamin B_{12} concentration on C-PC levels in this experiment rules out that possibility. The dissociation of the thylakoids is however, supported by the chl*a* cell^{-1} data, the drop in chl*a* cell^{-1} being intrinsically associated with a decrease in thylakoid structure. Thus it appears that the affect of vitamin B_{12} may be to alter the availability of structural components required to maintain thylakoid integrity.

The amount of vitamin B_{12} per cell in the medium, defined by a comparison of cell densities with vitamin B_{12} concentrations, declines to 256 molecules per cell at the level of 5 ng L^{-1}, equivalent to 6.15×10^{-10} ng cell^{-1} (Table 20). Guillard and Cassie (1963) reported that, for seven clones of marine centric diatoms, the molecules of vitamin B_{12} required per cell varied from 1035.3 to 35,711. However, standardizing this to cell volume, the values decreases from 5.1 to 13.4 molecules vitamin B_{12} μm^{-3}; less than the

Table 20. Vitamin B_{12} cell quotients in chemostat grown *Synechococcus* sp. PCC 7002. Quotients were determined from steady state cell densities.

Vitamin B_{12} ($\mu g\ L^{-1}$)	Cellular Quotient ($\mu g\ B_{12}\ cell^{-1}$)
500.0	1.40×10^{-5}
50.00	1.95×10^{-6}
5.000	2.11×10^{-7}
0.500	2.44×10^{-8}
0.050	2.88×10^{-9}
0.005	6.15×10^{-10}

requirements for *Synechococcus* sp. PCC 7002. Similar studies in autotrophically grown *Euglena gracilis* (Carell, 1969) have shown that the organism has a requirement of 4,900 to 22,000 molecules per cell (1.10-4.95 x 10^{-6} ng $cell^{-1}$). Considering the volume of a cyanobacterial cell ranges from 1-3 μm^3, it appears as though this cyanobacterium has a higher Q_{B12} μm^{-3} than the eukaryotes. Consideration is not given here to the volume of specific cellular components, particularly the chloroplasts and thylakoids in the eukaryotes. Cyanobacteria normally have a higher nitrogen content (4-9%) in comparison to eukaryotic algae (1-3%), impart do to the lower percentage of cellulose and other structural material within the cyanobacteria (Whitton 1992). Assuming that a similar situation exists for vitamin B_{12}, the higher Q_{B12} μm^{-3} of *Synechococcus* sp. PCC 7002 is to be expected.

Carell (1969) indicates that in vitamin B_{12}-deficient *Euglena gracilis*, chloroplast number increases by three to four fold, while total cellular concentrations of chlorophyll remain constant. This suggests is that, in eukaryotes, chloroplast biogenesis continues during vitamin B_{12}-deficient growth, while chlorophyll synthesis is affected, reducing the relative chlorophyll $chloroplast^{-1}$ levels. This concept is further complicated by reports of increases of cellular DNA, RNA and protein during periods of vitamin B_{12}-deficient growth as well as increases in cell size (Carell et al. 1970; Bertaux and Valencia 1973; Bertaux et al. 1991). This can be extrapolated to this cyanobacteria,

suggesting that this prokaryote responds to vitamin B_{12}-limitation in a similar manner to the eukaryotes chloroplast.

All the specific functions of vitamin B_{12} within cells remains to be determined; it appears, however, that mechanisms of *Synechococcus* sp. vitamin B_{12} utilization are likely to demonstrate similarities to the mechanisms of both eubacteria and plastids.

Appendix III: Statistical Analysis of Growth Data.

Chemostat Data: F-test and Paired T-test.

	17	18	19	20	21
17	XXXXXXX	20.898	30.864	**4.994F**	8.048
18	**3.56***	XXXXXXX	**1.476F**	**4.185F**	**2.597F**
19	**6.72*x**	**11.24*x**	XXXXXXX	**6.181F**	**3.835F**
20	**8.64*x**	**11.68*x**	**5.46*x**	XXXXXXX	**1.612F**
21	**6.04*x**	**8.64*x**	**1.09**	**5.38*x**	XXXXXXX

Upper Matrix: F-test, variance is homogeneous at less than 7.15 (F)
Lower Matrix (shaded): T-test; * $t_{0.05} = 2.132$, x $t_{0.005} = 4.604$
bold values demonstrate homogeneous variance.

Batch Culture Data: F-test and Paired T-test.

	17	18	19	20	21	22
17	XXXXXX	**.0148F**	25.0	11.111	**2.041F**	100
18	**2.17***	XXXXXX	169	**0.013F**	**0.072F**	**0.001F**
19	**7.45*x**	**0.60**	XXXXXX	**0.016F**	**0.032F**	**0.010F**
20	**9.00*x**	**1.28**	**4.96*x**	XXXXXX	**0.034F**	**0.014F**
21	**0.92**	**1.83**	**6.91*x**	**10.9*x**	XXXXXX	**0.032F**
22	**8.01*x**	**0.77**	**2.00**	**4.24***	**9.80*x**	XXXXXX

Upper Matrix: F-test, variance is homogeneous at less than 7.15 (F)
Lower Matrix (shaded): T-test; * $t_{0.05} = 2.132$, x $t_{0.005} = 4.604$
bold values demonstrate homogeneous variance.